MOLECULAR REQUIREMENTS AND EFFECTOR TARGETING OF THE INTERNALISATION OF PATTERN RECOGNITION RECEPTORS MEDIATING PLANT IMMUNITY

Jenna Caroline Loiseau

A thesis submitted to the University of East Anglia for the degree of Doctor of Philosophy

The Sainsbury Laboratory

Norwich Research Park

Norwich, UK

2019

Abstract

In order to perceive pathogen-associated molecular pattern (PAMPs) derived from pathogenic microbes, plants express pattern recognition receptors (PRRs) at their cell surface, which mediate PAMP-triggered immunity (PTI). In *Arabidopsis*, bacterial PAMP flg22 perception undergoes internalisation of its cognate PRR FLAGELLIN-SENSING 2 (FLS2). Ligand-activated FLS2 follows the endocytic pathway through the late endosome/multivesicular bodies (LE /MVBs) compartments to the lytic vacuole for degradation. Advances have been made regarding our understanding of the subcellular trafficking of these receptors but the molecular mechanisms underlying the regulation of their trafficking and the interplay it has with immunity remain poorly understood. Recent data demonstrate that post translational modifications (PTM) regulate PRRs internalisation and is critical for the execution of immune responses. To better understand regulation of PRRs trafficking during immunity, I investigated regulation of PRRs subcellular trafficking upon PAMP perception by using a combination of live-cell imaging microscopy together with effector interference. Here, I present FLS2 traffics to the LE/MVBs via the *trans*-Golgi network (TGN)/early endosome (EE) and that this is dependent on the ADP RIBOSYLATION FACTOR GUANINE-NUCLEOTIDE EXCHANGE FACTOR (Arf-GEF) HopM1 interactor 7 (MIN7). Further, confirming that endocytosis is a common process among PRRs mediating immunity, I demonstrate that the *Pseudomonas syringae* effector HopM1 targets flg22-induced endocytosis of FLS2 and elf18-induced endocytosis of EFR at the TGN/EE but not constitutive endocytosis of BRI1. Additionally, I indicate that receptor activation is uncoupled from its internalisation.

Table of Contents

1 GENERAL INTRODUCTION 18

1.1 Plant microbe interaction 18

1.2 Regulation of plant immunity mediated by cell surface-localised PRRs 20

1.2.1 General information 20

1.2.2 Receptor complex activation and defence signalling 23

1.2.3 PRRs regulation mediated by trafficking machinery 28

1.2.3.1 Delivery to the cell surface 28

1.2.3.1.1 Biogenesis 28

1.2.3.1.2 Spatial organisation 30

1.2.3.2 Uptake from the cell surface 30

1.2.3.2.1 Recycling 32

1.2.3.2.2 Endocytosis and signalling 33

1.2.3.2.3 Internalisation during MAMPs recognition 35

1.3 Regulation of defence responses mediated by the subcellular trafficking machinery 37

1.3.1 Re-adjustment of trafficking machinery during immunity 37

1.3.2 Effectors interference with host processes 38

1.3.2.1 Effectors of pathogenic bacteria 38

1.3.2.2 Effectors interference with trafficking components 40

1.4 Concluding remarks 41

1.5 Aims of the research project 42

2 MATERIAL AND METHODS 46

2.1 Plant material and growth conditions 46
2.1.1 *Arabidopsis* thaliana lines 46
2.1.2 *Arabidopsis* seeds sterilisation 47
2.1.3 Plants grown on soil 47
2.1.4 Plants grown on plates 47
2.1.5 Plants grown on liquid 47
2.1.6 Crossing of *Arabidopsis* lines 48
2.1.7 *Arabidopsis* mesophyll protoplasts isolation 48
2.1.8 Generating stable *Arabidopsis* lines 50
2.2 Bacterial strains 50
2.3 Culture media and reagents 50
2.3.1 Reagents and elicitors 50
2.3.2 Culture media recipes 50
2.3.3 Antibiotics 51
2.4 Molecular biology 51
2.4.1 Molecular cloning 51
2.4.1.1 GATEWAY cloning into pENTR vectors 54
2.4.1.2 Gateway cloning into pDEST vectors 54
2.4.2 Transformation of plasmids into *E. coli* by heat shock 54
2.4.3 Transformation of plasmids into *A. tumefaciens* by electroporation 55
2.4.4 DNA methods 55
2.4.4.1 Isolation of plant genomic DNA 55
2.4.4.2 Plasmid DNA isolation from *E. coli* 55

2.4.4.3 DNA extraction from Agarose gels 56
2.4.4.4 DNA sequencing 56
2.4.5 PCR methods 56
2.4.5.1 General PCR conditions 56
2.4.5.2 Colony PCR 58
2.4.6 RNA methods 58
2.4.6.1 Isolation of RNA from plants and cDNA 58
2.4.6.2 Reverse transcription PCR 59
2.4.6.3 DNA electrophoresis 59
2.5 Protein work 60
2.5.1 Protein extraction and IP experiments 60
2.5.1.1 Protein extraction for total extract 60
2.5.1.2 Protein extraction for Co-immunoprecipitation 60
2.5.1.2.1 Solubilisation buffer 61
2.5.1.2.2 SDS sample buffer (3X) 61
2.6 Biologicals assays 62
2.6.1 Chemicals and treatment 62
2.6.2 Ligand-induced internalisation 63
2.6.3 Seedling growth inhibition assay 63
2.6.4 OPERA 63
2.6.5 Confocal microscopy 64
2.6.6 Quantification of endosomes in *N. benthamiana* 64
2.6.7 Immunodetection 64
2.6.8 MAPK activation 65

2.6.9 TAMRA-flg22 uptake 65
2.6.10 Statistical analysis 65
3 DETECTION AND ANALYSES OF ENDOCYTOSIS OF PLANT RECEPTOR KINASES 66
3.1 Introduction 66
3.2 Materials 68
3.2.1 Samples 68
3.2.2 Experiment/Treatments 69
3.3 Confocal Microscopy 69
3.3.1 Sample Mounting 69
3.3.2 Image acquisition 70
3.3.3 Image Processing 70
3.4 Methods 71
3.4.1 Samples 72
3.4.2 Treatment 74
3.4.3 Experiment/Treatment 75
3.5 Confocal microscopy 76
3.5.1 Image acquisition 76
3.5.2 Image processing 78
3.6 Notes 81
4 THE FUNCTION OF 14-3-3S PROTEINS IS NOT REQUIRED FOR SUBCELLULAR LOCALISATION OF THE IMMUNE RECEPTOR FLS2 87
4.1 Abstract 87
4.2 Introduction 88

4.3 GRF4 localises to the cytosol, cell periphery and nucleus 92
4.4 GRF4 associates with FLS2 at the plasma membrane..... 94
4.5 GRF4 associates with FLS2 in a ligand and kinase-independent manner..... 96
4.6 GRF4 associates with EFR in a ligand-independent manner 98
4.7 GRF4 associates non-specifically with plasma membrane-localised proteins..... 99
4.8 The function of 14-3-3s is not required for flg22-induced FLS2 endocytosis..... 101
4.9 Other candidates tested..... 102
4.10 Conclusion 103
4.11 Discussion..... 104
5 POST-TGN TRAFFICKING OF FLS2 IS DEPENDENT ON THE ARF-GEF MIN7 AND IS TARGETED BY THE BACTERIAL EFFECTOR HOPM1 110
5.1 Abstract..... 110
5.2 Introduction 110
5.3 Activation dependent sorting of FLS2 occurs at the *trans*-Golgi-Network..... 114
5.4 The Arf-GEF MIN7 mediates FLS2 trafficking via the TGN/EE upon flg22 perception. 117
5.5 HopM1 interferes with ligand-induced endocytosis of PRRs in *N. benthamiana* 131
5.6 HopM1 interferes with FLS2 endocytosis at the *trans*-Golgi Network..... 140

5.7 Effector interference with FLS2 internalisation. 147
5.7.1 Effector secreted by Aphids 147
5.7.2 Effector secreted by *Xanthomonas*. 148
5.7.3 RIN4 148
5.8 General Conclusions..... 149
5.9 Discussion..... 152
6 REFERENCES 161

Table of tables

Table 2-1 List of *Arabidopsis thaliana* lines 46

Table 2-2 List of bacterial strains 50

Table 2-3 List of vector backbone used in this study 52

Table 2-4 Constructs used in this study. 52

Table 2-5 Programme for cloning PCRs 57

Table 2-6 List of primers used in this study. 57

Table 2-7 Programme used for colony PCR 58

Table 3-1 Receptor kinase localisation in *N. bemthamiana*. 84

Table 3-2 Markers used for co-localisation in heterologously expressing *N. benthamiana* leaves. 85

Table 3-3 Genetic interference of membrane trafficking in *N. benthamiana* leaves 86

Table of Figures

Figure 1-1 Schematic representation of FLS2 subcellular trafficking pathways. 44

Figure 3-1 General work flow for image acquisition and endosomes quantification. 72

Figure 4-1 Schematic representation of the distribution of proteins found in FLS2-GFP and GFP-Lti6B pull-downs by proteomic analysis. 89

Figure 4-2 FLS2 kinase domain exhibits a putative 14-3-3 binding motif mode Ⅰ. 92

Figure 4-3 GRF4-YFP localises to the cell periphery, cytoplasm and nucleus in *N. benthamiana*. 94

Figure 4-4 BiFC reveals GRF4 and FLS2 associate at the cell periphery. ... 96

Figure 4-5 GRF4 associates with FLS2 in a ligand and kinase-independent manner in *N. benthamiana*..... 97

Figure 4-6 GRF4 associates with EFR complex in an elf18-independent manner. 99

Figure 4-7 GRF4 associates with PM-localised proteins. 100

Figure 4-8 Chemical disruption of 14-3-3 function does not impair FLS2 internalisation. 102

Figure 4-9 Expression of GRF4-HA in five *Arabidopsis* transformants. 105

Figure 5-1 Recycling pathway of FLS2 is VHA-a1 positive. 115

Figure 5-2 Activated FLS2 partially co-localises with VHA-a1. 116

Figure 5-3 FLS2-GFP co-localises to VHa-a1-RFP after flg22. 117

Figure 5-4 *Arabidopsis* protoplasts are not suitable to observe flg22-induced FLS2 internalisation. 119

Figure 5-5 TAMRA-flg22 up take fails in Col-0 *Arabidopsis* cotyledons. 120

Figure 5-6 RT-PCR of *min7/*FLS2-GFP seedlings. 121

Figure 5-7 MIN7 is required for flg22-induced endocytosis of FLS2-GFP. . 122

Figure 5-8 flg22-induced endosomal number is reduced in *min7* mutant background compared to Col-0..... 123

Figure 5-9 RT-PCR of *min7/*RFP-ARA7 seedlings. 124

Figure 5-10 MIN7 is not required for RFP-ARA7 endosomes appearance. 124

Figure 5-11 MIN7 is not required for ARA7 endosomes. 125

Figure 5-12 Flg22-induced degradation of FLS2 is reduced in two independent *min7* mutant background, *min7* and in *ben1-2.* 126

Figure 5-13 ROS production is not impaired in *min7* background. 128

Figure 5-14 SGI induced by prolonged flg22 treatment is not impaired in *min7*. 129

Figure 5-15 MAPK activation is not altered in *min7*. 130

Figure 5-16 DEX::HopM1 *Arabidopsis* lines do not germinated on MS plates. 131

Figure 5-17 HopM1 reduces flg22-induced FLS2 endosomal number. 133

Figure 5-18 HopM1 reduces elf18-induced EFR endosomal number. 134

Figure 5-19 HopM1 does not affect BR1 endosomal number. 136

Figure 5-20 HopM1 truncated variants impair flg22-induced endocytosis of FLS2. 138

Figure 5-21 Anti-His antibody gives unspecific bands in *N. benthamiana*. . 139

Figure 5-22 HopM1 expression and tissues collapse in *N. benthamiana*. .. 140

Figure 5-23 Effect of HopM1 expression on endomembrane markers in *N. benthamiana.* 142

Figure 5-24 HopM1 reduced protein levels of SYP61. 143

Figure 5-25 HopM1 primary amino acid sequence does not display conserved known domains. 145

Figure 5-26 Structure prediction of HopM1. 146

Figure 5-27 MIN7-mediated Post-Golgi trafficking of FLS2 is targeted by HopM1. 151

List of publications arising from the work in this thesis

Chapter 3 has been compiled into the following manuscript:

Detection and Analyses of Endocytosis of Plant Receptor Kinases.

Loiseau J, *et al.* Methods Mol Biol. 2017.

Authors Loiseau J[1], Robatzek S[2]. Author information [1]The Sainsbury Laboratory, Norwich Research Park, Norwich, NR4 7UH, UK. [2]The Sainsbury Laboratory, Norwich Research Park, Norwich, NR4 7UH, UK. robatzek@tsl.ac.uk. Methods Mol Biol. 2017;1621:177-189. doi: 10.1007/978-1-4939-7063-6_1

Acknowledgements

I thank Silke Robatzek for giving me the opportunity to do a PhD in her group.

I would like to thank Cyril Zipfel, my secondary supervisor for his knowledge and support on my project. A great thanks to Sophien Kamoun for is wisdom and advise on writing.

Thank you to Christine Faulkner for her guidance.

Thank you to all my lab mates, you guys have helped me a lot through inspiring discussions or just unforgettable crazy talks involving fairy poneys, zombie unicorn or Harry Potter. Thank you, Mary and Kasia in particular for helping me during the writing process. Jelle, thank for the TGN and TGN/EE meetings. I would like to thank Martina and Heidrun for their help in the lab. Thanks to Malick, Anja and Rico who helped me at the very beginning of the project. It was a great pleasure to be part of the Robatzekretory pathway and I will never forget my time spend in Norwich.

Some huge thanks, to my office mates who witnessed too many “lost in translation” moments. Those who left already or those still around, Phon, Matt, Burkhard, Lucy, Jan, Jeoffrey, Jack, Lauren, Ana and a special thank you to the Fam for the good times and fun, Jelle, Janina, Jess, Sam, Helen, Rav, Ola.

I would like to thank Márcia for her faith in me, to Matt and Peter for their mentoring. Thank you to the admin Team, Karen, Lynda, Kim and Debbie, and to all the support team at TSL. Thank you to the Frenchies, Agathe and Baptiste for dragging me into social life.

Thank you to my friends Alicia and David, Jeanne and Nico for their moral support, your friendship is priceless. A special note for Oriane who knows that “les plantes ne sont pas des animaux”. Thanks to Alexandre Astier for is inspiring vision on science and for his work on Kaamelott which were helpful during doubtful moments.

And finally, a great thank to my parents and to my sister for believing in me and for their unconditional love.

Abbreviations

ADP	Adenosin diphosphate
Arf-GEF	ADP ribosylation factor guanine exchange factor
BAK1	BRI1-associated kinase 1
BIK	Botrytis-induced kinase
BIR1	BAK1-interacting receptor-like kinase 1
BIG	BFA-inhibited guanine nucleotide exchange protein
BRI1	Brassinosteroid insensitive 1
CBB	Coomassie brilliant blue
CCV	Clatrhin-coated vesicle
CEBiP	Chitin oligosaccharide elicitor-binding protein
CERK1	Chitin elicitor receptor kinase 1
CME	Clathrin-mediated endocytosis
CRT3	Calreticulin 3
DAMP	Damaged-associated molecular pattern
DRP2B	Dynamin-related protein 2B
ECD	Ectodomain
EE	Early endosome
EFR	EF-Tu factor receptor
EGFR	Epidermal growth factor receptor
ER	Endoplasmic reticulum
ER-QC	ER quality control
ERD2B	Endoplasmic reticulum detention defective 2B
ESCRT	Endosomal sorting complexes required for transport
ETI	Effector-triggered immunity
ETS	Effector-triggered susceptibility
FLS2	Flagellin-sensing 2
GA	Golgi apparatus
HRP	Hypersensitive response and pathogenicity
LE	Late endosomes
LeEiX	*Lycopersicum* ethylen-induced xylanase
LCSM	Laser confocal scanning microscopy
LORE	Lectin S-domain-1 receptor–like kinase
LPS	Lipopolyschaccaride

LRR	Leucine-rich repeat
MAMP	Microbes-associated molecular pattern
MAPK	Mitogen-associated protein kinase
MIN7	HopM1 interactor 7
MVB	Multi vesicular body
NLR	NOD-like receptor
PM	Plasma membrane
PR	Pathogenesis-related
PRR	Pattern-recognition receptor
PTI	PRR-triggered immunity
PTM	Posttranslational modification
pub12/13	*Plant U-box 12/13*
PVDF	Polyvinylidene fluoride
R genes	Resistance genes
RLCK	Receptor-like cytoplasmic kinase
RLK	Receptor-like kinase
RLP	Receptor-like protein
ROS	Reactive oxygen species
RTK	Receptor tyrosine kinases
SGI	Seedling growth inhibition
SNARE	N-ethylmaleimide-sensitive factor activating protein receptors
SOBIR1	Suppressor of BIR1-1
SP	Signal peptide
SYP61	Syntaxin protein 61
TfR	Transferrin receptor
TGN	*Trans*-Golgi network
TIR	Toll/interleukin receptor
TK	Tyrosine kinase
TLR	Toll-like receptor
TM	Transmembrane
TTSS	Type III secretion system
UGGT	UDP-glucose:glycoprotein glucosyltransferase
VPS	Vacuolar protein sorting

1 General introduction

1.1 Plant microbe interaction

Plants are continuously surrounded by a wide range of microbes that are present in their natural environment including viruses, nematodes, fungi, oomycetes and bacteria. Whilst some of them are beneficial to the plant, others can be harmful (Newton *et al*., 2010). Plants have physical barriers to prevent pathogens entry, cuticle (Serrano *et al*., 2014) and cell wall (Vorwerk *et al*., 2004) which constitute a line of passive defence. Some pathogens can break those barriers by mechanical forces, production of enzymes, or can enter the plant via pre-existing openings like stomata or wounds (Melotto *et al*., 2008). Pathogenic microbes invade the plant and multiply causing disease (Williamson, 1998). Nevertheless, disease is rather the exception than the rule, and through evolution plants have developed mechanisms to defend themselves (Dangl *et al*., 2013; Dodds and Rathjen, 2010; Jones and Dangl, 2006).

Unlike animals, plants lack specialised and mobile immune cells and rely on innate immunity (Chisholm *et al*., 2017; Da Cunha *et al*., 2006; Nürnberger *et al*., 2004). Remarkably, they have developed multi-layered strategies to counteract pathogen attacks at a molecular level where each individual cell is able to activate defence responses (Jones and Dangl, 2006). The first layer of defence is mediated by cell-surface localised receptors (Pattern Recognition Receptors) that recognise molecular determinants derived from the pathogen (Microbe-Associated Molecular Patterns) or from the host (Damage-

Associated Molecular Pattern) and activate PRR-triggered immunity (PTI). During PTI a set of signalling events are activated leading to defence responses preventing pathogen invasion. In most cases PTI is sufficient to resist pathogens (Jones and Dangl, 2006). However, successful pathogens have evolved to deploy mechanisms that disrupt PTI and promote disease (Dodds and Rathjen, 2010; Grant *et al*., 2006; Zhou and Chai, 2008). This process is mediated by molecules derived from the pathogen known as effectors (Chisholm *et al*., 2017). Effectors can manipulate plant processes to promote pathogenesis and colonise the host. For instance, effectors can target key components of defence responses to interfere at different level of PTI or they can promote pathogen growth by hijacking host processes. In these cases, effectors successfully promote infection resulting in the susceptibility of the plant (Effector-triggered susceptibility ETS). In turn, plants can deploy mechanisms to detect some of those effectors that relies on resistance (R) genes (Dodds and Rathjen, 2010; Jones and Dangl, 2006). Nod-like receptors (NLRs) are intracellular immune receptors that recognise directly or indirectly pathogen effectors, thus, triggering a second layer of defence known as Effector-Triggered Immunity (ETI) (Cesari *et al*., 2014; Dodds and Rathjen, 2010; Van der Hoorn and Kamoun, 2008; Jones and Dangl, 2006).

This co-evolutionary model where plants and pathogens deploy mechanisms to defeat each is the so-called “Zig-Zag” model (Jones and Dangl, 2006). In nature, pathogens and plants are both under pressure to select their best defeaters in an evolutionary arms race. Pathogens select effectors that avoid recognition by the plant surveillance system and plants select new alleles of R

genes that confer the recognition of these new effectors. Conceptually, PTI is activated by recognition of conserved molecular determinants indispensable for microbes, whereas ETI is activated by specific pathogen effectors, with transient defence responses activated by PTI and responses activated by ETI are stronger, often associated with cell death (Dodds and Rathjen, 2010; Tao *et al*., 2003). Nonetheless, both activate similar signalling pathways (Tsuda and Katagiri, 2010). Importantly, in some cases the classification between PRRs and NLRs, MAMPs and effectors is difficult to distinguish, hence, the line between PTI and ETI is blurry (Cook *et al*., 2015; Thomma *et al*., 2011). If the model based on the PTI/ETI dichotomy have help to decipher molecular mechanisms involved in resistance and susceptibly it is more complex in nature. Overall, the plant immune system is a surveillance system involving pathogen perception by plasma membrane-localised and intracellular receptors triggering responses to avoid pathogen invasion. This thesis will focus on plasma membrane-localised receptors.

1.2 **Regulation of plant immunity mediated by cell surface-localised PRRs**

1.2.1 **General information**

MAMPs are conserved molecular determinants of microbes and recognised as non-self by the host immune system (Medzhitov and Janeway Jr., 1997). In mammals, Toll-like receptors (TLRs) are evolutionary conserved PRRs that detect extracellular microbes and trigger immune cascades (Medzhitov, 2001; Tanji and Ip, 2005). TLRs are members of type 1 membrane receptors family,

which is characterised by an extracellular leucine-rich repeat (LRR) domain and an intracellular Toll-IL-(interleukin)-1 receptor (TIR) domain (Bell *et al*., 2017; O'Neill and Bowie, 2007). In plants, MAMP detection is mediated by two classes of PRRs, receptor-like kinases (RLKs) and receptor-like proteins (RLPs), which are structurally and functionally similar to TLRs (Mogensen, 2009). RLKs possess a highly variable ectodomain (ECD) involved in ligand detection, a single transmembrane region (TM), and an intracellular kinase domain required for response activation. RLPs share RLKs conformation but are lacking an intracellular signalling domain, thus, RLPs form complexes together with RLKs to mediate signal transduction (Gust and Felix, 2014; Liebrand *et al*., 2013; Shpak *et al*., 2005).

In animals, TLR5 is responsible for bacterial flagellin recognition and activates innate immunity (Smith *et al*., 2003).

Most plant species are sensitive to flagellin (Carrasco *et al*., 2014; Felix *et al*., 1999). In *Arabidopsis*, flagellin, or its 22 amino acids epitope, flg22, recognition is mediated by the LRR-RLK FLAGELLIN-SENSING 2 (FLS2) and activates PTI (Felix *et al*., 1999; Gómez-Gómez and Boller, 2018; Gómez-Gómez *et al*., 1999; Zipfel *et al*., 2004). Flg22 is the most conserved domain of the bacterial flagellin and has the highest affinity for FLS2 in *Arabidopsis* and tomato compared to other flagellin peptides and is used for most studies (Bauer *et al*., 2001; Meindl *et al*., 2000). Nonetheless, the flg22 epitope exhibits differences within the flagellin of bacterial species and strains (Sun *et al*., 2006). FLS2 orthologs display different flagellin perception (Helft *et al*., 2016; Lucie *et al*.,

2013; Robatzek *et al*., 2007; Vetter *et al*., 2012; Wang *et al*., 2015b). Some *Solanaceous* species including potato, tomato and pepper perceive the flgII-28 epitope independently of FLS2 and activate plant immune responses (Cai *et al*., 2011; Clarke *et al*., 2013; Hind *et al*., 2016). Those examples show evolutionary differences, likely to escape pathogen detection.

FLS2 and TLR5 are functional homologues, however, they have evolved separately (Smith *et al*., 2003). FLS2 and TLR5 do not share similar amino acid sequence and recognize different sites of flagellin (Felix *et al*., 1999). In plants, PRRs are cell-surface localised and can perceive a broad range of MAMPs from bacteria, fungi and oomycetes (Nicaise *et al*., 2009) but also DAMPs which are plant degradation products or secreted peptides present in the apoplast after pathogens attack. The ECD of PRRs is responsible for MAMPs/DAMPs detection, LRR types bind to proteins or peptides (Robatzek *et al*., 2006). For instance, the RLK ELONGATION FACTOR (EF)-Tu RECEPTOR (EFR) mediates Elongation factor Tu (EF-Tu), or it 18 amino acids epitope, elf18, perception in *Arabidopsis* (Zipfel *et al*., 2006). *At*PEP RECEPTOR 1 (PEPR1) and *At*PEP RECEPTOR 2 recognise the DAMP *At*pep1 (Yamaguchi *et al*., 2006, 2010). In *Arabidopsis*, RPL23 confers resistance to Necrosis and ethylene-inducing peptide 1-like proteins (NLPs) 20 (nlp20) from filamentous pathogens (Albert *et al*., 2015). The RLK Cold shock protein receptor (CORE), present in some Solanaceae species genome, mediates the recognition of the highly conserved nucleic acid binding motif RNP-1 of cold-shocks proteins (CSPs), represented by the MAMP csp22 during bacterial infection (Wang *et al*., 2016).

PRRs containing other domains than LRR mediate recognition of carbohydrate such as chitin, bacterial peptidoglycans, plant-cell-wall-derived oligogalacturonides (OG). For example, the Lysine-motif (LysM)-CONTAINING RECEPTOR-LIKE KINASE 5 (LYK5) binds chitin in *Arabidopsis* (Cao *et al*., 2014). Also, the LysM-containing TM protein chitin oligosaccharide elicitor-binding protein (CEBiP) and CHITIN ELICITOR RECEPTOR KINASE 1 (CERK1) mediates chitin perception in rice (Kaku *et al*., 2006; Miya *et al*., 2007). The *Arabidopsis* WALL-ASSOCIATED KINASE 1 (WAK1) mediates OGs perception (Brutus *et al*., 2010). LyM2, LyM3 and CERK1 mediate peptidoglycan (PGN) perception in *Arabidopsis* during bacterial attack (Willmann *et al*., 2011). The lectin S-domain-1 receptor–like kinase (LORE) protein mediates Lipopolysaccharide (LPS) sensing from gram-negative bacteria in plants (Ranf *et al*., 2015).

Importantly, heterologous expression of PRRs can confers responsiveness to several MAMPs (Lacombe *et al*., 2010). Thus, showing the downstream signalling components following MAMP perception must be at least partially functionally conserved within some plant species. Besides, in some plant species, ectopic expression of PRRs could confer resistance to different pathogens if downstream signalling components are present.

1.2.2 **Receptor complex activation and defence signalling**

In plants, upon ligand perception, signal transduction between extracellular signal and cytoplasmic signalling components is mediated by the recruitment of receptors kinases (RKs) responsible for phosphorylation and

transphosphorylation events. The LRR-RLK SOMATIC EMBRYOGENESIS KINASE 3 (SERK3/ BRASSINOSTEROID-INSENSITIVE 1 (BRI1)-ASSOCIATED KINASE 1 (BAK1) functions as a co-receptor for many RLKs in response to various stimuli, thus, this protein plays a central role in immunity (Chinchilla *et al*., 2007; Heese *et al*., 2007; Nekrasov *et al*., 2009). SERK3/BAK1 was first identified as a partner and positive regulator of the LRR-RLK BRI1 (Clouse *et al*., 1996). In *Arabidopsis*, brassinosteroids (BR) play important roles in plant growth, development and responses to the environment (Kim and Wang, 2010). After perception of its ligand, brassinolide (BL), BRI1 forms heterodimers with SERK3/BAK1 (Bücherl *et al*., 2013; He *et al*., 2000; Russinova *et al*., 2004; Sun *et al*., 2013) initiating phosphorylation cascades and downstream signalling (Wang *et al*., 2017). SERK3/BAK1 also plays a crucial role in immunity. Upon ligand perception, SERK3/BAK1 forms a complex with both RLKs FLS2 and EFR respectively and complex formation is crucial for ligand-induced responses (Chinchilla *et al*., 2007; Heese *et al*., 2007; Schwessinger *et al*., 2011; Sun *et al*., 2013). SERK3/BAK1 also serves as a co-receptor for the RLP Cf-4 upon AVR4 perception (Postma. *et al*., 2016). SERK3/BAK1 thus serves as a platform for the molecular assembly of signal competent receptors (Chinchilla *et al*., 2009; Liebrand *et al*., 2014). The *bak1-5* allele mutant shows impaired FLS2- and EFR-dependent signalling but not BR-mediated responses, (Schwessinger *et al*., 2011). Contrastingly to FLS2, BRI1 can form complexes with other member of the SERK family (Albrecht *et al*., 2008). This indicates distinct molecular mechanisms underline BAK1 function. Different hypotheses of BAK1 function were proposed.

Especially, C terminally tagged BAK1 are functional in BR signalling but not in PTI (Ntoukakis *et al*., 2011) and implies those tags affect BAK1 phosphorylation. Interestingly, a recent study using phophoproteomics identified conserved phophosites required for the function of BAK1 in PTI but not in growth (Perraki *et al*., 2018). This study suggests a phophocode dichotomy of BAK1 function in plant signalling.

Similarly, CERK1 serves a co-receptor for LyM-containing receptors. In *Arabidopsis*, CERK1 forms a complex with LYK5, and with LyM1 and LyM3 upon chitin perception (Miya *et al*., 2007). Whereas in rice, chitin perception induces recruitment of CERK1 by CeBiP, and by LYP5 and LYP6 (Liu *et al*., 2012).

To mediate signalling, LRR-RLPs associate with the RLK SUPPRESSOR Of BAK1-INTERACTING RECEPTOR-LIKE KINASE 1 (SOBIR1) or SOBIR1-like (Gust and Felix, 2014; Liebrand *et al*., 2014).

Interestingly, RKs acting as co-receptors with PRRs remain to be characterised, as it is the case for LORE-mediated signalling, which doesn't requires BAK1 or CERK1, but another yet uncharacterised RK (Ranf *et al*., 2015).

Ligand-induced heteromeric complexes with co-receptors recruit receptor- like cytoplasmic kinases (RLCKs). The *Arabidopsis* genome codes for over 160 RLCKs but most remain uncharacterised (Lehti-Shiu *et al*., 2009). Botrytis-induced kinase 1 (BIK1), the most studied RLCK, associates with FLS2 in is

resting state (Lu *et al*., 2010). Upon flg22 perception BIK1 dissociates from FLS2 in a BAK1-dependent manner (Lu *et al*., 2010). RLCKs act as substrates for PRRs complexes and mediate downstream signalling.

The signalling cascade that follows PRRs complex activation contains a series of early and late events (Zipfel and Robatzek, 2010). The early events appear within minutes following pathogen recognition, including phosphorylation events, activation of MITOGEN-ACTIVATED PROTEIN KINASE (MAPK) cascade, calcium burst, and reactive oxygen species (ROS) burst. Whereas, late events appear within hours or days following pathogen recognition, including defence-related gene expression, callose deposition, stomatal closure and seedling growth inhibition (SGI) (Monaghan and Zipfel, 2012). The signal transduction leads to a series of responses that ultimately restrict pathogen growth (Heath, 2000).

Molecular mechanisms underlying receptor complex activation and signalling transduction have been extensively studied over the past decade, reviewed by (Couto and Zipfel, 2016; Macho and Zipfel, 2014). In comparison, little is known regarding their subcellular trafficking and its contribution to PTI. Interestingly, flg22 perception induced an upregulation of the ADP rybosylation factor Guanine exchange factor (Arf-GEF) HopM1 interactor 7 (MIN7) protein levels (Gangadharan *et al*., 2013).

Arf-GEFs are trafficking determinants involved in vesicle trafficking (Anders and Jürgens, 2008). These large GTPases belong to a conserved eukaryotic protein family that are key players in cargo transport from one compartment to

another (Donaldson and Jackson, 2000). In *Arabidopsis*, this family is composed of eight members divided into two classes. The GBF1-related (Golgi Brefeldin A Resistant Guanine Nucleotide Exchange Factor 1) class includes three members, GNOM, GNOM-Like 1 (GNL1) and GNOM-Like 1 GNL2, closely related to the human cis-Golgi Arf-GEF GBF1 (Gerd and Niko, 2002; Richter *et al*., 2011). The role of GBF1-related members in trafficking has been described. GNOM localises to endosomal compartments and mediates the polar recycling of PIN1 to the PM which is essential for development (Geldner *et al*., 2003). (GNL1) localises to the Golgi apparatus and is involved in ER-Golgi transport (Sandra *et al*., 2009). GNOM-Like 2 (GNL2) is expressed in male gametophytes only and is involved in pollen germination (Richter *et al*., 2011). The second class is represented by the BIG family which includes five members, BIG1-4 and BIG5/BEN1/MIN7. Evidence shows that BIG1-4 perform essential functions in the late secretory pathway whereas the role of BIG5/BEN1/MIN7 remains elusive (Richter *et al*., 2014). So far, no link between Arf-GEFs and PRRs trafficking have been described.

BIG5/BEN1/MIN7 localises to the TGN/EE in *Arabidopsis* and *N. benthamiana* and is involved in the early endocytic pathway during development (Nomura *et al.*, 2011, Tanaka *et al.*, 2009). Phylogenetic analysis (Mouratou *et al*., 2005) revealed that the *MIN7* sequence diverges from the other BIG members suggesting that the same may be true for its function.

MIN7 does play a role in trafficking and is involved in polar trafficking of PIN proteins during developmental stage (Tanaka *et al*., 2009). Interestingly, MIN7

accumulation plays a role in callose deposition, PR-1 accumulation and establishment of aqueous apoplast during bacterial infection by a yet unknow mechanism (Gangadharan *et al*., 2013; Nomura *et al*., 2006, 2011; Xin *et al*., 2016). Taken together, MIN7 is a noteworthy candidate to investigate the contribution of trafficking to PTI responses.

1.2.3 **PRRs regulation mediated by trafficking machinery**

Eukaryotic cells are composed of an interconnected network of endomembrane system formed by membrane-bound organelles from secretory and endocytic pathways. In plants, the trafficking machinery involves regulators and adaptors to control the abundance and the distribution of proteins in and out of the cell and modulates many cellular responses.

1.2.3.1 **Delivery to the cell surface**

1.2.3.1.1 **Biogenesis**

Accumulation of functional PRRs at the cell surface is the key to activate defence responses. Newly synthetized proteins are translocated in the endoplasmic reticulum (ER), and follow the secretory pathway to reach their final destination where they carry out their function (Kim and Federica, 2014). The default or conventional secretion pathway is followed by most soluble or membrane proteins. In this case, proteins are exported from the ER to the Golgi apparatus (GA) via coat protein complex II (COPII)-coated vesicles and through the *trans*-Golgi network (TGN) (Gerd and Niko, 2002). The N-terminal sequence of PRRs contain a signal peptide (SP) that exports the PRR from

the ER into the secretory pathway (Gómez-Gómez and Boller, 2000). Importantly, the endoplasmic reticulum quality control (ERQC) components regulate transport of properly folded proteins (Anelli and Sitia, 2008). As a consequence, lack of ERQC components compromises PRRs accumulation and activity. For instance, loss-of–function mutants in ER-localised chaperones CALRETICULIN 3 (CRT3), URIDINE DIPHOSPHATE (UDP)-GLUCOSE:GLYCOPROTEIN GLUCOSYLTRANSFERASE (UGGT) and in ENDOPLASMIC RETICULUM RETENTION DEFECTIVE 2B (ERD2b) show impaired EFR accumulation and compromised elf18-induced responses, whereas FLS2 accumulation is not affected (Li *et al*., 2009; Nekrasov *et al*., 2009; Saijo *et al*., 2009). This indicates a difference between EFR and FLS2 delivery to the cell surface. FLS2 secretion is regulated by ER-resident reticulon-like proteins B 1 and 2 (RTLNB1 and 2), *rtlnb1* and *rtlnb2* mutants show accumulation of FLS2 in the ER (Lee *et al*., 2011). RLKs are glycoproteins and N-glycosylation in the ER and Golgi is required to mediate immunity (Häweker *et al*., 2010).

Additionally, an unconventional secretory pathway bypassing the GA has been observed in eukaryotes (Drakakaki and Dandekar, 2013; De Marchis *et al*., 2013). This pathway mediates trafficking from ER to PM in a Golgi-independent manner. In plants, this pathway occurs for proteins lacking a SP and in storage tissues like seeds (De Marchis *et al*., 2013).

1.2.3.1.2 **Spatial organisation**

Once arrived at the PM, PRRs are not randomly positioned but are spatially organised within the PM and this may contribute to defence activation by creating signalling platforms. For instance, FLS2 and LYSIN MOTIF DOMAIN-CONTAINING GLYCOSYLPHOSPHATIDYLINOSITOL-ANCHORED PROTEIN 2 (LYM2) both localise to PD(plasmodesmata)-PM and play a role in the regulation of intracellular flux during defences responses (Faulkner *et al*., 2013). BRI1 and FLS2 form distinct nanoclusters at the PM, suggesting spatial organisation of PRRs at the PM is associated with their signalling function (Bücherl *et al*., 2017). Several MAMPs induce changes in PM composition, fluidity and lateral organisation (Ali and Reddy, 2008; Keinath *et al*., 2010; Sandor *et al*., 2016). Signalling proteins are enriched in PM microdomains (Stanislas *et al*., 2009). Overall, PM biophysical characteristics are important to understand PRRs organisation within the PM and its link with activation of defence responses.

1.2.3.2 **Uptake from the cell surface**

Endocytic membrane trafficking involves the cellular internalisation and sorting of extracellular molecules, PM proteins and lipids generally termed cargoes (Conner and Schmid, 2003). It is a multi-step process involving activation, cargo capture/sorting, induction of membrane curvature, dilation of curvature and scission. From there, cargo is further sorted to destination organelles. In animal cells several types of endocytic processes such as phagocytosis (uptake of particles), pinocytosis (uptake of fluid), clathrin-mediated

endocytosis (CME), caveolae-mediated endocytosis, and clathrin- and caveolae-independent endocytosis occur (Conner and Schmid, 2003). The endocytic pathways differ with regard to the size of the endocytic vesicle, the nature of the cargo (ligands, receptors and lipids) and the mechanism of vesicle formation (Conner and Schmid, 2003). Nonetheless, CME is the main pathway, and is the best characterized in animals.

In plants, the existence, physical feasibility, and physiological significance of endocytosis have been a matter of debate for decades, specifically due to the presence of the cell wall and high cellular turgor pressure (Cram, 1980). However, microscopy experiments following internalisation of fluorescent dye in plant protoplasts demonstrate the existence of endocytosis in plants (Robinson and Milliner, 1990). Importantly, emerging evidence reveals CME is also the main entry portal into the plant cell (Pérez-Gómez and Moore, 2007). Orthologues for many of the well-characterized elements of this machinery in mammalian cells (clathrin heavy and light chains, adaptins, and scaffolding proteins such as AP180) have been found in plants (Barth and Holstein, 2004; Holstein, 2002; Holstein and Oliviusson, 2005). Moreover, one study has shown the internalization of the animal transferrin receptor (TfR) when expressed in plant protoplasts (Elena *et al*., 2006), strengthening the hypothesis supporting similarities between animal and plant cells. This suggests that many features of this pathway are evolutionarily conserved. Nevertheless, endocytosis is less studied in plants than in animals and many features remain poorly understood in comparison to the animal field.

1.2.3.2.1 **Recycling**

During the recycling process, internalised cargoes traffic via the Early Endosome (EE) and go back to the PM (Hsu and Prekeris, 2010). This early endocytic recycling pathway is essential for maintaining the proper composition of proteins and lipids in various organelles and for returning essential molecules that carry out specific functions to the appropriate organelles. Plants have independently evolved a different set of proteins and show considerable divergence in endosomal structures and trafficking components in comparison to animals (Geldner and Jürgens, 2006). For instance, in plants, no specific recycling endosomes have been identified so far. However, the TGN compartment has been proposed to sorts vesicles back to the plasma membrane or to late endosomes (LE) (Sandra *et al*., 2009). Moreover, the TGN/EE is a hub were cargo from the secretory and endocytic pathway merge thus can serve as a sorting platform (Viotti *et al*., 2010). As an example of receptor recycling, BRI1 undergoes constitutive endocytosis independently of its cognate ligand biding BL (Geldner *et al*., 2007). Non-activated FLS2 is constitutively recycled between the PM and the TGN/EE in a BFA-sensitive manner (Beck *et al*., 2012).

The fungal toxin Brefeldin A (BFA) has been extensively used as a tool to study recycling endocytosis in animals and plants (Robinson *et al*., 2008a). BFA inhibits GNOM which was described to be TGN-localised (Geldner *et al*., 2003). Thus, BFA was used to induce aggregation of cargoes which go through the TGN, thus, through the recycling and secretory pathway into the

so-called BFA compartments (Geldner *et al*., 2001; Robinson *et al*., 2008a). In 2014, Naramoto and collaborators shed the light on GNOM localisation using super-resolution confocal live imaging microscopy. Evidence shows GNOM localisation is predominantly at the Golgi rather than at the recycling endosomes as previously described by Geldner and his collaborators in 2003. This mis-localisation is owed to the fact that GNOM localisation was previously identified using long-term BFA treatment only. Naramoto and collaborators report long-term BFA treatment affects TGN integrity whereas short-term treatment affects Golgi and secretion. BFA must be used cautiously as it has a broad effect on TGN integrity rather than specifically on recycling pathway, thus, questioning the existence of a recycling endosome in plants (Naramoto *et al*., 2014).

1.2.3.2.2 **Endocytosis and signalling**

In animals, PRR endocytosis plays a role in downregulation of signalling because over activation leads to massive inflammation and can cause auto-immune diseases, chronic inflammation or death (Piccinini and Midwood, 2010). Data supports the hypothesis of receptor signalling, not only from the cell surface but also from endosomes (von Zastrow and Sorkin, 2007). The first observation that showed a requirement for endosomal localisation in signalling has been made in animals with the Epidermal Growth Factor Receptor (EGFR), a Receptor Tyrosine Kinases (RTKs). Ligand-binding of EGFR activates growth-modulating signalling pathways (Shuang *et al*., 1991). Activated EGFR initiates events leading to its endocytosis (Lamaze, C. &

Schmid) and is sorted to lysosomes in a clathrin-independent as well as a clathrin-dependent manner (Sigismund *et al*., 2008). In contrast, non-stimulated receptors are more efficiently recycled to the cell surface. Furthermore, various cellular signalling events appear to occur on endosome membranes and endosomes are considered to function as signalling compartments in animals (Howe *et al*., 2001). Conversely, it is becoming apparent that signalling events regulate the endocytic pathway (von Zastrow and Sorkin, 2007). Endocytosis is conserved among eukaryotes; therefore, it is tempting to propose a role for endosomes in plant signalling.

BRI1 can be localised at the PM and endosomes (Russinova *et al*., 2004) and a study shows a link between endocytosis and signalling in plants (Geldner *et al*., 2007). It has been shown that increased endosomal concentrations of BRI1 correlates with enhanced BR signalling (Geldner *et al*., 2007). It was therefore proposed that endosomes can serve as a platform for signalling, as it can allow interaction between key components in the cell cytosol. In tomato, disruption of the interaction between the adaptor-protein 2 (AP-2), required for internalisation of clathrin-coated vesicles (CCV) and a receptor involved in xylanase perception (Lycopersicon esculentum ethylene-inducing xylanase (LeEIX)) abolishes the induction of the hypersensitive responses upon xylanase treatments, suggesting that endocytosis plays key role in LeEIX2 signalling (Ron and Avni, 2004). In large scale proteomic analyses of vesicle pull-downs, it was revealed that signalling components are enriched in endosomes after flg22 perception (Heard *et al*., 2015). However, the role of endocytosis in plant signalling remains controversial and dependent on

studied models. Endocytic pathways play a role in many cellular processes; thus, it is likely that inhibition of those pathways has pleotropic effects.

1.2.3.2.3 **Internalisation during MAMPs recognition**

Upon flg22 perception, PM-localised FLS2 undergoes internalisation into the plant cell and transiently accumulates to mobiles vesicles (Robatzek *et al*., 2006). Co-localisation studies with the lipophilic endocytic tracer FM4-64 shows activated FLS2 receptors localise to *bona fide* endosomes (Beck *et al*., 2012). Activated FLS2 traffics through late endosomal pathway via LE/MVBs compartments in a BFA-insensitive manner (Beck *et al*., 2012). In contrast to the recycling pathway of non-activated FLS2, flg22-induced endocytosis of FLS2 requires co-receptor SERK3/BAK1 (Mbengue *et al*., 2016). Hence, FLS2 trafficking depends on its activation status (Beck *et al*., 2012). Co-localisation studies together with chemical interference revealed FLS2 localises to ARA7/RABF2b and ARA6/RabF1 positive compartments in *Arabidopsis* (Beck *et al*., 2012), labelling predominantly LE and MVBs (Takashi *et al*., 2004; Ueda,Takashi *et al*., 2001). The ENDOSOMAL SORTING COMPLEXES REQUIRED FOR TRANSPORT-I (ESCRT I) subunits VACUOLAR PROTEIN SORTING 37 (VPS37) are required to mediate flg22-induced MVB sorting of FLS2 (Spallek *et al*., 2013). Ultimately, FLS2 late endosomal pathway leads to its degradation in the vacuole (Lu *et al*., 2011).

By contrast, in *Nicotiana benthamiana*, upon flg22 perception FLS2 co-localises with TGN-resident SYNTAXIN OF PLANT (SYP)61 and with ARA7/RabF2b to a yet undefined compartment with hybrid characteristic of

TGN/MVBs (Choi *et al*., 2013). Evidence exists that FLS2 endocytosis requires clathrin and dynamins (Mbengue *et al*., 2016; Smith *et al*., 2014a). In animals, CME is mediated via the recognition of an endocytic motif Yxxϕ (where Y is a tyrosine x is any amino acid and ϕ is a hydrophobic amino acid) absent from the FLS2 amino acid sequence. So far, what mediates the internalisation of activated FLS2 from the PM remains poorly understood. Nevertheless, recent data support a role for post translational modification (PTM) in FLS2 endocytosis. This shows despite the fact that CME is a conserved mechanism among eukaryotes, different mechanisms exist for CME regulation in animals and plants.

Ligand-induced PRR internalisation pathways are conserved across the RLK family of PRRs. FLS2, EFR and PEPR1 all undergo endocytosis upon perception of their cognate ligands, flg22, elf18 and pep1 respectively in clathrin-dependent manner (Beck *et al*., 2012; Mbengue *et al*., 2016). Other PRRs following the late endosomal pathway have been reported. For instance, the RLP Cf-4 which undergoes internalisation after Avr4 recognition (Postma. *et al*., 2016). Recently, data demonstrates that after chitin perception, CERK1 mediates internalisation of the RLK LYK5 (Erwig *et al*., 2017) in *Arabidopsis*. The subcellular trafficking pathway of PRRs is now well-described in plants, but the molecular mechanisms underlying regulation of PRR endocytosis, and its interplay with PTI, remain poorly understood and its contribution to signal downregulation has not been shown.

1.3 Regulation of defence responses mediated by the subcellular trafficking machinery

1.3.1 Re-adjustment of trafficking machinery during immunity

During pathogen attack, the plant endomembrane system is re-adjusted to allow establishment of rapid responses. Up-regulation of the secretion pathway delivers defence-related molecules to the apoplast by exocytosis. Defence molecules include peptides with anti-microbial activities, like pathogenesis-related (PR)-1 (Wang *et al*., 2005), defensins (Ganz, 2003), and thionins (Asano *et al*., 2013), and also proteases (Bozkurt *et al*., 2011). Reinforcement of the cell wall by secretion of β-(1, 3)-d-glucan polymer (callose deposition) is commonly observed in response to pathogens (Luna *et al*., 2010; Ton and Mauch-Mani, 2004).

Evidence shows the plant trafficking process is altered during host-pathogen interactions. Plants can direct their trafficking pathways to the location of pathogen attack. For instance, RabE1d GTPases is a trafficking regulator localising to the GA and the PM, but focally accumulates in response to bacterial infection (Speth *et al*., 2009). Similarly, the secretion and focal accumulation to the PM of the PENETRATION RESISTANCE 1 (PEN1) syntaxin, also named SYP 121, is enhanced upon fungal attack (Assaad *et al*., 2004).Thus, PEN1/SYP121 facilitates secretion of anti-microbial compounds. Notably, flg22 induces phosphorylation of PEN1, but the role of this modification remains unknown (Nühse *et al*., 2003). The ATP binding cassette transporter PEN3 is a PM-resident protein. During powdery mildew infection,

PEN3 is directed to penetration sites and contributes to defence responses at the cell wall (Stein *et al*., 2006; Underwood and Somerville, 2013). The RabG3c protein (RAB7 GTPase) is rerouted to the extrahaustorial membrane (EHM) during *Phytophthora infestans* infection, showing that the late endosomal pathway is rerouted to the pathogen interface (Bozkurt *et al*., 2015). Focal accumulation of trafficking components is the most observed phenomenon during defence against filamentous pathogens and seems that MVBs play a role in this process (Lipka *et al*., 2005; Underwood and Somerville, 2013).

1.3.2 **Effectors interference with host processes**

Adapted pathogens have developed strategies to promote disease by producing virulence-associated proteins, known as effectors. Effectors are frequently small proteins that suppress host defence responses by targeting PTI (Jones and Dangl, 2006). Effectors can act as enzymes, structural mimics or adapters to modify the function of host targets (Abramovitch *et al*., 2006; Diao *et al*., 2007; Hicks and Galán, 2010). Therefore, they can modulate PTI at different levels.

1.3.2.1 **Effectors of pathogenic bacteria**

Gram-negative bacteria deliver effectors into the host cell via the type III secretion system (TTSS) which forms a syringe-like structure into the cell. TTSS is widely distributed among phytopathogenic bacteria and is essential to virulence (Ghosh, 2004). TTSS is a protein complex encoded by a cluster

of genes called hypersensitive response pathogenicity (hrp). As a result, bacterium lacking the *hrp* cluster in the genome can no longer inject effectors into the host and are not able to trigger HR in resistance plants (Alfano and Collmer, 2004; Collmer, 1998).

Bacterial strains can inject around 30 effectors into the host cytoplasm where they function. Effectors adopt different molecular strategies to subvert host processes, including PTI. Examples are listed below.

AvrPto and AvrPtoB target the complex FLS2-BAK1, thus, preventing activation of downstream signalling components (Shan *et al*., 2008; Xiang *et al*., 2008). *X. campestris* effector AvrAC uridylates host kinase BIK1 to dampen basal resistance at the receptor level (Wang *et al*., 2015a). *P. syringae* effector AvrPphB cleaves PBS-like proteins which inhibits PTI activation at the plasma membrane (Zhang *et al*., 2017). Bacterial effectors AvrRps4 and Pop2 target host WRKY transcription factors to suppress immune response (Le Roux *et al*., 2015; Sarris *et al*., 2015). *P. syringae* effector HopAI1 as phosphothreonine lyase activity that inactivates MAPKs to supress immunity (Zhang *et al*., 2007). HopM1 supresses MAMP-triggered stomatal aperture in a 14-3-3 dependant manner

Notably, if effectors injected into host are diverse they exhibit functional redundancy (Mukhtar *et al*., 2011). Proteomic approaches show pathogens effectors target an overlapping subset of host cellular process and is critical for pathogens to adapt to a range of hosts (Cunnac *et al*., 2009; Grant *et al*., 2006).

Other pathogens such as oomycetes and fungi also secrete effectors but will not be extensively presented in this thesis.

1.3.2.2 **Effectors interference with trafficking components**

The trafficking machinery is responsible for bringing host components to the right location in the cell, thus, it is an important player of establishment of defence (Bednarek *et al*., 2010). Accordingly, effectors target key components of vesicle trafficking to promote virulence. As described above, CME is the major entry portal in the cell, hence, evidence reports clathrin to be targeted by effectors by yeast-two-hybrid approach (Mukhtar *et al*., 2011).

Pathogen effectors with established host interactors that have a function in subcellular transport have been identified (reviewed (Ben Khaled *et al*., 2015)). For instance, the *P. infestans* effector AVRblb2 prevents secretion of papain-like cysteine protease C14 to the apoplast (Bozkurt *et al*., 2011). FLS2 endocytosis can be inhibited by co-expression of *P*. *infestans* AVR3a, a virulence protein interacting with *N. benthamiana* Dynamin-related protein 2 (DRP2) (Chaparro-Garcia *et al*., 2015). The bacterial effector HopW1 from *P. syringae*, which forms complexes with actin in plants and disrupts actin filaments during infection disrupts endocytosis (Kang *et al*., 2014) Besides, this suggests that HopW1's virulence is linked to its effect on actin and actin-dependent processes. *P. syringae* DC3000 effector HopM1 interacts with MIN7 and induces its degradation in a proteasome-dependent manner (Nomura *et al*., 2006).

HopM1 targeting of MIN7 leads to inhibition of MAMP-triggered callose deposition, suggesting inhibition of secretory trafficking (Gangadharan *et al*., 2013). However, the mechanism underlying this is unclear. Likewise, co-expression of pathogen virulence proteins can be used to interfere with receptor kinase localisation (Chaparro-Garcia *et al*., 2015), thus providing insights into the mechanisms by which pathogens re-adjust plant cellular responses. Co-localisation studies of trafficking markers with effectors can be used to study PRRs trafficking involvement in PTI (Loiseau and Robatzek, 2017).

1.4 **Concluding remarks**

To summarise, PRRs are sentinels of the plant surveillance system contributing to basal immunity and plants lacking PRRs or PTI components are more susceptible to pathogens (Miya *et al*., 2007; Schwessinger *et al*., 2011; Zipfel *et al*., 2004, 2006). Activation of PTI prevent invasion by a wide range of pathogens. Notably, fundamental discoveries on molecular mechanisms underlying activation of PTI and establishment of defence responses has become a strategy to engineer more sustainable crops (Lu *et al*., 2015; Schoonbeek *et al*., 2015).

In plants, PRR internalisation is a conserved process (Erwig *et al*., 2017; Mbengue *et al*., 2016; Postma. *et al*., 2016; Robatzek *et al*., 2006) but its contribution to signal downregulation has not been shown. Only indirect evidence shows a link between trafficking components and impairment of PTI. The ESCRT-I subunits VPS37 are required for flg22-triggered stomatal closure

(Spallek *et al*., 2013). The vesicular trafficking protein DYNAMIN-RELATED PROTEIN 2B (DRP2B) is involved in response to bacteria. Analysis of the *drp2b* null mutant showed increased flg22-induced ROS production and susceptibility to *Pto* DC3000 (Smith *et al*., 2014a). The clathrin heavy chain protein is involved in flg22-induced ROS burst (Mbengue *et al*., 2016). This shows trafficking components are important players during PTI.

1.5 **Aims of the research project**

Trafficking machinery plays a central role in defence responses (Bednarek *et al*., 2010). Overall, the role of the secretion pathway is to deliver functional PRRs to carry out their function in pathogen recognition and production of anti-microbial compounds. Recycling of non-activated PRRs allows the regulation of a competent pool of receptors at the PM. PRR internalisation appears to be required to maintain sensitivity to bacteria (Ben Khaled *et al*, unpublished). Nonetheless, the mechanism underlying regulation of PRRs internalisation remain elusive. A better understanding of the spatio-temporal regulation of PRRs is crucial for understanding the establishment of PTI. Co-expression with different fluorescent-tagged markers of defined subcellular compartments, e.g. PM, Golgi, TGN, and LE/MVBs, allows the probing of PRRs localisation along distinct trafficking routes and during infection (Choi *et al*., 2013; Loiseau and Robatzek, 2017; Postma. *et al*., 2016). In addition, chemical interference by vesicles trafficking inhibitors or with virus-induced or RNA-mediated gene silencing allows the identification of molecular determinants involved in ligand-induced endocytosis of PRRs (Beck *et al*.,

2012; Chaparro-Garcia *et al*., 2015; Choi *et al*., 2013; Frescatada-Rosa *et al*., 2015; Postma. *et al*., 2016; Smith *et al*., 2014a).

FLS2/flg22 is one of the best characterised models of PRR trafficking (Figure 1-1). Recently, data supported a link between post-translational events controlling PRR internalisation (ubiquitination and phosphorylation) and responsiveness to bacteria (Ben Khaled *et al*, unpublished). Ubiquitination-dependent FLS2 endosomal sorting is required for its vacuolar degradation (Lu *et al*., 2011; Spallek *et al*., 2013). Soon after defence activation, FLS2 is mono-ubiquitinated at the PM by the plant U-box E3 ligases (PUB) 12 and PUB13 (Lu *et al*., 2011). In the *pub12/13* double mutant FLS2 mono-ubiquitination and endocytosis is abolished whereas flg22-induced canonical responses remain unaffected (Ben Khaled *et al*, unpublished). However, defence responses to long term exposure to flg22 treatment are diminished. Taken together, this data suggested that FLS2 endocytosis is required to maintain responsiveness to long term flg22 treatment (Ben Khaled *et al.*, unpublished). In *pub12/13* accumulation of FLS2, likely deactivated, at the plasma membrane prevents the accumulation of newly synthesized receptors. Strikingly, this data suggests that flg22-induced endocytosis of FLS2 is coupled with the delivery of newly synthesized receptors in a cargo-specific manner. Similarly, data support a same mechanism underlying elf18-induced internalisation of EFR (Ben Khaled *et al.*, unpublished). Nevertheless, where does the coupling between receptor secretion and internalisation remain unknow.

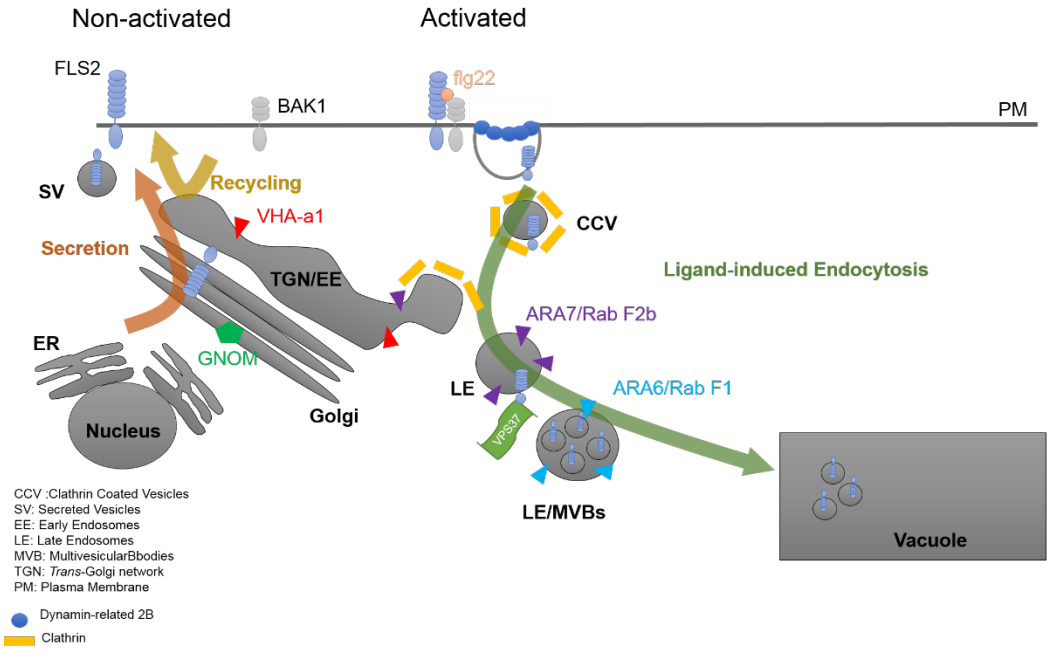

Figure 1-1 Schematic representation of FLS2 subcellular trafficking pathways.

Overview of FLS2 subcellular trafficking along compartments of the secretory-endosomal pathways. Secretory trafficking of FLS2 to the PM (dark orange arrow), constitutive recycling (yellow arrow) and ligand-induced endocytosis pathways (green arrow) are represented. Upon ligand binding FLS2 travels via CCV, LE and MVBs for vacuolar degradation. Marker proteins of endosomal compartments colocalising with FLS2 are shown by coloured tags. ER, endoplasmic reticulum; PM, plasma membrane; TGN, trans-Golgi network; MVB, multivesicular body; Adapted from Lu *et al.,* 2011; Beck *et al.,* 2012; Spallek *et al.,* 2013; Mbengue *et al.,* 2016; Smith *et al.,* 2014.

The purpose of the group's research is to better understand i) how are cell membranes and their cargoes, such as FLS2 and other PRRs transported through the cell? ii) how is this regulated during pathogen perception? iii) how is this contributing to defence activation?

The objectives of my project are:

1. Develop a standardised method to use PRRs internalisation observation as a tool to identify key trafficking routes targeted for virulence promotion.
2. Identify regulatory proteins that facilitates FLS2 endocytosis after flg22 treatment and investigate their role in establishment of PTI.
3. Determine whether FLS2 sorting to the late endosomal pathway is mediated via the TGN/EE in *Arabidopsis*. Then, identify the molecular determinant involved in FLS2 sorting to the TGN.
4. Investigate effector interference with sub-cellular trafficking to study its contribution to establishment of defence responses.

To summarize, my PhD project aim at identifying the protein complex that regulate FLS2 endocytosis and to a bigger extend to PRRs in general. Identifying components controlling PRRs trafficking after pathogens perception will unveil endomembrane trafficking role in immunity. Besides, addressing effectors targeting trafficking components to compromise defence responses could provide information to improve food security.

2 Material and Methods

2.1 Plant material and growth conditions

2.1.1 *Arabidopsis* thaliana lines

Arabidopsis thaliana lines genotypes belonging to the Columbia-0 (Col-0) ecotype were used as a control. The list of lines used in this study can be consulted in Table 2-1.

Table 2-1 List of *Arabidopsis thaliana* lines

Lines	AGI codes	Description	Reference
Col-0	-	Columbia-0, wild type	-
Col 0/FLS2p::FLS2-GFP (pCAMBIA 3000)	AT5G46330	Homozygous T4 transgenic line	(Beck *et al*., 2012)
Col 0/35Sp::GFP-LTi6B	AT3G05890	Homozygous T3 transgenic line	(Cutler *et al*., 2000)
min7 SALK_012013.54.75.x	AT3G43300	T-DNA insertion mutant	(Nomura *et al*., 2006)
ben1-2 SALK013761	AT3G43300	T-DNA insertion mutant	(Tanaka *et al*., 2009)
Col 0/UBQ10p::ARA7-mRFP (ubiquitin based vector)	AT4G19640	Homozygous T3 transgenic line	(Beck *et al*., 2012)
FLS2p::FLS2-GFPx min7 (pCAMBIA	AT5G46330 AT3G43300	Homozygous F3 crossing lines	Generated by Heidrun Häweker and Jenna Loiseau
UBQ10p::ARA7-mRFPx min7 (ubiquitin-based vector)	AT4G19640 AT3G43300	Homozygous F3 crossing lines	Generated by Heidrun Häweker

2.1.2 *Arabidopsis* seeds sterilisation

Seeds were gas sterilised in a desiccator with a beaker containing 97 mL sodium hypochlorite solution (Chlorine bleach) and 3 mL 37 % HCl. After a treatment time of 16 hours, seeds were dried in a sterile hood for 5 hours.

2.1.3 Plants grown on soil

Arabidopsis plants were grown on soil at 20 °C in a short-day photoperiod (10/14 hours) and 65 % humidity for 4-5 weeks. For seeds bulking, plants were transferred to a long-day photoperiod (16/8 hours). *Nicotiana benthamiana* plants were grown at 24 °C with 45-65 % humidity relative humidity under long-day conditions for 4-5 weeks.

2.1.4 Plants grown on plates

Sterile *Arabidopsis* seeds were sown on plates containing Murashige-Skoog (MS) salts medium (Melford Laboratories Ltdand) 0.8 % agar, incubated for 2 days at 4 °C and then grown at 20-22 °C with a long day photoperiod.

2.1.5 Plants grown on liquid

Arabidopsis seedling were grown in MS plates for 7-10 days as described above, and then transferred to liquid MS media containing 1 % sucrose in 24-well plates under sterile conditions and grown at 22 °C with a long day photoperiod.

2.1.6 **Crossing of *Arabidopsis* lines**

Individual flowers from mature *Arabidopsis* plants were emasculated using tweezers and fresh pollen from donor stamens was tapped onto each single stigma. Mature siliques containing F1 seeds were harvested. Genotyping of both parents for desired alleles were performed on plants to confirm success of crossing, and then were grown as described above and allowed to self-pollinate.

2.1.7 ***Arabidopsis* mesophyll protoplasts isolation**

Arabidopsis plants were grown for 4 weeks on soil under conditions previously described. Twenty-four leaves were detached using forceps and small stripes were cut using a razor blade. Leaves stripes were put in two 50ml falcon tubes containing each 25ml of a 55 C enzyme solution under gentle agitation (40 rpm) for 90 minutes. The enzyme solution containing protoplasts was filtered with a 50 mm nylon mesh into different round-bottom tubes and spinned down at 100 x g to pellet the protoplasts for 2 min. Pelleted protoplasts were suspended in 5 ml W5 solution by inverting the tubes very carefully. Protoplasts were kept on ice for 30 min before transfection. Protoplasts were spun down and resuspended in MMg solution (2-5 x 105/ml) before PEG transfection. 2ml of protoplasts were transferred into a at least 10ml round-bottom tube. 100µg of DNA were added and topped with 2ml of PEG solution and mixed by inverting the tube very carefully. Then it was incubated at 23 C for 10 min. Transfection was stopped by adding 5ml of W5 solution. Protoplasts solution was spun down at 100g for 3 min and the supernatant

was removed. 3-5ml W5 solution was used to resuspend the pellet and incubated 12-16 h at RT in the dark.

In this study, *Arabidopsis* mesophyll protoplasts were transfected with *RTL2p::FLS2-GFP* and imaged 16h after transfection .

Enzyme solution :

0.5 M sucrose, 10 mM MES-KOH (pH 5.7), 20 mM CaCl2, 40 mM KCl, 1% Cellulase (Onozuka R-10), 1% Macerozyme (R10), 0.1% BSA. Filter-sterilize and freshly use. Heat the enzyme solution at 55 C for 10 min (to inactivate proteases and enhance enzyme solubility) and cool it to room temperature before adding 10 mM CaCl2.

W5 solution:

0.1% (w/v) glucose, 0.08% (w/v) KCl, 0.9% (w/v) NaCl, 1.84% (w/v) CaCl2, 2 mM MES-KOH pH 5.7. Filter-sterilize and store at room temperature.

PEG solution (40%, v/v):

4 g PEG4000 (Fluka, #81240), 3 ml H2O, 2.5 ml 0.8 M mannitol, 1 ml 1M Ca (NO3)2 or CaCl2.

MMg solution :

0.4 M mannitol, 15 mM MgCl2, 4 mM MES (pH 5.7).

2.1.8 Generating stable *Arabidopsis* lines

2.2 Bacterial strains

Bacterial strains used for this study are listed in Table 2-2.

Table 2-2 List of bacterial strains

Species	Strain	Use	Resistance
Escherichia coli	DH5 a	Molecular cloning	-
Agrobacterium tumefaciens	GV3101	Plant transformation Expression in *N. benthamiana*	Rifampicin, Gentamicin
	GV3101pMP90	Expression in *N. benthamiana*	Rifampicin, Gentamicin Kanamycin
	GV3101pMP90; pSOUP	Expression in *N. benthamiana*	Rifampicin, Gentamicin

2.3 Culture media and reagents

2.3.1 Reagents and elicitors

Unless otherwise indicated, all reagents were purchased from Sigma-Aldrich.

Flg22 and elf18 peptides were purchased from EZ Biolab.

2.3.2 Culture media recipes

All recipes are scaled for 1L. Solutions were sterilized by autoclaving.

LB (Lysogeny broth):

10 g NaCl, 10 g tryptophane, 5 g yeast extract, pH 7.0. For solid medium, 10 g agar was added.

MS (Murashige Skoog):

4.3g MS salts, 0.59 g MES, 0.1 g myo-inositol, 1 mL of 1000x MS vitamin stock, 10 g sucrose, pH 5.7. For solid medium, 8 g Phyto agar.

2.3.3 **Antibiotics**

Antibiotics were used at the following final concentrations.

Carbenicillin: 100 µg/mL for bacteria

Gentamycin: 25 µg/mL for bacteria

Kanamycin: 50 µg/mL for bacteria and plants

Rifampicin: 50 µg/mL for bacteria

Tetracyclin: 15 µg/mL for bacteria

Spectinomycin: 100 µg/mL for bacteria

2.4 **Molecular biology**

2.4.1 **Molecular cloning**

In this study, I used the GATEWAY (Invitrogen) method for cloning. PCR fragments were separated on agarose gel and extracted. After cloning into entry vector, the insert was confirmed by colony PCR followed by DNA sequencing (GATC LIGHT*run* sequencing).

Table 2-3 List of vector backbone used in this study

Backbone	Use	Method	Resistance	Source/Reference
pGWB15 (Nter 3x ter HA)	Plant expression	GATEWAY	Hygromycin	(NAKAGAWA *et al*., 2007)
pGWB14(Cter 3x ter HA)	Plant expression	GATEWAY	Hygromycin	(NAKAGAWA *et al*., 2007)
pAM-pAT-GW (Nter Split YFP)	Plant expression	GATEWAY	Chloramphenicol	(NAKAGAWA *et al*., 2007)
pAM-pAT-GW (Cter Split YFP)	Plant expression	GATEWAY	Chloramphenicol	(NAKAGAWA *et al*., 2007)
pENTER-D-TOPO	Sub-cloning	GATEWAY	Kanamycin	Invitrogen

Table 2-4 Constructs used in this study.

Construct	Backbone	Use	Source/Reference
35Sp::GRF4-YFP	pGBW45	*N. benthamiana* expression	Cloned by Anja and Rico Brentke (intern students)
35Sp::GRF4-HA	pGBW45	*N. benthamiana* expression	Cloned by Anja and Rico (intern students)
FLS2p::AtFLS2-3xmyc-GFP	pCAMBIA	*N. benthamiana* expression	(Beck *et al*., 2012)
FLS2p::AtFLS2^{D997N}-GFP	pEarly Gate 103 - 35S	*N. benthamiana* expression	(Schwessinger *et al*., 2011)
35Sp::CLV1-eGFP	pK7FWG2.0	*N. benthamiana* expression	Obtained from C. Zypfel, The Sainsbury Laboratory.
35Sp::SOBIR1-eGFP	pBIN-KS	*N. benthamiana* expression	(Liebrand *et al*., 2013)
35Sp::Cf4-eGFP	pBIN-KS	*N. benthamiana* expression	(Postma. *et al*., 2016)
FLS2p::SlFLS2-myc-GFP	pCAMBIA 2300	*N. benthamiana* expression	(Mbengue *et al*., 2016)
35Sp::AtFLS2-YFPc	PAMPAT35S-GW-YFPc	*N. benthamiana* expression	Cloned by Malick Mbengue

35Sp::AtFLS2-YFPn	PAMPAT35S-GW-YFPn	*N. benthamiana* expression	Cloned by Malick Mbengue
35Sp::GRF4-YFPc	PAMPAT35S-GW-YFPc	*N. benthamiana* expression	Cloned by Jenna Loiseau
35Sp::GRF4-YFPn	PAMPAT35S-GW-YFPn	*N. benthamiana* expression	Cloned by Jenna Loiseau
35Sp::EFR-GFP-His	pEarly Gate 103 - 35S	*N. benthamiana* expression	Obtained from C. Zypfel, The Sainsbury Laboratory, England
35Sp::BRI1-GFP	pUB-C GFP	*N. benthamiana* expression	Obtained from C. Zypfel, The Sainsbury Laboratory, England
DEXp::HopM1-His	pTA7002	*N. benthamiana* expression	(Nomura *et al*., 2006)
DEXp::HopM1$_{1-300}$-His	pTA7002	*N. benthamiana* expression	(Nomura *et al*., 2006)
DEXp::HopM1$_{301-712}$-His	pTA7002	*N. benthamiana* expression	(Nomura *et al*., 2006)
UBQ10p::RFP-ARA7	pUBQ10 based vector	*N. benthamiana* expression	Obtained by Karin Schumacher, University of Heidelberg, Germany
UBQ10p::mCherry-MEMB12	pGREEN(NIGEL)	*N. benthamiana* expression	(Mbengue *et al*., 2016)
UBQ10p::VHA-a1-RFP	pUBQ10 based vector	*N. benthamiana* expression	Obtained by Karin Schumacher, University of Heidelberg, Germany
SYP61p::CFP-SYP61	Information not available	*N. benthamiana* expression	(Robert *et al*., 2008)
pRTL2::FLS2-GFP	pRTL2 based vector	*Arabidopsis thaliana*	Cloned by Michaela Kopischkhe-Stegmann

2.4.1.1 **GATEWAY cloning into pENTR vectors**

For GATEWAY cloning, all forward cloning primers contained a CACC extension at the 5'-end. First, PCR fragments were cloned into pENTR-D-TOPO (Invitrogen) by combining 0.5 µL plasmid DNA, 0.5 µL salt solution (Invotrogen), 2.5 µL insert DNA and 1.5 µL water. The reaction was incubated for 1 hour at room temperature and transformed into chemically competent cells.

2.4.1.2 **Gateway cloning into pDEST vectors**

To clone inserts from pENTR D-TOPO into a destination vector Table 2-3, the GATEWAY LR reaction was performed. Reactions contained 1 µL pENTR clone, 2 µL pDEST vector, 1 µL LR clonase II mix (Invitrogen), and were incubated 2 hours at room temperature and transformed into chemically competent cells.

2.4.2 **Transformation of plasmids into *E. coli* by heat shock**

Chemically competent cells were thawed on ice. For each transformation, 5 µL DNA were gently mixed with 50 µL chemically competent cells and incubated for 15 minutes on ice, followed by heat shock at 42 °C for 30-45 sec, and incubation on ice for 3 minutes. 1 mL of LB were added, and cells were incubated at 37 °C for 45 minutes and then 200 µL of cells and of 1/10 dilution in LB were both plated on selection plates (LB with appropriate antibiotics) and grown ON at 37 °C.

2.4.3 Transformation of plasmids into *A. tumefaciens* by electroporation

Electro-competent cells were thawed on ice. For each transformation, 3 µL DNA were gently mixed with 50 µL electro-competent cells in a 1mm electroporation cuvette. Electroporator (Bio-Rad0 set as follows: 1800 V with a capacity of 25 µF over 200 Ω resistance. After adding 500 µL LB pre-heated at 28 °C, cells were incubated with shaking at 28 °C for 1 hour and plated on selection plates (LB with appropriate antibiotics), and grown for 2-3 days at 28 °C.

2.4.4 DNA methods

2.4.4.1 Isolation of plant genomic DNA

Plants genomic DNA was isolated for genotyping and cloning purposes using the “Edward’s buffer method” (ref). Three 7-10-day old *Arabidopsis* seedlings were ground in 400 µL extraction buffer (200 mM Tris-HCl (pH 7.5), 250 mM NaCl, 25 mM EDTA, 0.5 % SDS) and centrifuge for 5 min at 14, 000 g. Supernatant was transferred to new tubes and 1:1 volume of isopropanol was added. The solution was vortexed and centrifuged as before. The remaining pellet was washed with 70 % ethanol, air-dried at room temperature and dissolved in 100 µL of sterile water.

2.4.4.2 Plasmid DNA isolation from *E. coli*

Cultures of single *E. coli* colony in 5 mL LB supplemented with the appropriate antibiotics were pelleted by 1 min centrifugation at 14, 000 g. plasmid DNA

was extracted using the Necleospin Plasmid Miniprep Kit (QUIAGEN) according to the manufacturer's instructions, Isolated DNA was dissolved in 30 uL water.

2.4.4.3 **DNA extraction from Agarose gels**

DNA fragments were excised from gel under UV light. DNA was extracted using the NucleoSpin Gel and PCR clean-up (Macherey-Nagel) following the manufacturer's instructions.

2.4.4.4 **DNA sequencing**

Each reaction was composed of 2.5 uL DNA c, 2.5 uL of primer (10 µM stock) and 5 uL water. Sequencing was performed by GATC Biotech AG (Cologne Germany) and results analysed using the vector NTI software (Invitrogen).

2.4.5 **PCR methods**

2.4.5.1 **General PCR conditions**

Primers used for this study were purchased from Sigma-Aldrich and used in 0.5 uM final concentration. dNTPs were purchased from Invitrogen and used in 200 µM final concentration. Cloning and genotyping PCRs were performed using the proof-reading Phusion High-Fidelity DNA polymerase (NEB) or the Q5 polymerase (Thermo fisher), respectively with the supplied reaction buffers. Reactions were incubated in a G-Storm Thermocycler (Life Science Research) programmed as described in Table 2-5.

Table 2-5 Programme for cloning PCRs

Step	Temperature	Duration	Number of Cycles
Initial denaturation	98 °C	3 min	1
Denaturation	98 °C	30 sec	30-35
Annealing	50-60 °C *	30 sec	
Elongation	72 °C	0.5-X min**	
Final extension	72 °C	5 min	1

* Annealing temperature was set according to the melting temperature of the primer pair.

** Elongation time was set according to the length of the PCR fragment (30 sec per 1 Kb for phusion polymerase)

Table 2-6 List of primers used in this study.

Primer name	Primer sequence (5'-3')
Molecular cloning	
GRF4 F_GW	CACCATGGCGGCACCACCAGCATC
GRF4 R_noStop	GATCTCCTTCTGTTCTTCAGCAGGC
M13_F	GTAAAACGACGGCCAG
M13_R	GGAAACAGCTATGACCATG
FLS2_Forward	TGGAGCTGATGACGAAACAG
Genotyping	
35S_F	ATGACGCACAATCCCACTATCCTTCGCA
GFP_R	
LBb1.3	ATTTTGCCGATTTCGGAAC
SALK_012013_	
SALK_013761	TGGAAAGTGAAATTGGTGAGC CAAGGATTCTTCTCTGCATGG
MIN7_F1	TTCTTCTCTGCTGTCAGGCTC
MIN7_R1	TTGACCAACGAATTTTTCACC
MIN7_F2	
MIN7_R2	
HopM1_F	ATGATCAGTTCGCGGATCGGC
HopM1_R	ACGCGGGTCAAGCAAGCCCTC
$HopM1_{1-300}$_R	CCCTGCACCTTTCCAGCCACC
$HopM1_{301-712}$_F	CTGGTCTCGGGAATCGTGTC

2.4.5.2 **Colony PCR**

A small part of a single *E. coli* or A. *tumefaciens* colony was resuspended in 10 uL of PCR reaction mixture. Colony PCR were performed using Q5 polymerase (Thermo Fisher). Reactions were run in a G-Storm Thermocycler (Life Science Research) programmed as described in Table 2-7.

Table 2-7 Programme used for colony PCR

Step	Temperature	Duration	Number of Cycles
Initial denaturation	98 °C	3 min	1
Denaturation	98 °C	30 sec	30-35
Annealing	50-60 °C *	30 sec	
Elongation	72 °C	0.5-X min**	
Final extension	72 °C	5 min	1

* Annealing temperature was set according to the melting temperature of the primer pair.

** Elongation time was set according to the length of the PCR fragment (30 sec per 1 Kb for phusion polymerase)

2.4.6 **RNA methods**

2.4.6.1 **Isolation of RNA from plants and cDNA**

RNA was isolated from soil-grown *Arabidopsis* or *N. benthamiana* plants or *Arabidopsis* 2-week-old seedling grown in liquid MS medium. Total RNA was extracted using RNeasy kit (Qiagen). Briefly, leaves were collected in Eppendorf tubes, frozen in liquid nitrogen and ground to a fine powder using a rotating drill (pre-chilled in liquid nitrogen). 100 mg was used for total RNA

extraction following the manusfacturer's instruction. For the elution step, the manufacturer's instruction recommends eluting in 100 μg elution buffer but I re-suspended the RNA in 30-50 μg RNase-free water to concentrate the RNA. DNAse was treated according to the DNase I RNase-free protocol (Roche). 10% SDS and proteinase K were added to the RNA and the solution incubated for 15 min at 42 °C. RNA was then purified using the RNeasy MinElute cleanup kit (Qiagen) and eluted in RNase-free water. Total RNA was quantified with a Nanodrop (Thermo Scientific).

2.4.6.2 **Reverse transcription PCR**

First-strand cDNA was performed using 30 μg total RNA with SuperScript II transcriptase (Invitrogen) and oligo (dT 18)-primers, according to the manufacturer's instructions.

2.4.6.3 **DNA electrophoresis**

Presence and length of DNA fragments after PCR were confirmed using electrophoresis. PCR products were mixed with 6x loading dye and in gels containing 1% agarose diluted in TBE and ethidium bromide. DNA migration was tested in an electrophoresis tank filled with TBE buffer applied with 100 V for 30 minutes. Fragment length was estimated using the 1 kb DNA ladder (40 ng/μl from NEB) loaded on the same gel. DNA was visualised by exposing the gel to UV light in a UV transilluminator from BIO-RAD.

2.5 Protein work

2.5.1 Protein extraction and IP experiments

2.5.1.1 Protein extraction for total extract

Three leaves disks were excised from soil-grown 4-week old plants with a cork borer No. 3 (ø 6.5mm) and put in a 2 mL Eppendorf tube containing 2 stainless beads, then kept at – 80 °C. Plant material were grinded in liquid nitrogen with a tissue lyser (TissueLyser II, Qiagen) and for total extract preparation, sample were mixed with 150 µL of 1X SDS Sample Buffer and 1mM of freshly add protease inhibitors (P9599; Sigma-Aldrich), 1 mM PMSF and 5 mM DTT. Extracts were cooked for 10 minutes at 75 °C then centrifuged. Proteins were separated by SDS/PAGE 10% and analysed by Western blot.

2.5.1.2 Protein extraction for Co-immunoprecipitation

Plant material were grinded in liquid nitrogen with pre-chilled pestle and mortar and transferred to pre-chilled 50 ml Falcon tubes. To normalise the amount of protein between sample, 5 mL of solubilisation buffer was added to 1.5 mg of grinded tissue and was incubated on ice for 30 minutes. Extracts were then centrifuged for 30 minutes at 16, 000 g and 4 °C (Sorvall RC-5B centrifuge with SM-34 rotor). Supernatants were filtered through Bio-Spin exclusion columns (Bio-Rad) into 50 mL Falcon tubes at 4 °C. Filtrates was then used for total extract and for Co-immunoprecipipatation.

For total extract preparation used as INPUT, 50 µL of filtrates was mixed with 50 µL 3 X SDS sample buffer and 5 mM DTT.

For Co-immunoprecipitation, 1.5 ml of filtrates were incubated with 15 µL of GFP-Trap beads (Chromotek) for 1h30 at 4 °C with gentle agitation. I recommend using an incubation time inferior or equal to 2h when immunoprecipitation FLS2-GFP because I observed its degradation when incubation was superior at 2h. Beads were collected by centrifugation for 30 seconds at 500 g and washed 3 times with solubilisation buffer + 0.2% Igepal (SiGMA). After the last wash, the remaining supernatant was carefully removed with a needle fitted on a syringe. Proteins were eluted from the beads by adding 50 µL 1X SDS sample buffer and 5 mM DTT. Proteins were denatured by incubation for 10 minutes at 75 °C, centrifuged for 10 minutes at 8,000 g. At this point, extract can be directly loaded on polyacrylamide gel for separation or kept at - 20°C up to six months (protein degradation can occur when sample is kept more than six month). Proteins were separated by SDS/PAGE 10% and analysed by Western blot.

2.5.1.2.1 **Solubilisation buffer**

25 mMTris, 15% (v/v) glycerol, 2% (w/v) SDS, 2% (v/v) protease inhibitor cocktail (P9599; Sigma-Aldrich), 2% (v/v) phosphatase inhibitor mixture 2 and 3 (P0044 and P5726; Sigma-Aldrich), 1 mM PMSF, and 5 mM DTT.

2.5.1.2.2 **SDS sample buffer (3X)**

150 mMTris HCL pH 6.8; 50% (v/v) glycerol; 6% SDS (w/v) ; 0.015% Bromophenol Blue (w/v); 5 mM DTT (added fresh), PMSF (added fresh), protease inhibitor (P9599; Sigma-Aldrich, added fresh).

2.6 **Biologicals assays**

2.6.1 **Chemicals and treatment**

Flg22 and elf18 (EZBiolab) 100 mM stock solution were prepared in water and kept at – 20°C. All chemicals were purchased from Sigma-Aldrich, if not otherwise indicated, and used as previously described (Beck *et al*., 2012). Briefly, chemicals were prepared at the following concentrations: BFA (10 mM in ethanol, working solution 30 µM), ConCA (10 mM in DMSO, working solution 10 µM). Detached two-week old *Arabidopsis* cotyledons were vacuum infiltrated for 5 minutes in inhibitor solutions, followed by 55 minutes incubation at room temperature. Flg22 (working solution 10 µM) was added to the inhibitor solutions, and imaging was performed at different time points after flg22 treatment. For *N. benthamiana* analysis, flg22 (working solution 100 µM) was infiltrated in an agro-infiltrated leaf by a needless syringe and incubated 60-80 min at room temperature and imaged as previously (Loiseau and Robatzek, 2017; Mbengue *et al*., 2016).

AICAR (Sigma-Aldrich) treatment was performed as described before (Lozano-Durán *et al*., 2013). Briefly, detached two-week-old *Arabidopsis* cotyledons were vacuum infiltrated for 5 minutes in AICAR solutions, followed by 1h55 min incubation at RT. Flg22 (working solution 1 µM) was added to the AICAR solution, and imaging was performed at different time points after flg22 treatment. For *N. benthamiana* analysis, agro-infiltrated leaves were incubated in flg22 or elf18 (working solution 10µM) at room temperature for 15, 30 and 60 min.

2.6.2 **Ligand-induced internalisation**

Freshly prepared MAMP solution were prepared at the desired concentration and applied 60 or 80 minutes prior to microscopy observation on *Arabidopsis* seedling or Agro-infiltrated *Nicotiana Benthamiana* leaves respectively. Cotyledons were dipped into solution and vacuumed for five minutes and left at RT whereas *Nicotiana Benthamiana* leaves were hand-infiltrated with MAMP solution.

2.6.3 **Seedling growth inhibition assay**

Seedling growth inhibition assays were performed as described in (Nekrasov *et al*., 2009). In brief, four-day old *Arabidopsis* seedlings were grown in liquid MS medium containing 1% sucrose supplemented with 100nM flg22 or not (mock). Twelve seedlings were weighed individually using a scale linked to a computer at 5 and 18 days after treatment.

2.6.4 **OPERA**

Cotyledons from soil-grown F3 seedlings were imaged using the spinning disc high-throughput automated Opera microscope (Perkin-Elmer Cellular Technologies) as described (Beck *et al*., 2012) and were analysed with the image processing software Acapella (version 2.0; Perkin-Elmer) with an algorithm previously described (Beck *et al*., 2012) for quantification of endosomal numbers.

2.6.5 **Confocal microscopy**

Subcellular localisation of fluorescently tagged proteins transiently expressed in *N. benthamiana*, was determined by confocal laser-scanning microscopy with a DM6000B/TCS SP5 microscope (Leica). Four-week-old *N. benthamiana* plants were used for transient expression assays as described before (Loiseau and Robatzek, 2017; Mbengue *et al*., 2016).

2.6.6 **Quantification of endosomes in *N. benthamiana***

Quantification of endosomes was performed as described previously (Loiseau and Robatzek, 2017). Briefly, maximum projections of 10 x 1 μm slices were opened and processed with FIJI open-source platform using the built-in BioFormats plug-in. Spots were manually quantified using the multipoint tool, informations were extracted from the analyze tab and saved in a spreadsheet software.

2.6.7 **Immunodetection**

For GFP detection, the rabbit anti-GFP (Roche; 1:1,000 dilution) primary antibodies, followed by the secondary anti-rabbit, coupled to HRP (Sigma-Aldrich; 1:20,000 dilution) were used. For HA detection, the anti-HA-HRP (Sigma-Aldrich 1:2, 000 dilution) conjugated antibody was used. For His detection, the anti-His-HRP (Sigma-Aldrich 1:2, 000 dilution) conjugated antibody was used. HRP was detected using ECL reagents (Pierce ECL substrate; Thermo Fisher Scientific) and a CCD camera (ImageQuant LAS 4000 series, GE healthcare).

2.6.8 **MAPK activation**

For *N. benthamiana*, MAPK activation by flg22 was done essentially as described previously (Schwessinger *et al*., 2011). Briefly, total extracts form *N. benthamiana* were denatured for 10 min at 75 °C before separation on 10% SDS/PAGE gels and transfer to PVDF membrane (Immobilon-P; EMD Millipore) using the Bio-Rad semidry transfer apparatus, following the manufacturer's instructions. The anti-p42p44 (Cell Signaling Technology; 1:1,000 dilution) primary antibodies, followed by the secondary anti-rabbit, coupled to HRP (1:20,000 dilution; Sigma-Aldrich), were used for protein detection. HRP was detected using ECL reagents (Pierce ECL substrate; Thermo Fisher Scientific) and an SRX-101A film developer (Konica Minolta).

2.6.9 **TAMRA-flg22 uptake**

TAMRA-flg22 uptake was performed accordingly to previous study in *Arabidopsis* lines (Mbengue *et al*., 2016). Briefly, four-day-old *Arabidopsis* seedling grown on MS plates were incubated with 20 μM TAMRA-labelled flg22 prepared in MS solution in a 2ml Eppendorf tube for 20 seconds, then, washed twice in liquid MS for one minute. Samples were image immediately for 1h.

2.6.10 **Statistical analysis**

Statistical significances based on t-test and ANOVA analyses were performed with excel software.

3 Detection and Analyses of Endocytosis of Plant Receptor Kinases

This chapter is based on a book chapter I co-authored with Dr Silke Robatzek.

3.1 Introduction

While working on my thesis project, several methods were available on the study of receptor internalisation. If all were suitable different materials (developmental stage, location in the cell and timing) were used (Choi *et al*., 2013; Mbengue *et al*., 2016; Smith *et al*., 2014a) and it occurred to me that a standardise method was necessary to facilitate comparison and understanding of data between laboratories. Therefore, I sat up a standardized method to study PRRs internalisation based on current methods available and on observations/experiments I made. I have improved the method and it is now available as a book chapter co-authored with Dr Silke Robatzek for other scientists to use.

Specially, since endosomes are very dynamic structures and a quantitative parameter it was important to analyse a defined area to be sure data were comparable between samples. Hence, I selected parameters, that are crucial to analyse endosomes in transient systems such as volume, number of maximum projections, zoom, laser intensity and sat up standard to use as a reference for flg22-induced internalisation of FLS2-GFP.

In this chapter, we provide instructions for transient expression of FLS2-GFP in *N. benthamiana* leaves and how to monitor FLS2-GFP localisation by confocal microscopy. We describe how to ensure correct FLS2-GFP expression and imaging of FLS2-GFP fluorescent signals and provide tools for

quantification of endosomes from images. Although we focus on FLS2-GFP in this chapter, this method can be broadly applied for imaging other fluorescent tagged receptor kinases in *N. benthamiana* (Postma. *et al*., 2016), and combined with co-expression of subcellular markers, pathogen virulence proteins and genetic interference to functionally dissect their dynamic sub-cellular localisation.

Fluorescence confocal microscopy is essential to identify the sub-cellular locations of receptor kinase trafficking routes. The investigation of trafficking components role in PTI is ongoing, thus, PRRs localisation can be used to resolve trafficking changes after microbial perception. Besides, it can be used in screens to identify pathogen effectors that target these trafficking routes for virulence promotion.

To advance the time-intensive limitations that typically occur from generating stable transgenic plants, *Agrobacterium tumefaciens*-mediated transient transformation of *Nicotiana benthamiana* leaves is a powerful system for simple and fast genetically encoded expression. This approach is routinely used e.g. to monitor bimolecular fluorescence complementation (Postma. *et al*., 2016), and assess the localisation and function of virulence proteins secreted by pathogens to suppress plant defences (Bozkurt *et al*., 2011, 2015; Dagdas *et al*., 2016). We have adapted heterologous expression in *N. benthamiana* leaves combined with confocal microscopy to dissect the endocytic routes of pattern recognition receptor kinases tagged with fluorescent proteins. Co-expression with different fluorescently tagged

markers of defined subcellular compartments, e.g. plasma membrane (PM), Golgi, trans-Golgi network (TGN), and multivesicular bodies (MVBs), allows the probing of pattern recognition receptor localisation along distinct trafficking routes and during infection (Postma. *et al*., 2016). In addition, genetic interference by overexpressing dominant negative variants of trafficking regulators, virus-induced and RNAi-mediated gene silencing allows the identification of molecular determinants involved in ligand-induced endocytosis of pattern recognition receptor kinases (Chaparro-Garcia *et al*., 2015; Frescatada-Rosa *et al*., 2015; Postma. *et al*., 2016) . Likewise, co-expression of pathogen virulence proteins can be used to interfere with receptor kinase localisation (Chaparro-Garcia *et al*., 2015), thus providing insights into the mechanisms by which pathogens re-program plant cellular responses. For example, FLS2 endocytosis can be inhibited by co-expression of *Phytophthora infestans* AVR3a, a virulence protein interacting with *N. benthamiana* Dynamin-related protein 2 (DRP2) (Chaparro-Garcia *et al*., 2015).

The following material is necessary to start the experiment. The age of plants and growth conditions presented here are the one showing best results.

3.2 **Materials**

3.2.1 **Samples**

- Four weeks-old *Nicotiana benthamiana* plants (see Figure 3-1) grown on soil under 16 hrs light at 22°C / 80% humidity.

- *pFLS2:FLS2-3xmyc-GFP* cloned in pCAMBIA2300 (Robatzek *et al*., 2006) Table 3-1.

- *Agrobacterium tumefaciens* strain GV3101 carrying pMP90.

3.2.2 **Experiment/Treatments**

- LB Medium (Tryptone 10g/L Merck 1.07213.1000, yeast extract 5g/L Merck 1.03753.0500, Sodium Chloride 10g/L Sigma-Aldrich 31434-1KG-R).

- Antibiotics: Rifampicin (Melford Laboratories Ltd, R0146, prepare stock solution at 50mg/L in DMSO), Gentamycin (VWR/Applichem, A1492.0008, stock solution at 30mg/L in water), and Kanamycin (Melford Laboratories Ltd, K0126, stock solution at 50mg/L in water); all are kept at -20°C.

- 3′,5′-Dimethoxy-4′-hydroxyacetophenone (acetosyringone; Sigma-Aldrich, D134406-5G; stock solution of 250 mM in DMSO, use 100 µM final concentration in water).

- flg22 peptide: QRLSTGSRINSAKDDAAGLQIA (custom produced; EZbiolabs/USA).

MW=2,272.5 g/l.

3.3 **Confocal Microscopy**

3.3.1 **Sample Mounting**

Samples are mounted in water or 100 µM flg22 solution for mock or for treated conditions, respectively. Leaf disks are excised from *A. tumefaciens*-infiltrated

leaves with a cork borer No. 3 (ø 6.5mm) and mounted between a cover glass (22x50 mm, Slaughter Ltd, R&L 631 0137) and glass microscope slide (76x26mm SKAN LTD).

3.3.2 **Image acquisition**

- Confocal laser scanning microscope.

- Lasers: Argon ion, DPSS 561.

- Detectors coupled with cameras.

- Scan parameters: Acquisition: *xyz* for single plane and for z-sectioning, and *xyt* for time lapse movies. Format: 512x512 pixel, scan speed 400Hz (400 lines/s); Pinhole size as default at 1 Airy Unit (AU). Averaging: line 1x, frame 1x (see Notes 1).

- Objectives: Start with a low magnification to find the sample (e.g. 10x), then switch to higher magnification to detect spots (63x).

- Zoom factor: 2x zoom, image size 122 µm x 122µm.

3.3.3 **Image Processing**

1. EndoQuant

EndoQuant is a modification of EndomembraneQuantifier (Beck *et al*., 2012), runs on the PerkinElmer Acapella image analysis software package, and can be used for spot detection and quantification for standard confocal images (Postma. *et al*., 2016).

2. FIJI

FIJI ('FIJI Is Just ImageJ') is an open-source platform for biological image analysis that comes pre-loaded with an extended set of used plugins:

FIJI homepage: http://pacific.mpi-cbg.de/wiki/index.php/Fiji

ImageJ homepage: http://rsb.info.nih.gov/ij/

3.4 **Methods**

General workflow: the general workflow; sample preparation and treatments, image acquisition and image processing are represented in the Figure 3-1.

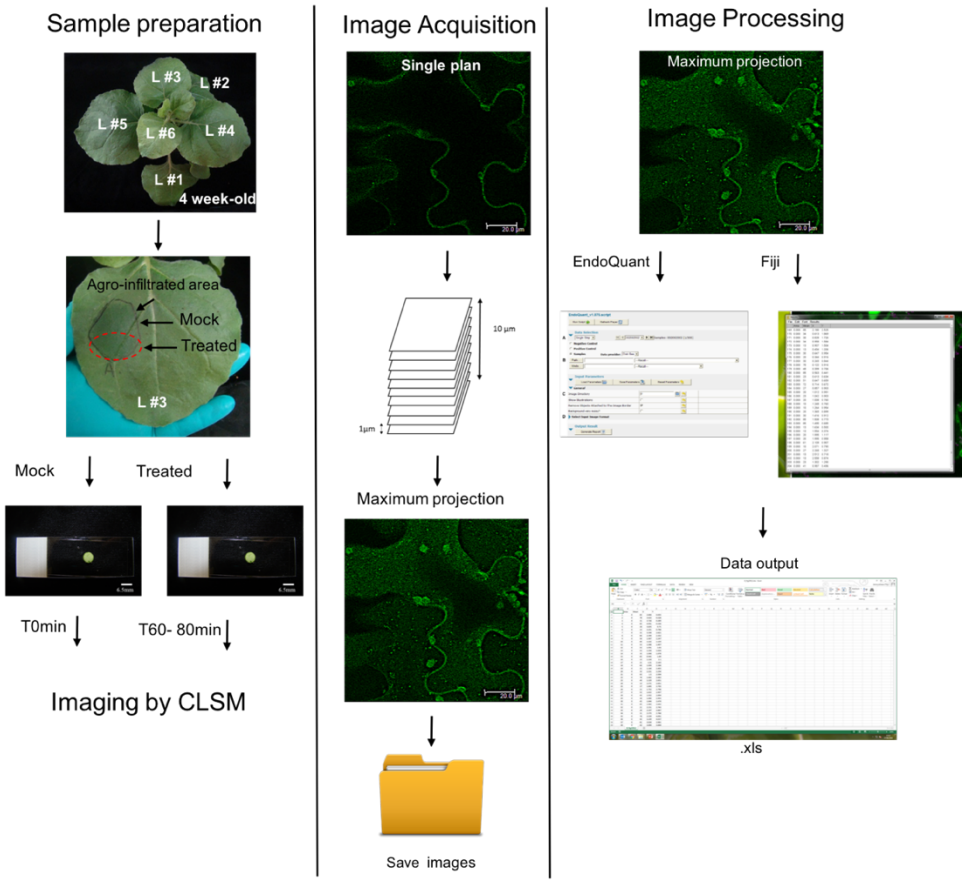

Figure 3-1 General work flow for image acquisition and endosomes quantification.

For sample preparation, leaf disks are mounted on microscopy slides and cover glass in water and 100 µM flg22 for mock and treatment respectively. Sample treatments are performed by infiltration in the epidermal tissue before mounting process. The Image acquisition is performed with a confocal laser scanning microscope (CLSM). The generated files are analysed with EndoQuant or with Fiji. The *Data output* is generated in table format. Adapted from (Loiseau and Robatzek, 2017).

3.4.1 **Samples**

1. For transient expression of FLS2 fused to the green fluorescent protein (GFP) in *N. benthamiana*, the pCAMBIA2300 plasmid carrying pFLS2:FLS2-3xmyc-GFP is introduced into Agrobacterium tumefaciens GV3101 by

transformation. Leaves of *N. benthamiana* will be used for transient transformation. Imaging is performed on leaf discs.

2. Inoculate 10 mL LB medium supplemented with antibiotics (Rifampicin 50 mg. L^{-1}, Gentamycin 30 mg. L-1, Kanamycin 50 mg.L-1) with A. tumefaciens GV3101 carrying pFLS2:FLS2-3xmyc-GFP and incubate for 16h shaking at 28°C.

3. Centrifuge the bacterial culture for 10 min at 5000 rpm. Remove supernatant and re-suspend the pellet in 5 ml dH_2O (see Notes 2).

4. Take 100 µl of bacterial suspension and dilute 1/10 in water to measure OD_{600}.

5. Prepare 5-10 ml of bacterial suspension at final OD_{600}=0.1-0.2 in dH20 and add 100 µM 3′,5′-Dimethoxy-4′-hydroxyacetophenone (acetosyringone). Incubate for 1h at RT in the dark (see Notes 3).

6. Turn leaf #3 or #4 of a four weeks-old N. benthamiana plant (see Figure 3-1) to face its abaxial side upwards and pinch the leaf carefully with a needle.

7. Where the leaf has been pinched, carefully inject the bacterial suspension (‘infiltration’) using a needleless syringe and fill about 0.5 ml and infiltrated leaf.

8. Mark the inoculated area with a soft permanent marker on the leaf apical side and incubate plants in growth chamber for 1-3 days (see Notes 2, 3, 4 and 5).

9. To observe localisation of non-liganded and liganded, activated FLS2-GFP in *N. benthamiana*, perform co-localisation studies (see Table 3-2). Organelle markers are heterologoulsy co-expressed by A. tumefaciens-mediated transient transformation as described above. To express several constructs (up to four), pre-mix Agrobacterium suspensions to infiltrate each construct at OD_{600} = 0.1-0.4 (see Notes 5).

3.4.2 **Treatment**

1. Non-liganded FLS2-GFP resides predominantly in the plasma membrane (Choi *et al*., 2013) and co-localises with the plasma membrane marker ACA8-mCherry (Mbengue *et al*., 2016).

2. Liganded, activated FLS2-GFP is detected at endosomes around 80-90 min after flg22 treatment and observed as mobile spots. Endosomal FLS2-GFP co-localises with mRFP-SYP61 at 90-120 min after flg22 treatment, and localises to RFP-ARA7/RabF2b-positive late endocytic compartments from 30 up to 200 min after flg22 treatment (Choi *et al*., 2013). Additional markers can be used to trace FLS2-GFP endocytic trafficking (see Notes 10), (Dettmer *et al*., 2006; Geldner *et al*., 2009; Spallek *et al*., 2013).

3. To validate that the observed mobile spots are bona fide endosomes and not e.g. secretory vesicles, co-localisation experiments using the Golgi marker mCherry-MEMB12 should be negative (Geldner *et al*., 2009; Postma. *et al*., 2016).

4. FLS2-GFP endocytic trafficking can be genetically dissected using transient silencing approaches, overexpression of dominant negative trafficking regulators, and co-expression of pathogen virulence proteins (see Table 3-3; (Chaparro-Garcia *et al*., 2015; Choi *et al*., 2013; Postma. *et al*., 2016)). For example, the *P. infestans* effector AVR3a has been identified to target N. benthamiana DRP2 (Chaparro-Garcia *et al*., 2015). In agreement with ligand-induced endocytosis depending on DRP2b in *Arabidopsis* (Smith *et al*., 2014a), co-expression of AVR3a impaired FLS2 endocytosis (Chaparro-Garcia *et al*., 2015). Consistently, using a hairpin-based RNA-mediated silencing approach, FLS2 endocytosis was affected upon knockdown of N. *benthamiana* DRP2 expression (Chaparro-Garcia *et al*., 2015). This demonstrates that heterologous expression in *N. benthamaina* leaves is a suitable system to dissect endocytic trafficking of receptor kinases.

3.4.3 **Experiment/Treatment**

1. Excise leaf disks with a cork borer No. 3 (ø 6.5mm) from the inoculated area. Drop 70 µl of dH_20 in the middle of a cover glass. Using tweezers to grasp the disk edge, place a single leaf disk on the liquid drop with the abaxial-surface facing down. Add two drops of 60 µl water at each side of the disk. Cover with microscope slide. Carefully invert the mounted leaf disk. Abaxial leaf side is now facing up. Fill the remaining space between slide and cover glass with water. Image samples to observe FLS2-GFP at the plasma membrane.

2. For flg22 treatments, pinch the abaxial leaf side of the inoculated area close to where it has been done before for bacterial inoculation. Using a 1 ml needleless syringe, infiltrate ca. 0.1 ml of 100 µM flg22 solution filling an area about ø 3.5cm. Mark the infiltrated area on the apical leaf side. Incubate at RT for ca. 70-90 min. Then, excise leave disks with a cork borer and mount the disks as described above in 100 µM flg22 solution instead of water, to ensure continued treatment. Image samples between 80-200 min of flg22 treatments to observe FLS2-GFP positive endosomes.

3.5 **Confocal microscopy**

3.5.1 **Image acquisition**

1. Excitation of the samples is performed with the 488 nm argon laser for GFP and emission is collected between 495-550 nm. For co-localisation studies and use of other fluorescent proteins (see Table 3-1)

2. A water immersion 63x/NA1.20 objective is used for subcellular imaging of FLS2-GFP on the abaxial side of the sampled leaf disk. Depending on the microscope lasers, detectors, camera and/or resolution, unspecific signals may be recorded. Therefore, when setting up the system, it is critical to image N. benthamiana leaves that were inoculated with A. tumefaciens not carrying a vector with FLS2-GFP, preferably an empty vector. Following the microscopy instructions, set up the imaging parameters such that epidermal cells are clearly detected and in focus when viewing the bright field channel, and such that autofluorescence of chloroplasts is detected in the autofluorescence

control channel (e.g. 700-800 nm), but no or negligible signal should be observed in the GFP channel. Using these settings, start imaging discs from FLS2-GFP-expressing N. benthamiana leaves. It might be necessary to adapt the image acquisition settings in order to optimize detection in the GFP channel, but when imaging leaf discs that were not transformed with FLS-GFP, no or negligible signal should be observed using the same settings (see Notes 6, 7).

3. Epidermal puzzle-shaped cells are visualized. In the acquisition mode, select xyz to allow acquisition of z-stacks. Choose scan parameters: Tick the pinhole box to control the image contrast, format 512x512 px, 400Hz speed, line averaging 1x and frame averaging 1x (see Notes 11). Unidirectional scanning is best for image quality, avoiding artefacts that originate from interlacing after bidirectional scanning. Select cells with good GFP signal at the plasma membrane (see Figure 3-1; see Notes 8 and 9). Perform a 2x zoom (area size: 122 µm x 122µm). Take a z-stack from to the top of the cell downward (see Notes 9). Take ~10 z-sections that are 1 µm separated (see Notes 9). FLS2-GFP positive endosomes can be observed as mobile spots (see Notes 6) and co-localise with endosomal markers (see Table 3-2). To ensure that the signal observed is truly GFP, perform a lambda wavelength scan according to microscopy instructions.

4. Save your experiments (format depends on microscope manufacturer).

3.5.2 **Image processing**

Confocal images (see section 1 below for image format) can be processed automatically using EndoQuant or manually with FIJI.

1. EndoQuant

EndoQuant is a modification of EndomembraneQuantifier (Beck *et al*., 2012), runs within the PerkinElmer Acapella image analysis software package, and can be used for spot detection and quantification for standard confocal images (Postma. *et al*., 2016).

2. Generate maximum projections of confocal z-stacks and save as PNG, TIFF, JPG or BMP files.

3. Place all resulting images to be analysed in a single folder.

In order to run EndoQuant, you need the PerkinElmer Acapella image analysis program.

4. Start Acapella

5. Open EndoQuant, for example by dragging the .script file onto the open Acapella screen.

6. Set ‘Data Selection’ to ‘Single Step’

7. Set ‘Path’ and ‘Image Directory’ to the location of the folder with images to be analysed.

8. Set ‘Select Input Image Format’ to match the format of images to be analysed.

It is recommended to switch on ‘Remove Objects Attached to The Image Border’ and switch off ‘Background very noisy?’, but these can be adjusted based on preference.

9. Click ‘Run Script’

EndoQuant generates comma-separated value .csv files, which can be opened using MS Excel or another spreadsheet software. For each analysed confocal micrograph, EndoQuant also generates images that show which spots were detected, which size they were classified as (red: big, yellow: medium, green: small), and how they were numbered. These images can be used as a visual evaluation of the quality of spot detection.

10. Go to the automatically generated ‘results’ folder in the image folder that was analysed

11. Open ‘overall results.csv’ and separate values in column A based on symbol ‘#’.

In the resulting spreadsheet, the column ‘Endosome_No’ can be found, and this data is used as a value for number of endosomes in each individual confocal micrograph.

The detected spots are further separated into three size classes for more detailed information on size distribution.

‘Endosome_No’ values can be used for further statistical data analysis.

2. FIJI

FIJI is an open-source platform for biological-image analysis and can read most confocal microscope data formats using the built-in BioFormats plugin. Maximum projections are opened and processed with FIJI.

1. Launch the FIJI software and open the saved experiment and process as a maximum projection.

2. Open the maximum projection in FIJI to analyse and quantify spots.

3. Within the FIJI menu, right click on the multi point tool. A window will appear that allows setting the parameters of the selection (type: circle, color: magenta and size: large; tick the box label points).

4. Select and click on spots/endosomes with pointer. Numbers appear as you click (selection).

5. Upon completion of manual spot detection, extract the information. In the Analyse tab click on ‘Measure’ or press Ctrl+M: a table will appear in a new window. Number of spots and the corresponding coordinates will be listed in the table. In the ‘File’ tab of the results window clicks on save as all file *.*. The table is saved and can be later open with Excel or another spreadsheet software.

6. To save the circled spots (selection) on the maximum projection as an image, the selection created must be added to the maximum projection as an

overlay (Image overlay, add selection or CTRL+ B) and the overlay must be flattened (Image, Overlay, Flatten or Ctrl + Shift + F).

3.6 **Notes**

1. To enhance FLS2-GFP signals and reduce noise, background, or blurry signals, scan parameters can be adjusted (e.g. change to format 1024x1024 px, 200Hz speed, line average 3x). However, enhanced laser power or longer local exposure can damage leaf cells, which in turn induces the accumulation of autofluorescing compounds recorded as false-positive signal, introduce stresses that may cause aberrant receptor localisation, and bleach the GFP signal.

2. Interpretation of localisation or co-localisation results must be done cautiously and insure that the tag does not affect the protein function. As an example c-terminally tagged BAK1 is not functional in PTI signaling but functional in BR signalling (Ntoukakis *et al*., 2011). Testing functionality of tagged protein function can be performed. For instance, NbSERK3a/b can be silenced and functionally complemented with untagged AtBAK1 (Postma. *et al*., 2016).

3. Expression levels and accumulation of the full-length fluorescent tagged FLS2-GFP (other receptor kinase fluorescent fusions, and organelle marker fluorescent fusions; see Tables 1 and 2) should be validated by immunoblot analysis for different OD_{600} (0.1 to 0.5) and time points after inoculation (e.g. 1-3 dpi) prior to confocal microscopy.

4. Transient expression can trigger cell death symptoms. To avoid triggering cell death, remaining LB medium and antibiotics should be removed by a second wash.

5. To improve bacterial inoculation, plants can be watered or humidified 1-2 h prior the infiltration.

6. To enhance transient expression of p35S-driven constructs, the Plant Viral Protein p19 silencing suppressor (Lu, Y *et al*., 2012) can be co-inoculated at OD_{600}= 0.2.

7. Autofluorescence of chloroplasts is collected between 700-800 nm. This is important to record in the red channel as it can also be detected in the GFP channel and misinterpreted as signal from receptor kinase GFP fusions. Likewise, chlorophyll autofluorescence might be misinterpreted as RFP/mCherry signal when using those fluorophores to image organelle markers.

8. Save the settings used to image the control material (laser power and intensity, pinhole, gain, zoom, numbers of z-sections, slide size) and use the same parameters to acquire the signal of the treated experiment to prevent variation due to confocal settings.

9. The extent to which constructs are expressed in transiently transformed *N. benthamiana* leaves varies between individual cells, leaves and plants. Thus, when comparing mock and treated conditions, use samples from the same leaf. Such within-leaf comparisons are critical when quantifying FLS2-GFP endosomes from genetic interference experiments (Figure 3-1).

10. Since epidermal cells of *N. benthamiana* mature leaves are highly vacuolated, FLS2-GFP-positive endosomes are best observed close to the cell periphery. Therefore, it is recommended to acquire z-stacks of ca. 10 µm depth and to include the top of cells where the orientation of the periphery is horizontal. Endosomes are visible as mobile signal-positive punctae. Acquire time lapse movies to capture vesicle mobility. For this, choose a single plane where spots are detected (e.g. near the top of cells), select xyt mode in acquisition parameters and record a movie for up to 1 min (movies are saved as .avi files).

11. To enhance transient transformation efficiency, OD_{600} or 3′, 5′-Dimethoxy-4′-hydroxyacetophenone (acetosyringone) concentration can be increased.

12. Co-localisation studies with organelle markers are performed to observe FLS2-GFP transit trough the late endosomal pathway after activation, and to dissect its trafficking (see Table 3-2).

Table 3-1 Receptor kinase localisation in *N. benthamiana*.

PM= plasma membrane; dpi = day post infiltration. * *Putative N. benthamiana* orthologues obtained by sequence similarity (BLAST) against *N. benthamiana* v1.0.1 predicted cDNA.

Receptor kinase	**Organelle**	**Heterologous expression**	**Excitation-emission**	*** Putative *N. benthamiana* orthologues genes**	**Reference**
FLS2-GFP	PM, endosomes	2-3dpi	488nm-495/550nm	Niben101Scf03455g01008.1	(Choi *et al*., 2013)
EFR-GFP	PM, endosomes	2-3dpi	488nm-495/550nm	-	(Mbengue *et al*., 2016)
BRI1-GFP	PM, endosomes	2-3dpi	488nm-495/550nm	Niben101Scf13404g00002.1	(Mbengue *et al*., 2016)
PEPR1-YFP	PM, endosomes	2-3dpi	514nm-520/560nm	No hits	(Mbengue *et al*., 2016)
SOBIR1-GFP	PM, endosomes	2-3dpi	514nm-520/560nm	Niben101Scf03816g01001.1 Niben101Scf04099g05004.1 Niben101Scf05437g06022.1	(Peng *et al*., 2015; Postma. *et al*., 2016)

Table 3-2 Markers used for co-localisation in heterologously expressing *N. benthamiana* leaves.

PM = plasma membrane, TGN = trans-Golgi network, LE= Late Endosomes, MVB = multivesicular body; dpi= day post infiltration. * Putative *N. benthamiana* orthologues obtained by sequence similarity (BLAST) against N. benthamiana v1.0.1 predicted cDNA.

Marker	**Organelle**	**Heterologous expression**	**Excitation-emission**	*** Putative *N. benthamiana* orthologues genes**	**Reference**
ACA8-mCherry	PM	2-3dpi	561nm-580/620nm	Niben101Scf04852g01008.1	(Postma. *et al*., 2016)
mCherry-MEMB12	Golgi	2-3dpi	561nm-580/620nm	No hits	(Postma. *et al*., 2016)
mRFP-SYP61	TGN	2-3dpi	561nm-580/620nm	Niben101Scf02944g02004.1	(Choi *et al*., 2013)
VHA-a1-RFP	TGN	2-3dpi	561nm-580/620nm	Niben101Scf11756g01025.1	(Lu, Y *et al*., 2012)
RFP-ARA7	Endosomes	3dpi	561nm-580/620nm	Niben101Scf02976g01015.1 Niben101Scf00271g01020.1	(Lu, Y *et al*., 2012)
ARA6-RFP	LE	2-3dpi	561nm-580/620nm	Niben101Scf29276g00003.1 Niben101Scf00648g00003.1	(Lu, Y *et al*., 2012)
RFP-VPS37-1	MVB	3dpi	561nm-580/620nm	No hits	(Lu, Y *et al*., 2012)
YFP-RabG3c RFP-RabG3c	Tonoplast, vacuole Tonoplast, vacuole	3dpi 3dpi	488nm-495/550nm 561nm-580/620nm	Niben101Scf05709g00001.1 Niben101Scf01374g03034.1 Niben101Scf07008g01002.1	(Bozkurt *et al*., 2011)

Table 3-3 Genetic interference of membrane trafficking in *N. benthamiana* leaves.

TRV = Tobacco Rattle Virus; hp = hairpin; PM = plasma membrane; LE= late endosomes; TGN= *trans*-Golgi network.

Construct	**Target**	**Effect on FLS2 localisation**	**FLS2 localisation after flg22 treatment**	**Reference**
DN-RABA6ab^{N126I} DN-RABA4c^{N128I}	RABA6a RABA4c	Delayed maturation from TGN to LE Inhibition of FLS2 transport to the TGN	TGN Endosomes	(Choi *et al*., 2013)
TRV::*Nb*SERK3a/b	*Nb*SERK3a/b	Inhibition of FLS2 internalisation	PM	(Mbengue *et al*., 2016; Postma. *et al*., 2016)
hp*Nb*CHC	6 *Nb*CHCs	Inhibition of FLS2 internalisation	PM	(Mbengue *et al*., 2016)
hp*Nb*DRP2	Nb05397 Nb31648	Reduced number of FLS2-GFP punctae	PM, punctae	(Chaparro-Garcia *et al*., 2015)
AVR3a	DRP2	Reduced number of FLS2-GFP punctae	PM, punctae	(Chaparro-Garcia *et al*., 2015)

4 The function of 14-3-3s proteins is not required for subcellular localisation of the immune receptor FLS2

4.1 Abstract

Cell surface-localised pattern recognition receptors (PPRs) mediate perception of microbe-associated molecular patterns (MAMPs) and activate plant defence responses in a process known as PRR–TRIGGERED IMMUNITY (PTI) (Dodds and Rathjen, 2010). In *Arabidopsis*, flagellin perception or its conserved N-terminal 22-amino acid sequence (flg22) is mediated by FLAGELLIN-SENSING 2 (FLS2) which acts together with the co-receptor SOMATIC EMBRYOGENESIS RECEPTOR KINASE 3/BRASSINOSTEROID INSENSITIVE 1-ASSOCIATED KINASE 1/ (SERK3/BAK1) in defence against bacterial infection in most plant species. FLS2 is endocytosed after binding of flg22, with endosomal sorting depend on its activation status. However, how the activated FLS2/BAK1 complex recruits the endocytic machinery necessary for the internalisation of FLS2 at the plasma membrane (PM) remains unknown. A better understanding of protein complexes that regulate FLS2 internalisation is critical to unravel its role in defence activation. To investigate regulation of PRRs subcellular trafficking during immunity I used a combination of live-cell imaging microscopy together with chemical interference. The 14-3-3 protein general regulator factor 4 (GRF4) have been identified as an FLS2 interactor by immunoprecipitation (IP)/mass spectrometry (MS) and co-IP (Mbengue *et al.*, unpublished). I found that GRF4 associates with PRRs including FLS2 and the EF-TU RECEPTOR (EFR) but also with other PRRs regardless of their biological function.

Furthermore, using chemical interference between GRF4 and its targets I demonstrated 14-3-3 function has no role in FLS2 internalisation.

4.2 **Introduction**

In *Arabidopsis*, ligand-activated FLS2 is internalised (Robatzek *et al*., 2006) and traffics via the late endosomal pathway (Beck *et al*., 2012). However, the mechanism through which the activated FLS2/BAK1 complex recruits the endocytic machinery leading to translocation into endosomes remains unknown. We speculated that the binding partners of FLS2 regulate its trafficking. FLS2-GFP pull-downs followed by a large-scale proteomics approach in stable *Arabidopsis* lines identified putative regulators of FLS2 subcellular trafficking (Mbengue *et al.,* unpublished). To test the specificity of the interaction between putative candidates and FLS2 complex Low Temperature Induced protein 6 (LTi6B), a PM-localised protein who has no role in endocytosis nor in plant defence was used as a negative control. The LC (liquid chromatography)/MS-MS MS analysis performed by the TSL proteomic team had identified +/- 500 proteins and 17 % were specifically found in complex with FLS2 but not with Lti6B. To verify the integrity of the data the presence of well-described FLS2 interactors in the list of proteins were confirmed. As shown in Figure 4-1 BAK1, which is found in FLS2 complex after flg22 perception (Chinchilla *et al*., 2007) was specifically found in FLS2 complex after flg22. Therefore, I concluded the approach used and data obtained were valid to identify FLS2 interactors.

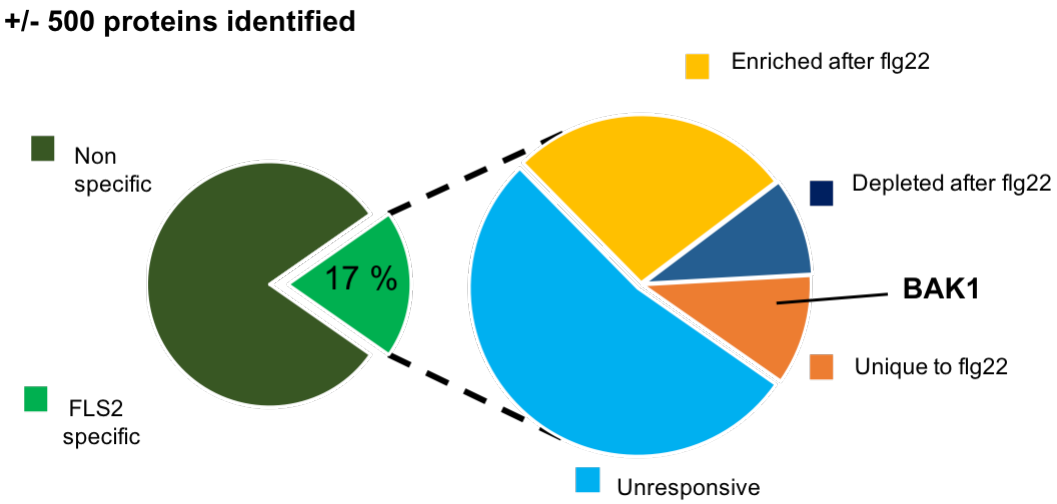

Figure 4-1 Schematic representation of the distribution of proteins found in FLS2-GFP and GFP-Lti6B pull-downs by proteomic analysis.

The pie chart on the left represent the distribution of proteins found with FLS2-GFP (light green) or with GFP-Lti6B (dark green) pull-downs by proteomic analysis. Proteomic analysis has identified +/- 500 proteins in complex with the GFP pull-downs. Among them, 85 proteins (17 %) are specially find in complex with FLS2 but not with LTi6B. The pie of pie chart (right) displays the distribution of proteins found in complex with FLS2. In accordance with previous studies, the well-described FLS2 ligand-dependant interactor BAK1 was found in FLS2-GFP pull-downs after flg22 treatment (orange section), thus, validating the method we used to study FLS2 interactors. Proteomics analyses were performed by Dr Malick Mbengue and TSL proteomic team on *Arabidopsis* seedlings.

The 14-3-3 protein general regulation factor 4 (GRF4 or also designated as GRF ϕ) was found specifically in the FLS2 complex (Mbengue *et al.,* unpublished). In addition, GRF4 was found in CALCIUM PROTEIN KINASE 28 (CPK28) pull-downs (Monaghan *et al .,* unpublished), which is a regulator of PRR-mediated immunity (Monaghan *et al*., 2014).

The 14-3-3 proteins are small soluble proteins belonging to a highly conserved family in eukaryotes (Yaffe *et al*., 2017). Proteins belonging to this family

display redundant functions, therefore genetic analysis are challenging. Although displaying no enzymatic activity, this family of proteins forms homo or heterodimers and bind in most but not all cases to serine/threonine-phosphorylated residues in their interactors (De Boer *et al*., 2013). These associations with the target proteins (also called clients) modulate their activities, localisation, or interaction with other proteins (Aitken, 2006; Jaspert *et al*., 2011; Muslin *et al*., 1996; Paul *et al*., 2012). As a consequence, 14-3-3s appear to regulate important pathways by protein-protein interactions (Denison *et al*., 2011; Jaspert *et al*., 2011). In plants, several studies report a role for 14-3-3s in several pathways (Denison *et al*., 2011) including cellular trafficking (Aducci *et al*., 2002) and plant immune responses (Lozano-Durán and Robatzek, 2015). For instance, GRF6 regulates the subcellular localisation of BRASSINAZOLE-RESISTANT (BZR) proteins and consequently plays a role in brassinosteroid (BR) signalling (Gampala *et al*., 2007; De Vries, 2007). Recently, site directed mutagenesis (SDM) in the 14-3-3 binding motif of VIRE2-INTERACTING PROTEIN 1 (VIP1) revealed that the change in VIP1 localisation from cytosol to nucleus is regulated by 14-3-3 during mechanical or hyper-osmotic stress (Takeo and Ito, 2017).

The role of 14-3-3s in pathogen-induced responses is emerging, as several 14-3-3 proteins have been shown to interact with components of the plant immune system (Chang *et al*., 2009) and to play a role in plant immune responses. For instance, the tomato 14-3-3 protein 7 (TFT7) is required for plant *Pseudomonas syringae pv*. tomato (*Pto*)-induced programmed cell death, as it interacts with a Mitogen-Activated Protein Kinase Kinase (MAPKK)

to regulate immunity in both tomato and in *N. benthamiana* (Oh and Martin, 2011). In rice, 14-3-3 GF14e expression is upregulated during Effector-Triggered-Immunity (ETI) and this negatively affects cell death during bacterial and fungal rice disease (M. *et al*., 2011). More recently, it has been shown in *Arabidopsis* that the 14-3-3 GRF6 interacts with MPK11 after Potyvirus infection and this triggers its degradation by the proteasome to promote infection (Carrasco *et al*., 2014). Interestingly, studies have shown 14-3-3 function is required for MAMP-induced reactive oxygen species (ROS) burst and stomatal closure in *Arabidopsis* and *N. benthamiana* (Lozano-Durán *et al*., 2013). Altogether, these results suggest a role for 14-3-3s in the regulation of plant immunity at different levels.

In addition, FLS2 primary amino acid sequence showed a putative consensus 14-3-3s binding motif mode Ⅰ (K/RXXXS/TXR, where K is a lysine, R an Arginine, X is a , S a serine, T a threonine) in the intracellular kinase domain at the position 1159 (Valérie Cotelle, INRA Toulouse, unpublished) (

Figure 4-2 C).

Figure 4-2 FLS2 kinase domain exhibits a putative 14-3-3 binding motif mode Ⅰ.

(A) The kinase domain of FLS2 amino acid sequence exhibits a putative 14-3-3 binding motif mode Ⅰ R/KXXXS/TXR (software designed by Valérie cotelle, INRA Toulouse). (B) The motif in the FLS2 sequence is KANSFR (K represents lysine, A alanine, N asparagine, S serine, F phenylalanine and R arginine). (C) The putative binding motif is positioned between the 1151-1173 amino acids in the FLS2 sequence. LRR= leucine rich repeat; TM= transmembrane.

This suggests that the FLS2 intracellular domain displays 14-3-3s binding sites and can interact with 14-3-3s proteins. Taken together, GRF4 was selected as a potential FLS2 regulator and I speculated that GRF4 functions as a scaffold or adaptor proteins in the recruitment of the endocytic machinery upon receptor activation. To test this hypothesis, I performed GFR4 localisation by live-cell-imaging microscopy. I carried out GRF4 association with PRRs by Co-immunoprecipitation. I tested the involvement of 14-3-3s function in FLS2 internalisation by chemical interference.

4.3 GRF4 localises to the cytosol, cell periphery and nucleus

LC/MS-MS analysis revealed GRF4 association with FLS2 complex but not with LTi6B complex (Mbengue *et al.*, unpublished) indicating a putative

interaction between GRF4 and FLS2. FLS2-GFP localises to the PM in *N. benthamiana* (Choi *et al*., 2013). Prior to confirming GRF4 and FLS2 association GRF4-YFP expression were tested by western blot in *N. benthamiana* performed by undergraduate students and showed expression of the full protein at 2 dpi (data not shown). I tested subcellular localisation of GRF4-YFP using laser scanning confocal microscopy (LSCM) in *N. benthamiana* transient expression system. I detected a YFP signal in the cytosol observed by characteristic cytosolic strand (CS), in the nucleus (N), and at the cell periphery (CP). This result indicated GRF4-YFP mainly localised to the cytosol in *N. benthamiana*.

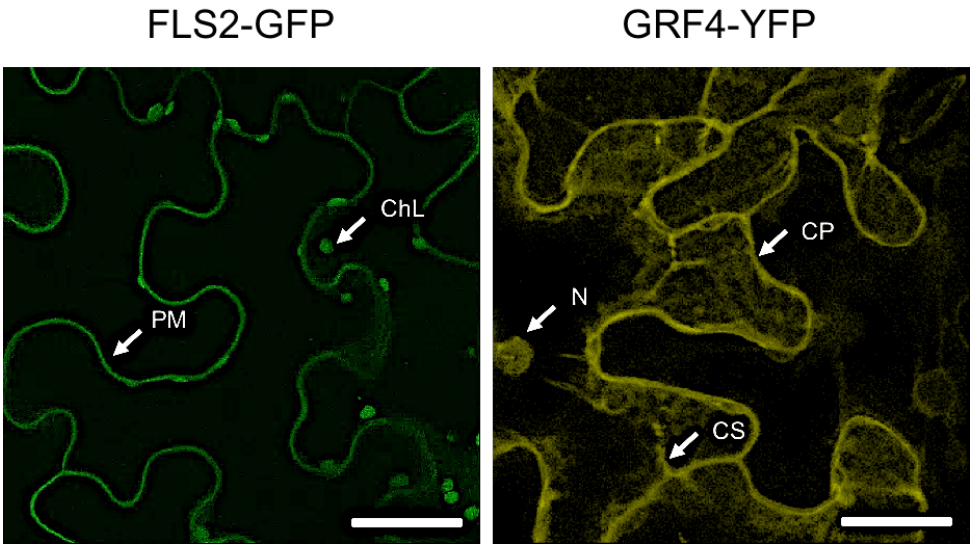

Figure 4-3 GRF4-YFP localises to the cell periphery, cytoplasm and nucleus in *N. benthamiana*.

Confocal micrographs were taken at 2 dpi. Plasma membrane (PM); chloroplast (ChL); cytoplasm (CP); nucleus (N) and cell periphery (CP). Confocal micrographs show maximum projection of 10 z-stack of 1 µm each. Three independent biological replicates were performed.

Previous studies demonstrate cytoplasmic proteins can interact with and regulate PM-protein complex (Kadota *et al*., 2014; Lu *et al*., 2010). Thus, I concluded that *in planta* interaction and regulation between GRF4 and FLS2 is feasible.

4.4 GRF4 associates with FLS2 at the plasma membrane

Based on the localisation study I speculated GRF4 and FLS2 associate at the cell periphery. To test this, I performed Biomolecular Fluorescence Complementation (BiFC) experiments in *N. benthamiana*. BiFC is based on the restoration of fluorescence after the two non-fluorescent halves of a fluorescent protein are brought together by a protein-protein interaction event (Hu *et al*., 2001). Therefore, BiFC assay enables simple and direct

visualisation of protein interactions in living cells and it is relatively quick to perform. I observed GRF4-YFP localisation to the CP, CS and N (Figure 4-3). It is established the 14-3-3 proteins form homo/hetero dimers (Gardino *et al*., 2006), therefore if the constructions are functional, co-expression of GRF4-YFPc with GRF4-YFPn should show a reconstruction of YFP. As a consequence co-expression of GRF4-YFPn and GRF4-YFPc showed reconstitution of YFP protein by detection of a fluorescent signal in the cytoplasm (CS), nucleus (N) and cell periphery (CP) (Figure 4-4 right panel) whereas co-expression of GRF4-YFPc with an empty vector used as a control showed a background signal from the chloroplast autofluorescence but no reconstituted signal (Figure 4-4; left panel). Notably, when FLS2-YFPn and GRF4-YFPc were transiently co-expressed I observed a fluorescent signal at the cell periphery (CP) (Figure 4-4; middle panel). This suggests that FLS2-YFPn and GRF4-YPFc associated at the PM. I concluded that the interaction between FLS2 and GRF4 occurred at the PM. Next, I wanted to address whether the association undergoes dynamic changes in response to flg22 perception.

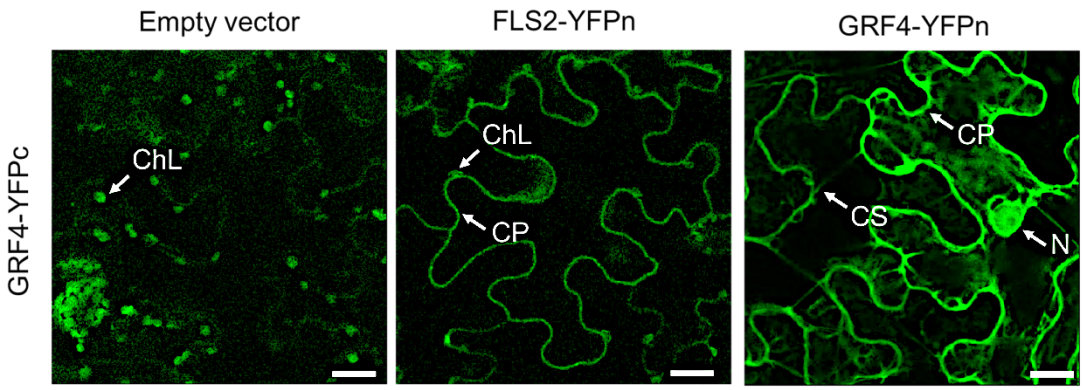

Figure 4-4 BiFC reveals GRF4 and FLS2 associate at the cell periphery. Subcellular localisation of the association between GFR4-YFPc and FLS2-YFPn in *N. benthamiana* by BiFC. The left panel shows a background signal from the chloroplast autofluorescence but not a YFP signal when GRF4-YFPc is co-expressed with a YFPn empty vector used as a control; the middle panel shows a YFP signal at the cell periphery (CP) when GRF4-YFPc is co-expressed with FLS2-YFPn; the right panel shows a cell periphery (CP), chloroplast (ChL); cytoplasmic strand (CS) and nucleus (N) signal when GRF4-YFPc is co-expressed with GRF4-YFPn. Scale bars = 10 μm. Confocal micrographs were taken at 2 dpi. Three independent biological replicates were performed.

4.5 GRF4 associates with FLS2 in a ligand and kinase-independent manner

To test if the association between FLS2 and GRF4 was responsive to flg22 treatment I performed a Co-IP between GRF4-HA and FLS2-GFP in *N. benthamiana* transient system in the absence or presence of flg22. FLS2-GFP pull-downs were followed by immunoblot to detect the presence of GRF4-HA.

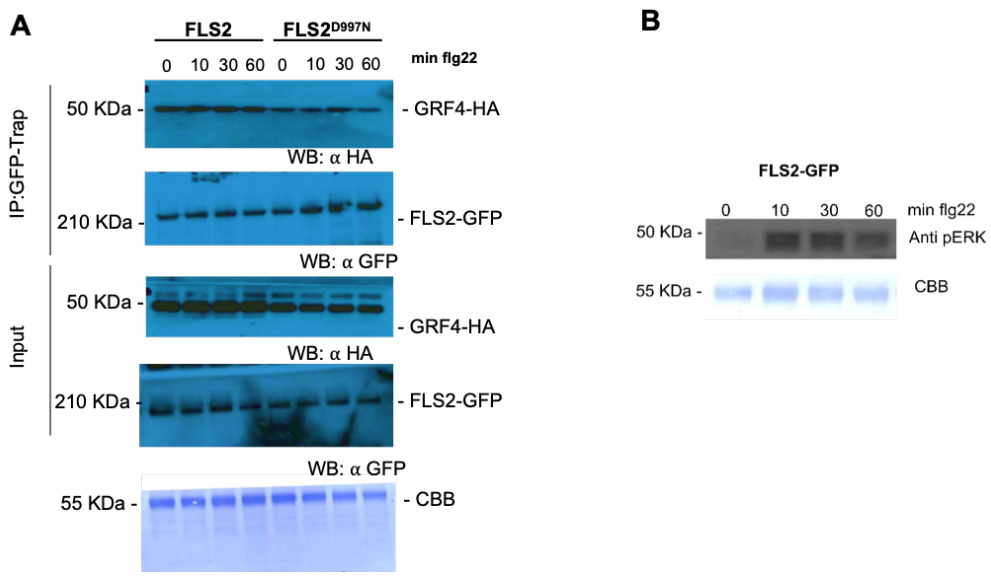

Figure 4-5 GRF4 associates with FLS2 in a ligand and kinase-independent manner in *N. benthamiana*.

(A) Immunoblots shows expression of FLS2-GFP and GRF4-HA presence in GFP-pull-downs from *N. benthamiana* leaves. Solubilised proteins were either IP with anti-GFP antibody or not (Input) or immunobloted using anti-HA and anti-GFP antibodies (FLS2-GFP (left panel) or $FLS2^{D997N}$-GFP (right panel) pull-downs with GRF4-HA before and after flg22 treatment. Note that different exposure times are presented between blots to facilitate the reading (B) flg22-induced MAPK activation in total proteins extract of FLS2-GFP pull-downs. Bars = 20 µm. Dpi=days post infiltration. six and three independent biological replicates were performed for FLS2 and $FLS2^{D997N}$ respectively.

No significant change in GRF4 protein levels was detected before compared to after flg22 (Figure 4-5 A), indicating GRF4 constitutively associated with FLS2 complex. To confirm the competence of the flg22 treatment I performed a flg22-induced MAPK phosphorylation assay on total protein extract (input) (Figure 4-5 B). I observed MAPK activation after flg22 treatment in total protein extract used for Co-IP experiments (Figure 4-5 B) showing the competence of the treatment. Therefore, I concluded association between FLS2 complex and GRF4 is independent of flg22 elicitation. Many studies demonstrate 14-3-3s

function as phosphoregulatory proteins (De Boer *et al*., 2013; Carrasco *et al*., 2014; Yaffe *et al*., 2017). Consequently, I speculated GFR4 association with activated FLS2 is mediated via phosphorylation events. To address this question I performed Co-IP between $FLS2^{D997N}$, a kinase-inactive variant of FLS2 (Schwessinger *et al*., 2011) and GRF4. Similar to FLS2-GFP pull-downs I observed no significant change in GRF4 protein levels in $FLS2^{D997N}$-GFP pull-downs. Thus, showing GRF4 constitutively associated with $FLS2^{D997N}$ (Figure 4-5). I concluded FLS2 kinase activity is not required for GRF4 association with active FLS2 complex. Overall, my Co-IP results indicated GRF4/FLS2 association is independent of ligand activation and kinase activity.

4.6 **GRF4 associates with EFR in a ligand-independent manner**

FLS2 and EFR, are both members of the same Leucine-Rich Repeat-Receptor-like kinases (LRR-RKs) family (Shiu and Bleecker, 2001), and both follow the late endosomal pathway upon ligand activation (Mbengue *et al*., 2016). Similar to FLS2, EFR internalisation is ligand (elf18) dependent. To test whether GRF4 also interacts with EFR, I studied the association between EFR and GRF4 upon elf18 treatment in *N. benthamiana* transient system. As observed with FLS2, I did not detect a significant difference in GRF4 protein levels in EFR-GFP pull-downs after elf18 elicitation (Figure 4-6). I concluded GRF4 constitutively associated with EFR complex in an elf18-independent manner. Taken together my results showed GRF4 associated with RLKs in a ligand-independent manner. This result prompted me to investigate whether

GRF4 interacts with PRRs, regardless of their involvement in immunity and belonging to different subfamilies.

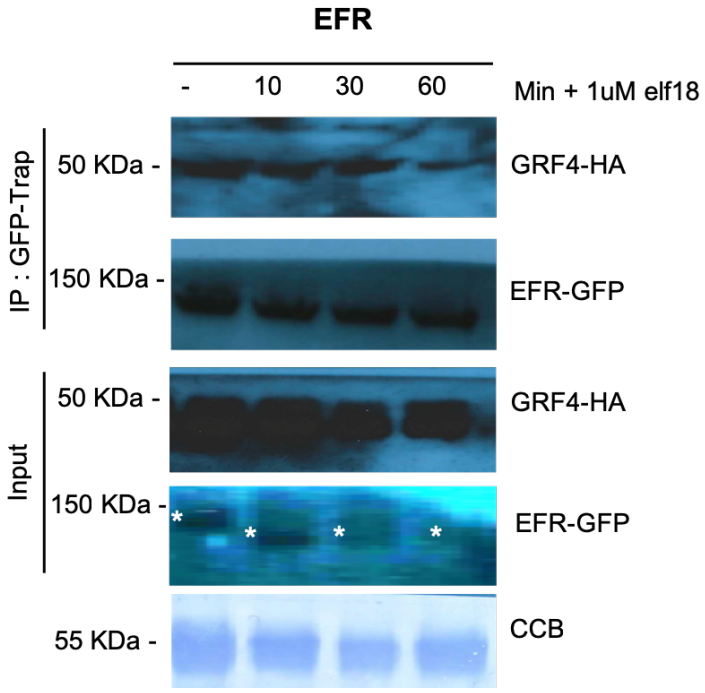

Figure 4-6 GRF4 associates with EFR complex in an elf18-independent manner.

Immunoblots show expression of EFR-GFP and GRF4-HA presence in GFP-pull-downs from *N. benthamiana* leaves. Solubilised proteins were either IP with anti-GFP antibody or not (Input) or immunoblotted using anti-HA and anti-GFP antibodies. EFR-GFP pull-downs with GRF4-HA before and after elf18 treatment. Note that different exposure times are presented between blots to facilitate the reading White asterics show bands of interest. Three independent biological replicates were performed.

4.7 GRF4 associates non-specifically with plasma membrane-localised proteins

To test the specificity of GRF4 association with PRRs I performed Co-IP with other PRRs such as the LRR-RLK CLAVATA1 (CLV1) involved in stem cell proliferation (Nimchuk *et al*., 2011) and SUPPRESSOR OF BIR1-1 involved in

plant defence (SOBIR1) (Clark *et al*., 1997; Gao *et al*., 2009). I also included the RLP *Cladosporium fulvum*-4 (Cf-4), lacking an intracellular kinase domain (Rivas and Thomas, 2005). GRF4 presence was detected in all Co-IP performed with several PRRs (Figure 4-7). I concluded GRF4 associated with SOBIR1, CLV1, Cf-4 (Figure 4-7). Altogether, these findings demonstrated GRF4 associated non-specifically with plasma membrane-localised proteins, suggesting a role as a PM-chaperone. To test this hypothesis, I investigated the function of 14-3-3s in FLS2 subcellular trafficking.

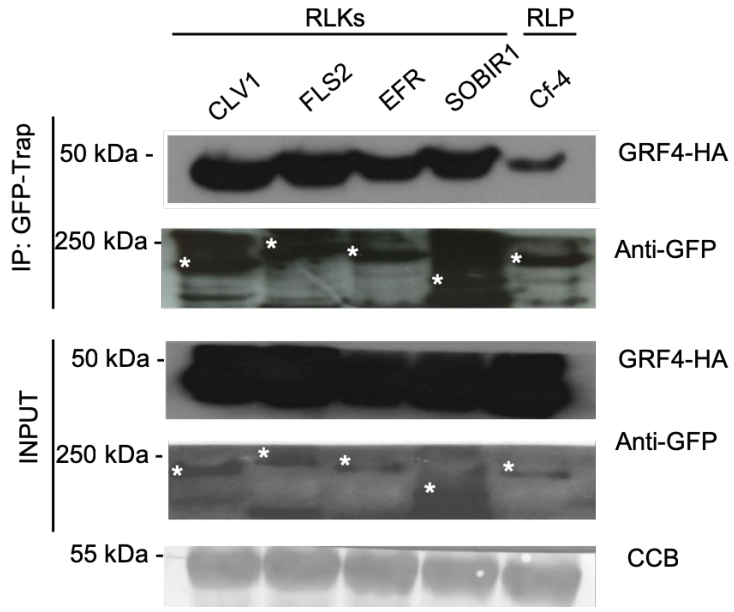

Figure 4-7 GRF4 associates with PM-localised proteins.

Immunoblots show expression of GFP-tagged plasma-membrane localised proteins (PRRs pull-downs (RLKs; CLV1, FLS2, EFR, SOBIR1) and RLP pull down (Cf-4) and GRF4-HA presence in GFP-pull-downs from *N. benthamiana* leaves. Solubilised proteins where either IP with anti-GFP antibody or not (INPUT) or immunoblotted using anti-HA and anti-GFP antibodies. White asterics indicate GFP pull downs. Three independent biological replicates were performed.

4.8 The function of 14-3-3s is not required for flg22-induced FLS2 endocytosis

Genetic analysis of 14-3-3s are challenging due to their highly redundant functions in plants (Paul *et al*., 2005, 2009). To obtain irrefutable data, multiple 14-3-3s must be knock-out. Besides, 14-3-3 proteins are involved in broad processes making multiple mutants not only time consuming but also unusable to address their involvement in a specific pathway. Therefore, to overcome those issues, I carried out a pharmacological approach to test if 14-3-3 functions was involved in FLS2 subcellular trafficking. AICAR is a 5′ AMP analogue that is known to disrupt the biochemical and biological influence of 14-3-3s upon their target clients (Paul *et al*., 2005). To this end, stably FLS2-GFP expressing *Arabidopsis* plants (Beck *et al*., 2012) were pre-treated with the 14-3-3 inhibitor AICAR (Paul *et al.*, 2005, Lozano-Durán *et al.*, 2014) and challenged with flg22. High-throughput live-cell imaging (Beck *et al*., 2012) revealed FLS2-GFP localised to the PM in both conditions, untreated and AICAR-treated (Figure 4-8 A, left panel). This suggested GRF4 is not required for FLS2 localisation at the PM. In addition, I observed FLS2-GFP localised to endosomes in untreated and AICAR-treated samples upon flg22 perception (A, right panel). I concluded that the 14-3-3s function is not required for FLS2 localisation before and after flg22 perception. Moreover, quantification of endosomes with EndomembraneQuantifier (Beck *et al.*, 2012) showed no significant difference between AICAR-treated and untreated tissues (Figure 4-8 B). This indicated AICAR did not prevent FLS2 internalisation. I concluded

14-3-3s function is not required for flg22-induced endocytosis of FLS2.

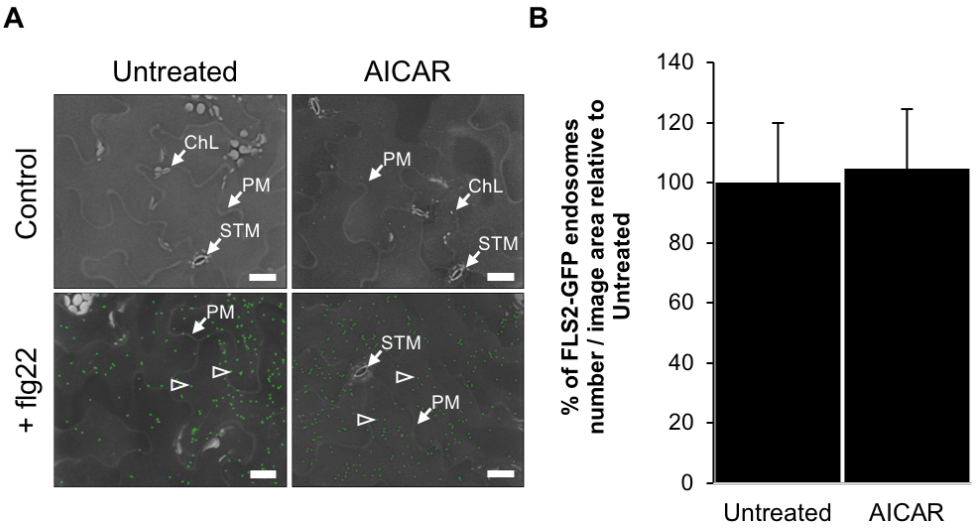

Figure 4-8 Chemical disruption of 14-3-3 function does not impair FLS2 internalisation.

(A) High-throughput confocal micrographs of *Arabidopsis* FLS2-GFP transgenic lines show maximum projections of cotyledon epidermis treated or not (untreated) with flg22 after 60 min. Detected spots are surrounded by green circled. Bars = 30 µm. (B) Quantification of FLS2-GFP endosomal numbers *per* imaged area in samples challenged with flg22 in the presence or absence (untreated) of AICAR. Graph represents mean values ± SEM (standard error of the mean); untreated *n* =69, flg22 *n* = 70 images graphs shows one representative experiment. Micrographs are in black and white, the white signal at the PM is the GFP signal collected by the OPERA microscope. The green "dots" are processed by the ACAPELLA software which recognises endosomes and circle them to facilitate counting by EndomembraneQuantifier. Four independent biological replicates were performed.

4.9 **Other candidates tested**

Other notable candidates found in FLS2 pull-downs were short-listed (literature-based) but were not investigated further. Indeed, it appeared some of those candidates were already investigated by other groups.

4.10 **Conclusion**

By using co-IP experiments, I demonstrated GFR4 associates with PM-localised proteins which is not surprising for scaffold and adaptors proteins. Nevertheless, I demonstrated GRF4 association with PRRs is not specific because co-IP experiments showed GRF4 associated with PM-localised protein regardless of their function. Using a chemical approach with AICAR, an inhibitor of 14-3-3 proteins function I exhibited 14-3-4 function is not required for FLS2 internalisation. Since 14-3-3 function is required for two flg22-induced responses ROS burst and stomatal closure (Lozano-Durán *et al*., 2013) but not for flg22-mediated internalisation of FLS2 (Figure 4-8), I concluded FLS2 internalisation is uncoupled from FLS2 complex activation. It appears this study does not improve our understanding of FLS2 internalisation. Nevertheless, knowing 14-3-3s function is not required for FLS2 internalisation still bring important information and suggests FLS2 internalisation and PTI follow separate signalling pathway after flg22 perception. Interestingly, it might the same for other PRRs than FLS2. Analyses of MAMP-induced PRR internalisation other than FLS2 under AICAR treatment is a key experiment to perform to confirm the results found in this study can be generalised to PRRs.

4.11 **Discussion**

GRF4 associates with PM-localised proteins in *N. benthamiana*

By using BiFC assays I observed GRF4 associates with FLS2 at the PM (Figure 4-4 B). Nevertheless, a positive BiFC signal does not necessarily confirm that the tested proteins are actually interacting *in vivo* in a specific way as BiFC is known to promote protein-protein interactions through the high affinity of the both split YFP halves. Using more sensitive technique such as FRET-FLIM (Bücherl *et al*., 2014) can further dissect subcellular localisation or GRF4 and FLS2 association.

GRF4 associates with FLS2 and EFR in a ligand-independent manner

Co-IP experiments revealed GRF4 associates with FLS2 and with EFR complexes in a ligand-independent manner in *N. benthamiana* (Figure 4-5 and Figure 4-6). GRF4 was overexpressed under a 35S promotor, in a transient system, thus, it is possible that a specific or dynamic association are not detectable because of the limitations of the transient system. For instance, expression in transient system allow *in vivo* studies, high accumulation and fast screening of proteins but it has limitations. To address those issues several experiments could be carried out. First, transient expression of GRF4 driven by its native promotor would show GRF4 expression at a native level. Secondly, stable expression of tagged *At*GRF4 in *Arabidopsis* system would provide physiological conditions for its function than its transient expression *in N. benthamiana*. To address this, transformation of *Arabidopsis* plants with

Agrobacterium carrying GRF4-HA construct was performed by TSL transformation team. I tested GRF4-HA protein expression in transformants (T1) and I obtained two lines, T1#1 and T1#5 expressing GRF4-HA (Figure 4-9). Nonetheless, no further experiments were carried out because by the time I obtained those lines I already excluded a role of 14-3-3 proteins in FLS2 internalisation.

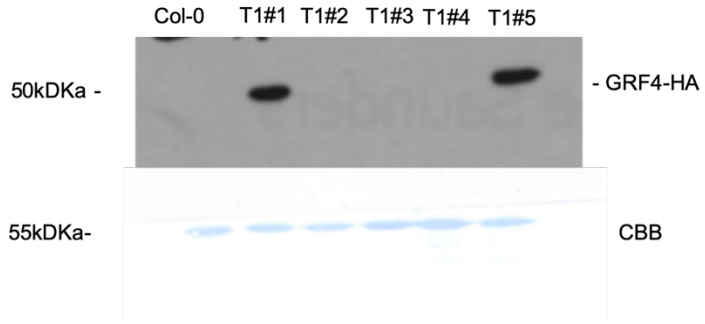

Figure 4-9 Expression of GRF4-HA in five *Arabidopsis* transformants.
Immunoblot shows expression of GRF4-HA in crude extracts from five different *Arabidopsis* T1 plants T1#1 to T1#5. Solubilized proteins where immunoblotted using anti-HA antibodies. The experiment was performed one time.

Besides, 14-3-3s are highly conserved proteins among eukaryotes families (Yaffe *et al*., 2017), and data present *Arabidopsis* 14-3-3s can complement yeast 14-3-3s mutants (van Heusden, G *et al*., 1996), hence, expression of *Arabidopsis* GRF4 in *N. benthamiana* system is suitable. Thirdly, pull-downs and co-IP experiments using antibodies against GRF4 and PRRs would show endogenous accumulation and expression in *Arabidopsis*. Additionally, I used different stringency to avoid unspecific interactions. For instance, I used different incubation times with the GFP Trap ® (from 2 to 4 hours). Indeed, at one point the system gets saturated and a too long exposure can lead to

agglomeration of proteins revealing unspecific interactions. Two hours seemed the best incubation time. I used different non-ionic detergent concentrations (IgePal) in the solubilisation buffer and additional washing steps to remove unspecific interaction and I observed no difference. The best conditions are provided in chapter 2.

Overall, using *N. benthamiana* system allow a fast screening of candidates, I can conclude testing GRF4 involvement in FLS2 subcellular trafficking using *N. benthamiana* is sufficient to demonstrate GRF4 is not specifically interacting with FLS2.

GRF4 associates with all PM-proteins tested

Additionally, I observed GRF4 constitutively associated with other RLKs/RLPs in *N. benthamiana* (Figure 4-7). Therefore, I demonstrated GRF4 interacted with PRR proteins regardless of their biological function. *In silico* study indicated a putative 14-3-3s binding motif in FLS2 intracellular domain (Valérie Cotelle, INRA Toulouse unpublished). Site directed mutagenesis (SDM) in the putative K/RXXX**S/T**XR motif of FLS2 sequence together with *in vitro* pull-downs will address whether the motif is genuine and characterise the interaction.

It would be interesting to use the search tool set-up by Valérie Cotelle in Toulouse to know if the amino acid sequences of the other tested proteins carry or not a 14-3-3s binding motif. This experiment is key to determine that the association with 14-3-3s is feasible. Besides, absence of a 14-3-3s motif

in the protein sequence does not mean that association is impossible, it only reveals that a direct interaction is unlikely to occur. Furthermore, if 14-3-3s are chaperone proteins which regulate protein function or localisation by protein-protein interaction, it is not necessarily by direct interaction. Indeed, 14-3-3s can modify a protein function or localisation by association to a binding partner of this protein (De Boer *et al*., 2013). For instance, when I start the project, I speculated that GRF4 could either associate to FLS2 directly or to another protein present in FLS2 complex such as BAK1. This is why I carried out *in-vivo* Co-IP experiments to reveal protein complex interactions. Co-IP experiments between GRF4 and PRRs in the presence of the 14-3-3 inhibitor AICAR will unravel specific interactions. If GRF4 associates with PRRs in a specific manner via 14-3-3 binding motifs AICAR should disrupt the interaction and in co-IP experiments GRF4 would no longer associate with PRRs complex. Nonetheless the effect of AICAR on 14-3-3 in *N. benthamiana* is unknown and its effect should be confirming prior to carrying out experiment in *N. benthamiana*.

The possibility that GRF4 is sticky to GFP protein or GFP beads were excluded as preliminary pull-downs experiments performed by Malick Mbengue showed GRF4 did not associated with GFP-LTi6B in *Arabidopsis* (Figure 4-1). Nevertheless, a negative control using protein extract containing GRF4-HA incubated with GFP trap ® only could be performed to exclude the GFP stickiness. A negative control for the co-IP could be Lti6B because it was the control used in *Arabidopsis* to perform the MS experiment. Unfortunately, this was not performed.

14-3-3 function is not required for FLS2 subcellular localisation in *Arabidopsis*

Due to functional redundancy I did not use a genetic approach to study GRF4 involvement in FLS2 internalisation (Paul *et al*., 2005). AICAR has been previously described as an inhibitor of 14-3-3 function in *Arabidopsis.* AICAR disrupt 14-3-3 binding to its designated targets by associating with 14-3-3 and preventing interaction with targets (Dikran *et al*., 1998).

Live-cell imaging revealed AICAR treatment had no effect on FLS2 subcellular localisation nor on FLS2 internalisation (Figure 4-8). This demonstrates that chemical interference of 14-3-3s with their targets does not impair subcellular localisation of FLS2 in the presence or absence of flg22. Therefore, I demonstrated 14-3-3 function is not required for flg22-induced internalisation of FLS2. The 14-3-3 proteins are highly redundant, although this inhibitor targets more than one 14-3-3 protein, including GRF4 (Paul *et al*., 2005), I cannot rule out the possibility that other 14-3-3 members are insensitive to AICAR and can thus functionally replace GRF4. However, evidence argues against this hypothesis as GRF2, the closest homologue of GRF4 is also targeted by AICAR in *Arabidopsis* (Paul *et al*., 2005). Other 14-3-3 functional inhibitors such as R18 peptide (Petosa *et al*., 1998; Wang *et al*., 1999), could be used to provide more robust conclusion. High-throughput quantification revealed no effect on FLS2 endosomal number in AICAR-treated samples. Nevertheless, I cannot exclude the possibility that AICAR affects one particular population of FLS2 endosomes. To address this possibility, co-localisation

studies of activated FLS2-GFP with endomembrane markers in the presence of 14-3-3 inhibitor could be carried out.

Interestingly, AICAR-treated *Arabidopsis* plants shows impairment of two early PTI responses, the ROS burst and stomatal closure (Lozano-Durán *et al*., 2013). This shows 14-3-3 function is required for establishment of defence responses and can explain why 14-3-3 are found in PRRs complexes.

Additionally, the fact that AICAR-treated samples show impaired PTI responses (Lozano-Durán *et al*., 2013) whereas FLS2 internalisation was unaffected (Figure 4-8)suggests FLS2 endocytosis is uncoupled to complex activation.

Overall, despite the fact that GRF4 was found in FLS2 pull-downs, and the presence of a 14-3-3 binding motif in FLS2 extracellular domain our study provides no evidence for a direct regulation of FLS2 internalisation by 14-3-3s.

5 Post-TGN trafficking of FLS2 is dependent on the Arf-GEF MIN7 and is targeted by the bacterial effector HopM1

5.1 Abstract

To investigate regulation of PRRs subcellular trafficking during immunity I used a combination of live-cell imaging microscopy together with effector interference. Here, I present FLS2 traffics to the MVBs/LE via the trans-Golgi network (TGN)/early endosome (EE) and that this is dependent on the ADP RIBOSYLATION FACTOR GUANINE-NUCLEOTIDE EXCHANGE FACTOR (Arf-GEF) HopM1 interactor 7 (MIN7). Further, confirming that endocytosis is a critical component of overall immunity, I showed that the *P. syringae* effector HopM1 targets flg22-induced endocytosis of FLS2 at the TGN/EE.

5.2 Introduction

Pattern recognition receptors (PRRs) are plasma membrane (PM)-localized proteins that mediate recognition of pathogen-associated molecular patterns (PAMPs) derived from microbes (Dodds and Rathjen, 2010). PRR signalling is initiated at the cell surface, thus, PM-localisation of PRRs is crucial for defence activation (Zipfel *et al*., 2004). Moreover, in *Arabidopsis*, PRRs are spatially organised within the PM. For instance, FLS2 and LYSIN MOTIF DOMAIN-CONTAINING GLYCOSYLPHOSPHATIDYLINOSITOL-ANCHORED PROTEIN 2 (LYM2) both localise to plasmodesmata (PD)-PM and plays a role in the regulation of intracellular flux during defences responses (Faulkner *et al*., 2013). Additionally, BRASSINOSTEROID INSENSITIVE 1 (BRI1) and FLAGELLIN-SENSING 2 (FLS2) are involved in

growth and immunity respectively (Clouse *et al*., 1996; Gómez-Gómez and Boller, 2000), and form distinct nanoclusters at the PM (Bücherl *et al*., 2017). This suggests spatial organisation of PRRs at the PM is associated with their signalling function. Accumulation of functional PRRs at the PM is important to activate defence responses. Delivery of PRRs to the cell surface is mediated by the secretory pathway; FLS2 and ELONGATION FACTOR TU-RECEPTOR (EFR) biogenesis occurs through the endoplasmic reticulum (ER) and traffic through the Golgi apparatus (GA) and the *trans*-Golgi network (TGN) to reach the PM (Häweker *et al*., 2010; Saijo *et al*., 2009; Tintor and Saijo, 2014). Improperly folded PRRs are re-routed for degradation by ER-associated degradation (ERAD) (Su *et al*., 2011). PRR abundance at the PM is also regulated by turnover mediated by endocytic pathways. In *Arabidopsis*, both BRI1 and FLS2 undergo constitutive endocytosis independently of ligand binding (Geldner *et al*., 2007), but FLS2 is also actively and specifically endocytosed when activated. Activated FLS2 traffics via late endosomal pathway (Beck *et al*., 2012). The ligand-induced PRR internalisation pathway is conserved across receptor-like kinases (RLKs) PRRs. FLS2, EFR and PEP RECEPTOR 1 (PEPR1) all undergo endocytosis upon perception of their cognate ligands, flg22, elf18 and pep1 respectively (Beck *et al*., 2012; Mbengue *et al*., 2016). This is also true for the receptor-like protein *Cladosporium fulvum* (Cf-4) which undergoes internalisation after Avr4 recognition (Postma. *et al*., 2016). Recently, data demonstrate that after chitin perception, CERK1 mediates internalisation of the RLK LYK5 (Erwig *et al*., 2017) in *Arabidopsis*.

The subcellular trafficking pathway of PRRs is now well-described in plants, but the molecular mechanisms underlying PRR endocytosis regulation and its interplay with PRR-triggered immunity (PTI) remain poorly understood. Delivery of newly synthesised PRRs to the PM is mediated by the secretory pathway (Anelli and Sitia, 2008). In plants, the TGN serves as an early endosome (EE) (Dettmer *et al*., 2006; Robinson *et al*., 2008a). Moreover, the TGN/EE compartment sort vesicles back to the plasma membrane (recycling pathway) or to late endosomes (LE) (Sandra *et al*., 2009) and acts as a hub where cargo from the secretory and endocytic pathway merge. Thus, the TGN can serve as a sorting platform (Viotti *et al*., 2010) and different TGN subdomains coexist in the plant cell (Choi *et al*., 2013; Lee *et al*., 2011).

Together with Martina Beck, a postdoctoral researcher, we hypothesised that activation dependent sorting of FLS2 happens at the TGN/EE, i.e. endocytosis of inactive receptors and secretion of newly synthesised active receptor both pass though the TGN/EE during pathogen infection requiring active sorting within the TGN/EE. While secretion and endocytosis of these two forms of FLS2 are well documented, the role of the TGN/EE is not yet clear.

It has been suggested that in *N. benthamiana* FLS2 transiently co-localises to a yet unknown compartment hybrid between the TGN and multivesicular bodies (MVBs) after flg22 treatment (Choi *et al*., 2013). In *Arabidopsis*, FLS2 localises at the LE/MVBs compartment following flg22 treatment (Beck *et al*., 2012). Whether it bypasses the TGN/EE remains unknown. Interestingly, direct maturation from TGN to MVBs has been reported (Scheuring *et al*.,

2011), which might explain why FLS2 is not observed in the TGN/EE in *Arabidopsis*.

Recent data obtained by Sara Ben Khaled during her PhD in Silke Robatzek's laboratory, show post translational modification (PTM)-regulation (phosphorylation and ubiquitination) of PRR internalisation is required to maintain responsiveness to long term MAMP treatment. Thus, it is hypothesised PRR internalisation remove inactive receptors from the PM to allow accumulation of newly synthesised competent receptor (Ben Khaled *et al.,* unpublished). Notably, mutants impaired in flg22-induced FLS2 internalisation display a reduced *P. syringae* resistance to long term MAMP treatment (Ben Khaled *et al.,* unpublished). Similar results are observed in efl18-induced EFR internalisation (Ben Khaled *et al.,* unpublished). Thus, demonstrating a linked between PRR internalisation and pathogen resistance. Therefore, understanding how PRR internalisation and resistance are linked became a matter of interest in Silke Robatzek's laboratory. Team's members focused on investigating the regulation of PRR internalisation. In this chapter, together with Martina Beck, I performed characterisation of ligand-induced FLS2 endocytosis to identify the role of the TGN/EE in this process. We determined that FLS2 sorting follows the endocytic route through the TGN/EE in *Arabidopsis* and I determined that post-TGN trafficking of FLS2 is mediated by the guanine-nucleotide-exchange factors (Arf-GEF) MIN7. Further, my data demonstrate FLS2 endocytosis is targeted by the bacterial effector HopM1 at the TGN, likely in a MIN7-dependent manner.

5.3 Activation dependent sorting of FLS2 occurs at the *trans*-Golgi-Network

To find out whether FLS2 is following the canonical endocytic route through the TGN/EE together with Martina Beck we performed subcellular localisation of FLS2 with a TGN marker vacuolar H^+-ATPases (VHA-a1) (Dettmer *et al*., 2006) in the presence of flg22 together with trafficking inhibitors. Brefeldin A (BFA) is an inhibitor of the ADP ribosylation Factor of the guanine-nucleotide-exchange factors (Arf-GEF) GNOM and was used to promote accumulation of recycled proteins from TGN/EE but not LE and MVBs in BFA bodies in *Arabidopsis* root and cotyledons (Beck *et al*., 2012; Langhans *et al*., 2011; Naramoto *et al*., 2014; Robinson *et al*., 2008a). ConcanamycinA (ConcA) is an inhibitor of V-ATPase and prevents protein export from the TGN/EE to the MVBs (Dettmer *et al*., 2006). We observed FLS2-GFP and VHA-a1-RFP both localised to the BFA bodies (Figure **5-1**) typically observed by a cluster of vesicles caused by the accumulation of recycled proteins (Geldner *et al*., 2003). Therefore, we confirm non-activated FLS2 is sorted via the TGN/EE in *Arabidopsis*.

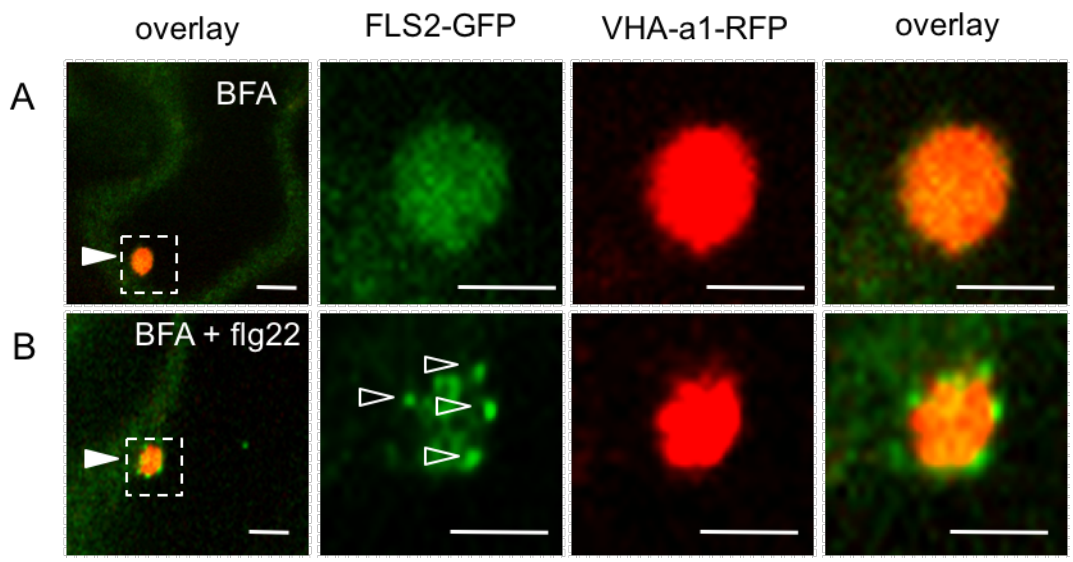

Figure 5-1 Recycling pathway of FLS2 is VHA-a1 positive.

Visualisation of FLS2-GFP and VHA-a1-RFP in 2-week-old cotyledons from FLS2-GFP/VHA-a1-RFP stable transgenic *Arabidopsis* lines generated by Martina Beck (A) FLS2 non-activated receptor localizes to the TGN/EE in BFA bodies whereas (B) flg22-activated receptor does not localize to VHA-a1-RFP in BFA bodies (bottom panel). The white arrow indicates a BFA body, arrowhead outlines show endosomes, inset images show details of BFA bodies. Three independent biological replicates were performed. NB the presented experiment was designed and performed by former post-doctorate researcher Dr Martina Beck.

As previously described we found activated FLS2 trafficking is BFA-insensitive (Beck *et al*., 2012), thus, did not co-localise with VHA-a1-RFP positives BFA bodies (Figure 5-1). FLS2-GFP was found around the VHA-a1 positive BFA body Figure 5-1) in agreement with previous data (Bauer *et al*., 2001; Beck *et al*., 2012). Interestingly, upon flg22 treatment FLS2-GFP endosomes partially co-localised with VHA-a1-RFP positive compartments (Figure 5-2).

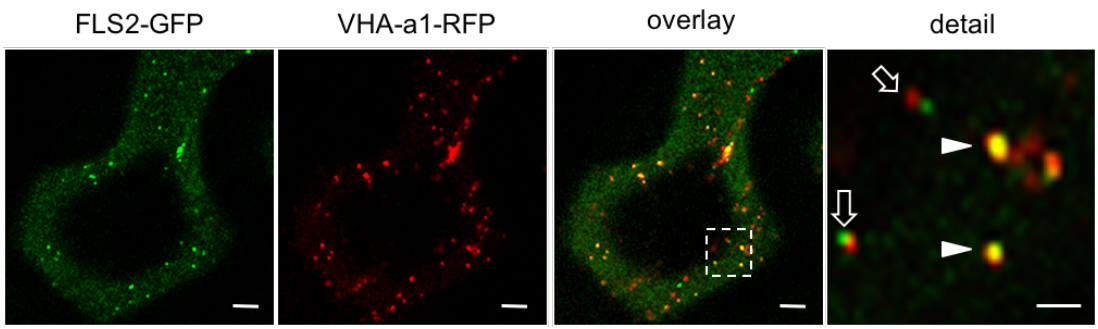

Figure 5-2 Activated FLS2 partially co-localises with VHA-a1.

Visualisation of FLS2-GFP and VHA-a1-RFP in 2-week-old cotyledons from FLS2-GFP/VHA-a1-RFP stable transgenic *Arabidopsis* lines generated by Martina Beck. Flg22-activated receptor does not localize to VHA-a1-RFP in BFA bodies (bottom panel). The white arrow indicates a BFA body, arrowhead outlines show endosomes, inset images show details of BFA bodies. Three independent biological replicates were performed. NB the presented experiment was designed and performed by former post-doctorate researcher Dr Martina Beck and by me.

High-throughput quantitative confocal microscopy showed 40% of co-localisation between FLS2-GFP and VHA-a1-RFP endosomes (Figure 5-3). To confirm FLS2 traffics to the MVBs/LE via the TGN/EE upon flg22 perception co-localisation between FLS2-GFP and VHA-a1-RFP was monitored after ConCA treatment. Co-localisation between FLS2-GFP and VHA-a1-RFP increased significantly in the presence of ConcA (Figure 5-3). This indicated FLS2-GFP TGN/EE population is targeted to LE/MVBs. In agreement with our observation in (Figure 5-2) this number was not affected by BFA treatment, showing that those compartments are following the late endosomal pathway. Therefore, we concluded activated FLS2 traffics to the LE/MVBs via the TGN/EE in *Arabidopsis*.

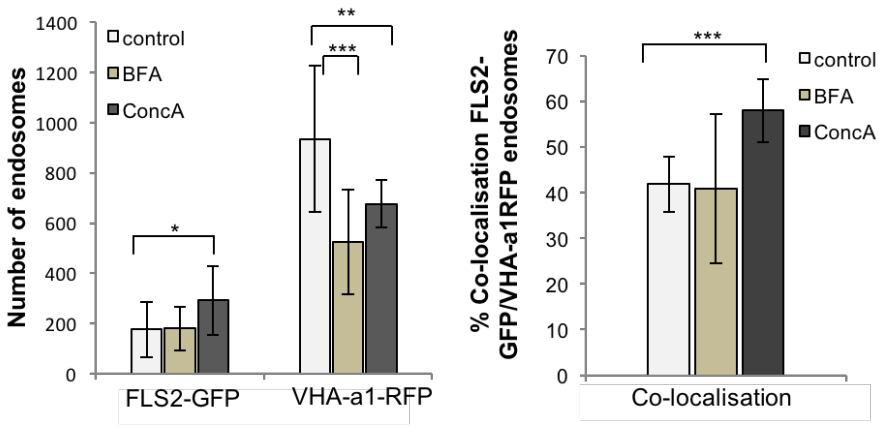

Figure 5-3 FLS2-GFP co-localises to VHa-a1-RFP after flg22.

Quantitative image analysis of FLS2-GFP and VHA-a1-RFP (left panel) endosomes and co-localisation between FLS2-GFP and VHA-a1-RFP under control conditions, BFA and ConcA. TGN=*trans*-Golgi network; EE=Early Endosome. NB the presented experiment was designed and performed by former post-doctorate researcher Dr Martina Beck and by me. Three independent biological replicates were performed.

Taken together, we observed activated and non-activated FLS2 both travelled via VHA-a1 positive compartments. Showing both non-activated and activated FLS2 pathways are shared by the TGN/EE. We concluded that, upon flg22 perception, FLS2 undergoes internalisation and enters the endocytic pathway through the TGN/EE. Thus, we demonstrated activation dependent sorting of FLS2 occurs at the *trans*-Golgi-Network. This result lead us to investigate by which mechanism FLS2 trafficking is mediated through the TGN/EE.

5.4 The Arf-GEF MIN7 mediates FLS2 trafficking via the TGN/EE upon flg22 perception.

To identify the molecular determinant of FLS2 sorting at the TGN/EE, IP/MS-MS were performed by TSL proteomic team using FLS2-GFP as a bait (Ben Khaled, unpublished). Interestingly, a TGN-localised Arf-GEF, BREFELDIN A-

INHIBITED GUANINE NUCLEOTIDE-EXCHANGE PROTEIN 5 / BFA-VISUALIZED ENDOCYTIC TRAFFICKING DEFECTIVE 1 / HOPM1 INTERACTOR 7 (BIG5/BEN1/MIN7), hereafter simply refer as MIN7 was found in FLS2 complex. MIN7 is a noteworthy candidate to investigate the link between PRR internalisation and establishment of defence (see introduction).

Taken together, I speculated that MIN7 mediates TGN/EE sorting of FLS2 upon flg22 perception. To test this, together with Heidrin Haweker the laboratory technician, we generated stable transgenic lines expressing FLS2-GFP in a *MIN7* mutant background. Meanwhile obtaining homozygous lines, I have tried to take advantage that mutants lines were available (Nomura *et al*., 2006; Tanaka *et al*., 2009) to obtain data using other tools. Thus, I wanted to observe i) FLS2-GFP endocytosis using protoplasts transformations of *min7* and *ben1-2* lines and ii) TAMRA-flg22 uptake in *min7* seedlings (Mbengue *et al*., 2016). Unfortunately, both experiments were unsuccessful, nor FLS2 internalisation or TAMRA-flg22 uptake were observed in the control conditions in protoplasts and seedlings respectively (Figure 5-4;Figure 5-5). Indeed, I could not observe FLS2 internalisation after flg22 treatment in *Arabidopsis* protoplasts. Previous study fails as well in observing FLS2 internalisation in protoplasts due to the possible involvement of cell-derived components in this process, missing in protoplasts (Ali and Reddy, 2008). Contrastingly, it seems it is suitable to study FLS2 complex activation (Lu *et al*., 2010) but not for its internalisation (Ali and Reddy, 2008). This suggests those two pathways are uncoupled.

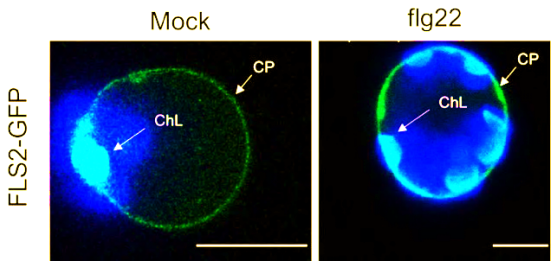

Figure 5-4 *Arabidopsis* protoplasts are not suitable to observe flg22-induced FLS2 internalisation.

Visualisation of FLS2-GFP in protoplasts. Confocal micrographs show a GFP signal localised at the cell periphery before (mock) and after flg22 treatment. Pictures were taken a day after transfection. Bar = 10 μm. Two independent biological replicates were performed.

TAMRA-flg22 is an N-terminally labelled fluorescent flg22 (Underwood and Somerville, 2013). A recent study shows TAMRA-flg22 is internalised together with FLS2, thus, can be used as a marker to follow FLS2 endosomes in *Arabidopsis* mutants lines (Mbengue *et al*., 2016). I expected to obverse the TAMRA-flg22 uptake to appear as dots inside the cell in a similar way of those observed for FLS2 endosomes (Ben Khaled *et al* ., unpublished). However, the TAMRA-flg22 experiment showed a signal at the cell periphery (CP) but not to the endosomes (Figure 5-5). Autofluorescence shows a false positive signal around the stomata (STM) but no uptake (Figure 5-5).

To summarize, both experiments were dropped out from the pipeline because the positive control did not give results

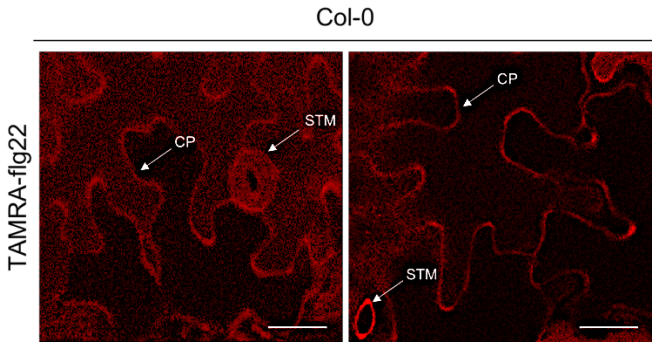

Figure 5-5 TAMRA-flg22 up take fails in Col-0 *Arabidopsis* cotyledons.
Visualisation of TAMRA-flg22 in 4-day-old Col-0 seedlings. Confocal micrographs show TAMRA-flg22 was not up taken in Col-0. Four independent biological replicates were performed.

I obtained homozygous lines from the cross between *min7* and FLS2-GFP to visualise flg22-induced Internalisation of FLS2-GFP in a *min7* mutant background. Two-week old *min7*/FLS2-GFP seedling showed no growth difference compared to FLS2-GFP (Figure 5-6; A).The expression of the T-DNA insertion and the lack of *MIN7* were tested by RT-PCR (Figure 5-6; B). I monitored FLS2-GFP subcellular localisation in the homozygous F4 line.

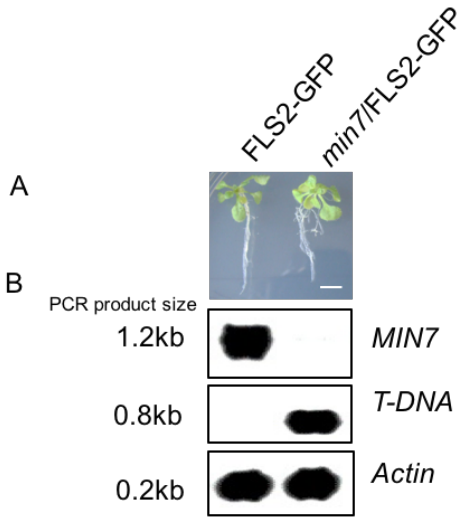

Figure 5-6 RT-PCR of *min7*/FLS2-GFP seedlings.

(A) two-week old *Arabidopsis* seedlings (B) RT-PCR to detect *MIN7* and T-DNA insertion in two-week old *Arabidopsis* seedlings. Amplification of actin is shown as a control.

Prior to flg22 treatment FLS2-GFP localised at the PM in both genotypes showing that MIN7 is not required for FLS2 secretion (Figure 5-7 left panel, Mock). By contrast, I observed that FLS2-GFP internalisation was affected in *min7* compared to Col-0 (Figure 5-7 right panel, +flg22).

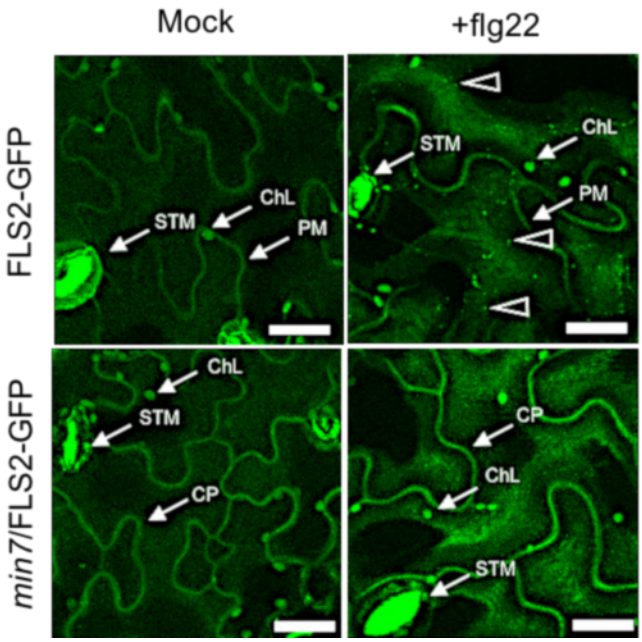

Figure 5-7 MIN7 is required for flg22-induced endocytosis of FLS2-GFP. Confocal micrographs show FLS2-GFP localisation in the absence (MOCK) or presence of 10 μM flg22 (60 min) in Col-0 and in *min7* backgrounds. Arrows show CP= cell periphery, STM = stomata, ChL = chloroplatst; arrowheads show endosomes. Scale = 20 μm. Three independent biological replicates were performed.

Confocal micrographs can be used to quantify the endosomal number in *min7* to check whether it was affected by the lack of MIN7. Thus, I performed high-throughput quantitative analysis (Beck *et al*., 2012) on *min7*/FLS2-GFP. Quantification of endosome numbers showed a significant reduction of FLS2-GFP positive spots detected in *min7* compared to Col-0 (Figure 5-8).

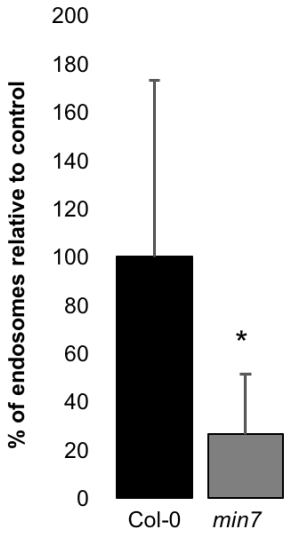

Figure 5-8 flg22-induced endosomal number is reduced in *min7* mutant background compared to Col-0.

Quantification of FLS2-GFP endosomal numbers *per* imaged area in samples challenged with flg22 in Col-0 or *min7*. Graph represents mean values ± SEM (standard error of the mean). Asterisks indicate statistical significance of P value < 0.05 based on Student's t test analysis.; Col-0 *n* = 67, min7 *n* = 106 images graphs shows one representative experiment. Four independent biological replicates were performed.

This result demonstrated FLS2 endocytosis is reduced in *min7* mutant background. Therefore, I concluded that MIN7 is required for FLS2 endocytosis. The function of ARA7/Rab F2b small GTPase is required for flg22-induced FLS2 endocytosis (Beck *et al*., 2012) and mainly label LE compartments (Takashi *et al*., 2004). I investigated whether the effect on FLS2 endocytosis in *min7* was mediated by ARA7/RabF2b by monitoring RFP-ARA7/RabF2b localisation in Col-0 and in a *min7* background. The *min7*/RFP-ARA7 lines were generated by our laboratory technician, Heidrun Häweker. Prior using those lines for microscopy, I performed a RT-PCR to observe the

expression of T-DNA insertion and the presence or absence of *MIN7* (Figure 5-9).

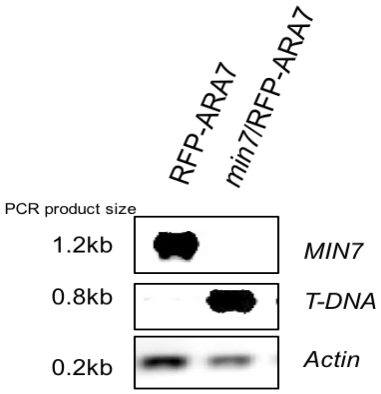

Figure 5-9 RT-PCR of *min7*/RFP-ARA7 seedlings.

RT-PCR to detect *MIN7* and T-DNA insertion in two-week old *Arabidopsis* seedlings. Amplification of Actin 2 is shown as a control.

I observed no difference in RFP-ARA7/RabF2b endosome appearance (Figure 5-11) between the two genotypes.

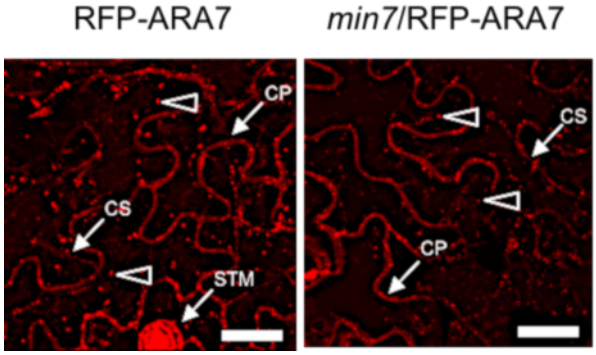

Figure 5-10 MIN7 is not required for RFP-ARA7 endosomes appearance.
Confocal micrographs show RFP-ARA7 localisation in Col-0 and in *min7* backgrounds. Arrows show CP= cell periphery, CS= cytoplasm, STM= stomata; arrowheads show endosomes. Scale = 20 μm. Three independent biological replicates were performed.

As described for *min*7/FLS2-GFP I performed high-throughput quantification of endosome numbers and showed no significant difference between the two genotypes (Figure 5-11).

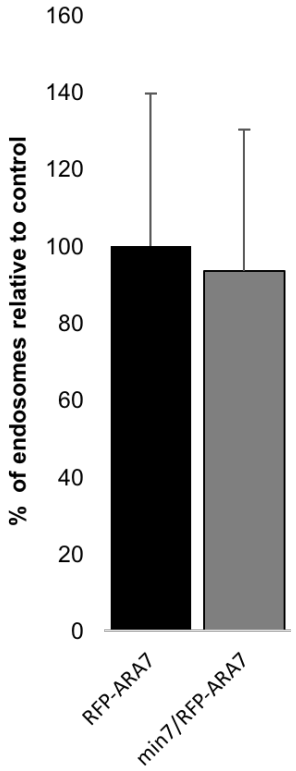

Figure 5-11 MIN7 is not required for ARA7 endosomes.
Quantification of FLS2-GFP endosomal numbers *per* imaged area in samples challenged with flg22 in Col-0 or *min7*. Graph represents mean values ± SEM (standard error of the mean); Col-0 *n* = 51, min7 *n* = 47 images graphs shows one representative experiment. Four independent biological replicates were performed.

I concluded MIN7 does not affect the late endosomal compartment. Therefore, I have evidence that MIN7 is required for FLS2 trafficking at the TGN/EE upon flg22 perception. Flg22-induced endocytosis of FLS2 leads to its vacuolar degradation (Lu *et al*., 2011; Spallek *et al*., 2013). Ligand-induced degradation of endogenous FLS2 in Ler and Col-0 has been reported (Smith *et al*., 2014b). Because ligand-induced FLS2 endocytosis is significantly reduced in *min7*

(Figure 5-8) I speculated FLS2 degradation is affected in *min7* upon flg22 elicitation. I performed an FLS2 accumulation assay in two knock-out independent lines, *min7* and *ben1-2* (Nomura *et al*., 2006; Tanaka *et al*., 2009).

I could not reproduce FLS2 accumulation assay using seedlings as described by (Smith *et al*., 2014b). Thus, I generated a different protocol for adult leaves (described in part 2.6.2 of this thesis). In *min7* and *ben1-2,* I observed FLS2 protein levels remained the same over 30 and 60 min after flg22 induction whereas I observed a lower signal in Col-0 at 30 and 60 minutes (Figure 5-12).

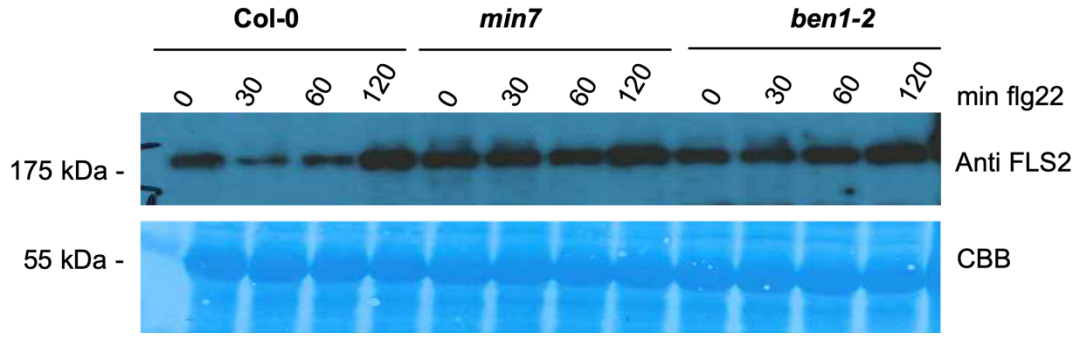

Figure 5-12 Flg22-induced degradation of FLS2 is reduced in two independent *min7* mutant background, *min7* and in *ben1-2.*

Immunoblots show FLS2 expression in 4-week-old *Arabidopsis thaliana* adult leaves treated with flg22 or with water (0) using anti-FLS2 antibody. Three independent biological replicates were performed.

This indicated that FLS2 is not degraded in *min7* and *ben1-2* compared to Col-0 after flg22 treatment. I therefore concluded MIN7 is required for ligand-induced degradation of FLS2. Interestingly, I observed an increase in FLS2 protein level at 120 minutes in all genotypes studied. This accumulation has been reported to be *de novo* accumulation of FLS2 in seedlings (Smith *et al*.,

2014b). This shows my method using adult plants is valid to observe FLS2 degradation. This suggested accumulation of newly synthesized FLS2 is not altered in *min7*. However, as described in (Smith *et al*., 2014b) a protein synthesis inhibitor must be used to confirm this hypothesis. I did not perform this experiment because protein synthesis inhibitor interferes with protein trafficking, thus, having a broad effect on the TGN integrity (Robinson *et al*., 1999).

Data shows loss-of *AtMIN7* gene function does not affect MAMP-triggered oxidative burst using *min7* (Lozano-Durán *et al*., 2013). To check if other *ben-1* responses toward flg22 treatment was similar to *min7*, I performed one ROS production assay.

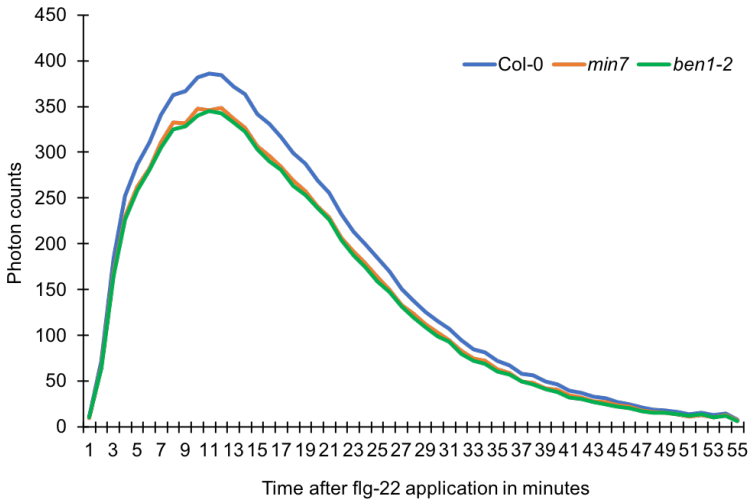

Figure 5-13 ROS production is not impaired in *min7* background.

ROS production was measured as photon count in Col-0, *min7* and *ben1-2* in response to 100 nM flg22 for 55 minutes. Two independent biological replicates were performed for Col-0 and *min7* and one biological replicate was performed for *ben1-2*.

ROS production in *ben1-2* is similar to the one observed in Col-0 and *min7*. Thus, showing flg22-induced ROS seems to be unaffected in *ben1-2.* Nevertheless, this experiment must be repeated to confirm this result.

MAPK activation and seedling growth inhibition (SGI) are canonical responses observed after flg22 treatment in *Arabidopsis* (Schwessinger *et al*., 2011). Thus, I observed that flg22-induced SGI and mitogen-associated protein kinase (MAPK) activation are not altered in *min7* (Figure 5-14;Figure 5-15). *min7* showed same growth phenotype than Col-0 before and after fl22 treatment (Figure 5-14 A). No SGI difference was observed between *min7* and Col-0 (Figure 5-14 B). After SGI, seedlings were recovered in fresh liquid MS for three days and treated with flg22 or not (mock) to observed MAPK activation. In *min7*, MAPK activation was similar then in Col-0 Figure 5-15.

Nevertheless, this experiment was performed only one time and must be repeated to confirm this result. This is in agreement with previous data revealing MAMP-induced ROS burst and stomatal closure are not impaired in *min7* (Lozano-Durán *et al*., 2013). Importantly, it is strengthening my data showing receptor internalisation and complex activation are uncoupled.

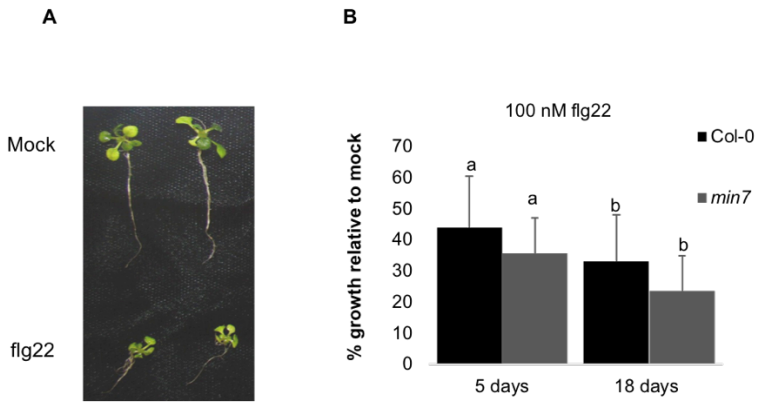

Figure 5-14 SGI induced by prolonged flg22 treatment is not impaired in *min7*.

(A) Seedling growth inhibition (SGI) was observed after 5 and (B) 18 days in a flg22 solution. Col-0 and *min7* both showed the same SGI response at 5 days this is also the case for 18 days. Growth is represented relative to untreated (mock) for each genotype ANOVA P <0.05. Three independent biological replicates were performed.

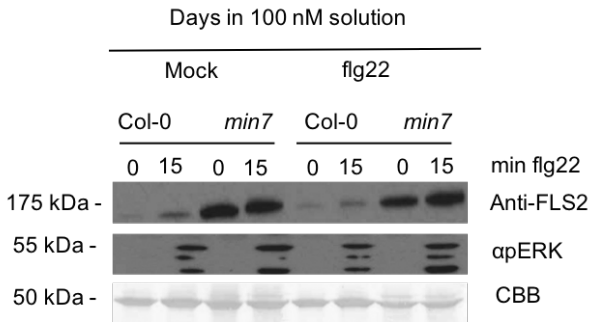

Figure 5-15 MAPK activation is not altered in *min7*.

FLS2 protein levels in *Arabidopsis* seedlings after 18 days in liquid MS (mock) or flg22 solution, were revealed by Western Blot using an anti-FLS2 antibody. A flg22 re-elicitation was performed to observe MAPK activation and was revealed using an anti pERK antibody. CBB (Coomassie brilliant blue) staining was used for loading controls. Experiment was performed once. After 15 min flg22 treatment MAPK are activated and FLS2 protein level increases in *min7*.

Interestingly, degradation of MIN7 by the bacterial effector HopM1 is required for *Pto* DC3000 virulence (Nomura *et al*., 2006).

HopM1 is a 75 KDa effector secreted by the TTSS of *Pto* DC3000 and is encoded by the conserved effectors loci (CEL) (Badel *et al*., 2006). Mutants *Pto* DC3000 strain lacking the CEL (∆ CEL) loss virulence in *Arabidopsis* (DebRoy *et al*., 2004). Expression of HopM1 in Col-0 restores virulence symptoms DC3000 ∆ CEL demonstrating HopM1 is required for DC3000 virulence despite displaying no enzymatic activity itself (Nomura *et al*., 2006). Importantly, HopM1 localises to the TGN (Nomura *et al*., 2011). HopM1 has been studied over a decade and it only recently that light was shed on HopM1-mediated virulence. For instance, evidence shows HopM1 forms complexes with host E3 ligases (Üstün *et al*., 2016) and creates an aqueous environment prone to bacterial growth (Xin *et al*., 2016). Nevertheless, if MIN7 degradation

and those two mechanisms are linked remains unknown. Therefore, I speculated HopM1-mediated degradation of MIN7 interferes with PRRs trafficking. To test this hypothesis, I observed PRR trafficking in the presence of HopM1 in a transient system. I have tried to used dexamethasone inducible HopM1 *Arabidopsis* lines (Nomura *et al*., 2006) numerous times but the lines did not germinate (Figure 5-16) despite using recommended conditions which hindered our progress towards obtaining these lines.

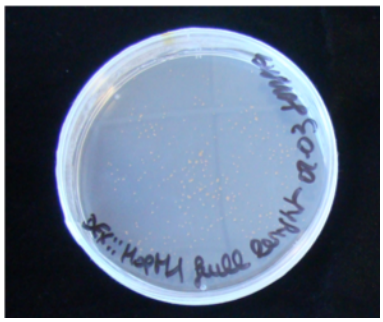

Figure 5-16 DEX::HopM1 *Arabidopsis* lines do not germinated on MS plates.

Sterilised DEX::HopM1 lines were sown on MS plates, stratified at 4°C for 2 days and placed in a growth chamber for 10 days. Seeds did not germinate despite several attempt using recommended conditions. Three independent biological replicates were performed.

5.5 HopM1 interferes with ligand-induced endocytosis of PRRs in *N. benthamiana*

To test the effect of HopM1 on PRR subcellular trafficking, I co-expressed FLS2-GFP with HopM1 or empty vector (control) in a transient *N. benthamiana* system. Similar to *Arabidopsis*, non-activated FLS2 localises to plasma membrane (PM), while flg22-induction leads to FLS2 translocation to

endosomes (Choi *et al*., 2013; Mbengue *et al*., 2016). Subsequently, I studied localisation of non-activated FLS2-GFP versus activated via laser scanning confocal microscopy (LSCM). Similarly, to what I observed in *min7* in *Arabidopsis*, I observed that HopM1 expression did not affect the subcellular localisation of non-activated FLS2 (Figure 5-17 A Mock left bottom panel), suggesting that FLS2 secretion is not affected. By contrast, FLS2 internalisation appeared reduced when co-expressed with HopM1 (Figure 5-17 A flg22 right bottom panel). Quantification of FLS2-GFP positive endosomal number revealed a strong decrease in the presence of HopM1 (Figure 5-17 B). This showed that HopM1 interfered with ligand-induced internalisation of FLS2.

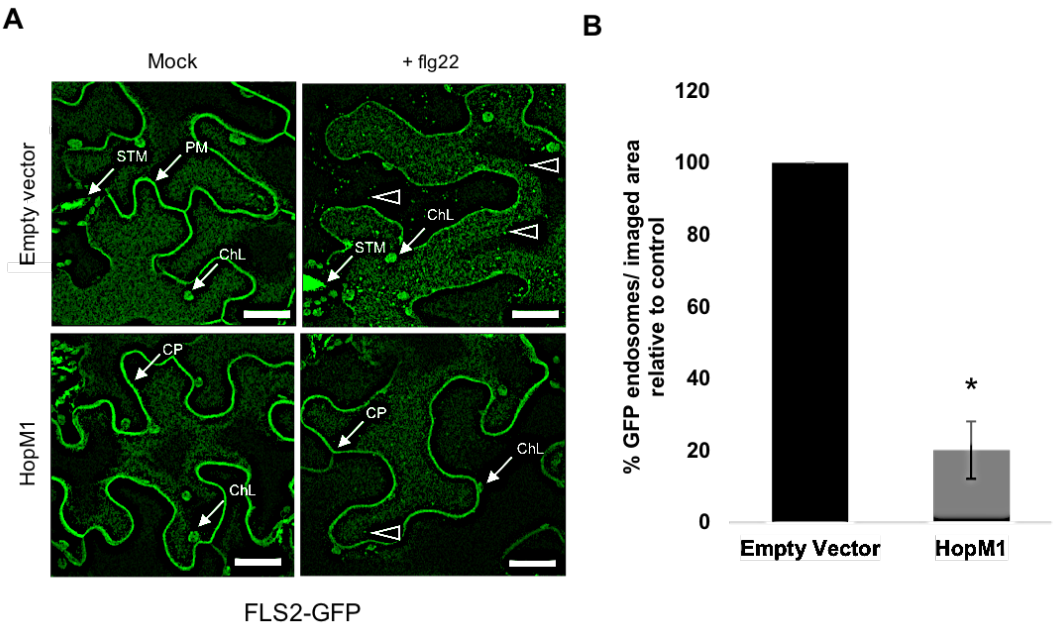

Figure 5-17 HopM1 reduces flg22-induced FLS2 endosomal number.

(A) Confocal micrographs show FLS2-GFP localisation in the absence (MOCK) or presence of 10 μM flg22 (60 min) in the presence of an empty vector or HOPM1. Arrows show cp= cell periphery, stm = stomata, clp = chlroplatst; arrowheads show endosomes. Scale = 20 μm. Confocal micrographs were taken at 2dpi (B) Quantification of FLS2-GFP endosomal numbers *per* imaged area in samples challenged with flg22 in the presence of an empty vector or HOPM1. Graphs show one representative experiment and represent mean values ± SEM (standard error of the mean); Five independent biological replicates were performed.

It has been recently described that other PRRs, like PEPR1/2 and EFR follow the same endosomal pathway after elicitation by their cognate ligands (Mbengue *et al*., 2016; Postma. *et al*., 2016). Therefore, I wanted to check whether HopM1 also affects the internalisation of other PRRs. In order to test this, I examined the effect of HopM1 on EFR-GFP endocytosis in the presence or absence (control) of elf18. I observed that expression of HopM1 did not interfere with inactive EFR-GFP localisation (mock), indicating that EFR secretion is not affected in the presence of HopM1 (Figure 5-18) A. However,

HopM1 did interfere with elf18-induced internalisation of EFR, which was observed via significant lower endosomal number compared to the control co-expressing an empty vector (control) (Figure 5-18 B). This demonstrated that HopM1 interference of ligand-induced endocytosis is not specific to FLS2, but affects also other PRRs.

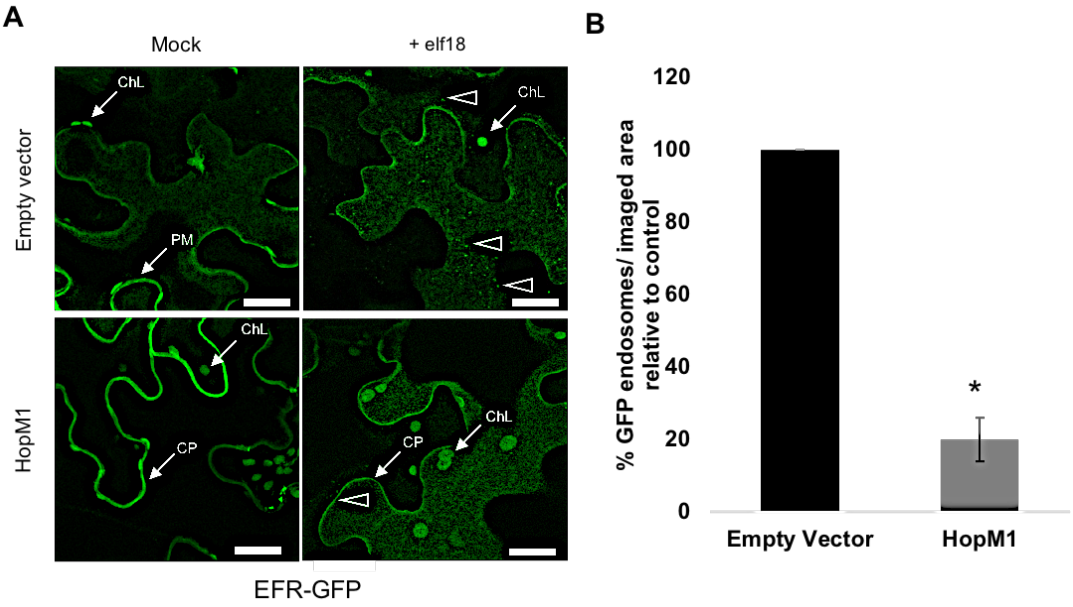

Figure 5-18 HopM1 reduces elf18-induced EFR endosomal number.
(A) Confocal micrographs show EFR-GFP localisation in the absence (MOCK) or presence of 10 μM elf18 (60 min) in the presence of an empty vector or HopM1. Arrows show CP= cell periphery, STM = stomata, ChL = chlroplatst; arrowheads show endosomes. Scale = 20 μm. Confocal micrographs were taken at 2dpi for HopM1 and 3dpi for EFR (B) Quantification of EFR-GFP endosomal numbers *per* imaged area in samples challenged with elf18 in the presence of an empty vector or HOPM1. Graphs show one representative experiment. Values represent means ± SEM; Asterisks indicate statistical significance of P value < 0.05 based on Student's t test analysis. Three independent biological replicates were performed.

Endocytosis is a conserved mechanism among PRRs and PRRs share a similar trafficking pathway (Erwig *et al*., 2017; Mbengue *et al*., 2016; Postma.

et al., 2016; Ron and Avni, 2004). Therefore, I wanted to examine whether HopM1 affects endocytosis in general or its action is specifically linked to PRRs-mediating immunity. For this reason, I tested the effect of HopM1 on BRI1. BRI1 receptor recognizes endogenously produced brassinosteroid (BL;(He *et al*., 2000) and is involved in development. In contrast to FLS2 and EFR, BRI1 undergoes endocytosis independently of its ligand (Geldner *et al*., 2007). Interestingly, HopM1 did not affect BRI1 internalization (Figure 5-23). The number of BRI1-GFP positive endosomes with and without HopM1 did not differ (Figure 5-23 B). That indicates that HopM1 does not affect the general endocytosis. Taken together, I concluded that HopM1 interferes specifically with PRR endocytosis during pathogen perception.

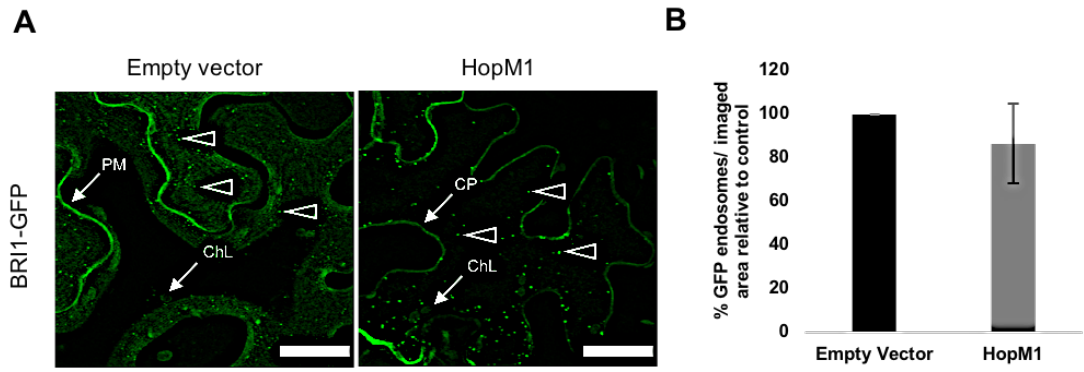

Figure 5-19 HopM1 does not affect BR1 endosomal number.

(A) Confocal micrographs show BRI1-GFP localisation in the presence of an empty vector or HopM1. Arrows show CP= cell periphery, ChL = chloroplatst; arrowheads show endosomes. Scale = 20 μm. (B) Quantification of EFR-GFP endosomal numbers *per* imaged area in samples challenged with elf18 in the presence of an empty vector or HOPM1. Graphs show one representative experiment. Values represent means ± SEM; Three independent biological replicates were performed.

Two truncated versions of HopM1 displays different functions (Nomura *et al*., 2006). HopM1$_{1\text{-}300}$ (which lacks the last 412 amino acids) is required for interaction with its host targets, whereas HopM1$_{301\text{-}712}$ (which lacks the first 300 amino acids) is suggested to be involved in host target degradation (Nomura *et al*., 2006) by recruiting host E3 ligases (Üstün *et al*., 2016). Thus, I decided to investigate which domain of HopM1 was required to disrupt flg22-induced FLS2 endocytosis. To address this question I tested the subcellular localisation of non-activated versus activated FLS2 in the presence or absence (control) of two truncated versions of HopM1 in a transient *N. benthamiana* system. I observed that HopM1$_{1\text{-}300}$ and HopM1$_{301\text{-}712}$ also affected endocytosis of activated FLS2. Quantification of FLS2 endosomes revealed a decreased of FLS2-GFP endosomal number when expressed with

truncated versions of HopM1 compared to control (Figure 5-20). Interestingly, statistical analysis showed the decrease of FLS2 positive endosomes observed with truncated versions of HopM1 was not as strong as with the full length HopM1. That shows that truncated versions were not able to fully phenocopy the effect observed with the full length HopM1 on FLS2 endocytosis. This result revealed that the full length HopM1 is required to disrupt FLS2 endocytosis. Additionally, it suggests that HopM1 interferes with FLS2 endocytosis by degradation of one/several of its targets potentially involving a host E3 ligases. It was not surprising that $HopM1_{1-300}$ affected FLS2 internalisation because it has been shown to interact with MIN7. Thus, it remains possible it has a dominant negative effect which prevent MIN7 from interacting with FLS2. The effect of $HopM1_{301-712}$ on FLS2 endocytosis was unexpected as it is not involved in interaction with MIN7 (Nomura *et al*., 2006). It suggests others yet unknow mechanisms are involved in HopM1-mediated degradation of MIN7.

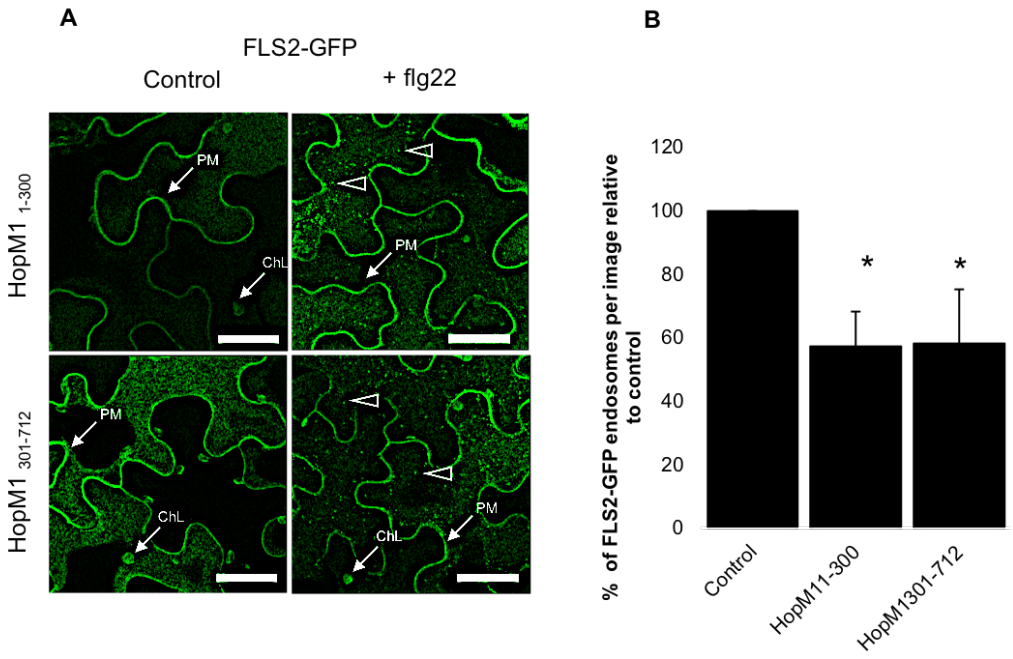

Figure 5-20 HopM1 truncated variants impair flg22-induced endocytosis of FLS2.

Transient co-expression of FLS2-GFP with an empty vector or with two HopM1 variants in *N. benthamiana* leaves at 2dpi (A) Confocal micrographs show flg22-induced endocytosis of FLS2-GFP in HopM1$_{1-300}$ or HopM1$_{301-712}$ expressing plants compared to Empty vector. Arrow indicate PM= plasma membrane, ChL= chloroplasts, arrowheads indicate endosomes. Bars = 20µm (B) FLS2-GFP endosomes number significantly decreases in HopM1 expressing cells (graph shows one representative experiment) $P<0.05$. error bars represent SD. Three independent biological replicates were performed.

To check the validity of experiments carried out with HopM1 in *N. benthamiana*, its expression was checked. The constructs used in this study were histidine-tagged, however, anti-His antibody did not give conclusive results in *N. benthamiana*. The signal observed in HopM1-His expressing tissues was comparable to the one observed in the negative control non-infiltrated *N. benthamiana* leaves (Figure 5-21). Thus, this approach was not suitable to check HopM1-His *in planta* expression.

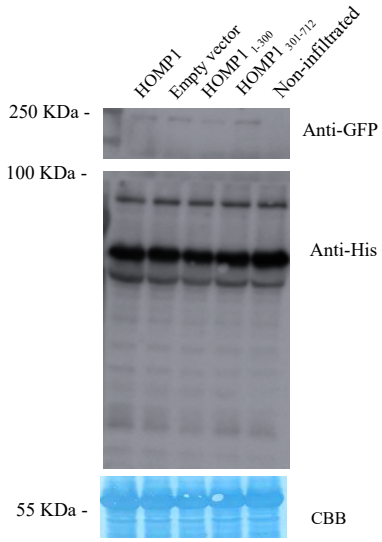

Figure 5-21 Anti-His antibody gives unspecific bands in *N. benthamiana*. Immunoblots show FLS2-GFP expression using anti-GFP antibody and unspecific bands using anti-His antibody in 2-days-old *N. benthamiana* leaves expressing HopM1 variants or why an empty vector and non-infiltrated leaves. Four independent biological replicates were performed.

Thus, RT-PCR and tissue collapse were performed to check HopM1 expression in *N. benthamiana* (Figure 5-22).

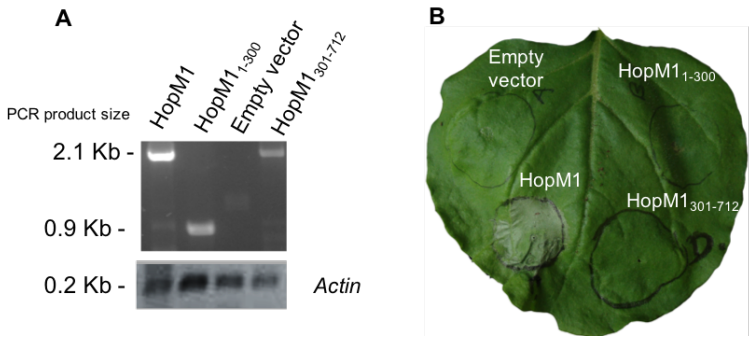

Figure 5-22 HopM1 expression and tissues collapse in *N. benthamiana*.
(A) RT-PCR to detect HopM1, HopM1$_{1-300,}$ and HopM1 $_{301-712}$ in *N. benthamiana* leaves agroinfiltrated with empty vector or with HopM1 variants at 2 dpi. Amplification of Actin is shown as a control (B) Tissue collapse in *N. benthamiana* leaves expressing HopM1 at 5 dpi. Dpi= days post infiltration. Four independent biological replicates were performed.

5.6 HopM1 interferes with FLS2 endocytosis at the *trans*-Golgi Network.

I presented post-TGN trafficking of FLS2 is mediated by MIN7 (Figure 5-7) and HopM1 interfered with FLS2 endocytosis possibly by degradation of one/several of its targets (Figure 5-17;Figure 5-20). I speculated HopM1 interferes with FLS2 endocytosis at the TGN/EE. To address this, I tested HopM1-interference with membrane compartments by LSCM. Different membrane trafficking markers have been shown to co-localize with flg22-activated FLS2 throughout the endocytic pathway (Beck *et al*., 2012; Choi *et al*., 2013). I used RFP-ARA7/RabF2b GTPase as a label for LE (Takashi *et al*., 2004), VHA-a1-RFP and CFP-SYP61 as markers for TGN/EE (Dettmer *et al*., 2006; Robert *et al*., 2008; Sanderfoot *et al*., 2001a) Additionally, I used

Golgi apparatus localised mCherry-MEMB12 (Geldner *et al*., 2009) to check HopM1 impact on the secretion pathway in *N. benthamiana*. In agreement with me finding MIN7 is not required for ARA7 internalisation in *Arabidopsis* (Figure 5-11), I observed that the localisation of RFP-ARA7 remained unaltered while co-expressed with HopM1 compared to the control (Figure 5-23). This indicated that HopM1 did not act at the late endosomal pathway. By contrast, HopM1 expression exhibited a slight effect on mCherry-MEMB12. In control conditions mCherry-MEMB12 localised to vesicles while in HopM1 expressing tissues mCherry-MEMB12 not only localised to vesicles but also to the cytoplasm which can be observed as characteristic cytoplasmic strand (CP) and nucleus (N) (Figure 5-23).This is consistent with the fact that HopM1 was shown to affect MEMB12-mediated PR-1 secretion (Gangadharan *et al*., 2013; Zhang *et al*., 2011). Interestingly, HopM1 affected the localisation and the accumulation of the TGN marker CFP-SYP61. I observed that characteristic CFP-SYP61 positive dots disappeared in the presence of HopM1 (Figure 5-23).

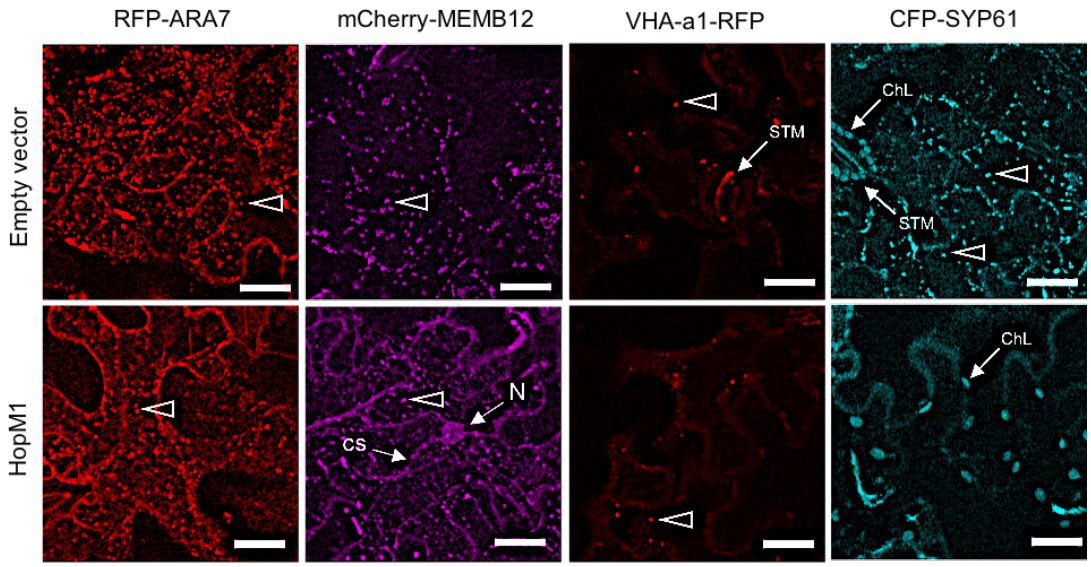

Figure 5-23 Effect of HopM1 expression on endomembrane markers in *N. benthamiana.*

Transient co-expression of endomembrane markers, RFP-ARA7, mCherry-MEMB12, VHA-a1-RFP and CFP-SYP61 in the absence (empty vector) or presence of HopM1. Confocal micrographs were taken at 2-3 dpi. ChL= chloroplasts, CS= cell periphery, N= noyau, STM= stomata. Bars = 20µm. Three independent biological replicates were performed.

Moreover, I observed HopM1 expression reduced CFP-SYP61 protein level (Figure 5-24). Notably, expression of an empty vector seems to reduce SYP61 protein as well but to a lower extend than HopM1 expression.

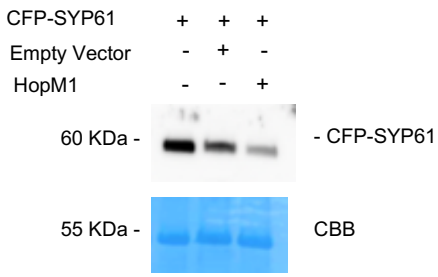

Figure 5-24 HopM1 reduced protein levels of SYP61.
Immunoblot shows CFP protein level in the absence or presence of an empty vector or HopM1 in *N. benthamiana* at 2 dpi. Protein levels were revealed by Western Blot using an anti-GFP antibody. CBB (Coomassie brilliant blue) staining was used for loading controls. Three independent biological replicates were performed. Note GFP protein level decreases in HopM1 expressing leaves compared to empty vector

Interestingly, effector expression did not impair localisation of VHA-a1-RFP (Figure 5-23). This might be attributed to the fact that SYP61 and VHA-a1 both used as TGN markers do not fully co-localise in *N. benthamiana* (Choi *et al*., 2013). Evidence shows FLS2 do not colocalises with VHA-a1 after flg22 treatment in *N. benthamiana*. Besides, evidence shows SYP61-labeled TGN domain is maturating to the MVBs whereas VHA-a1-labelled are directed back to the plasma membrane (Bottanelli *et al*., 2011; Scheuring *et al*., 2011). Hence, TGN domains exhibit different sorting function. Taken together, my data demonstrated that HopM1 interference with PRRs trafficking acts at the TGN/EE and its action is specific to SYP61-labeled TGN domain. I conclude HopM1-mediated inhibition of FLS2 acts at the TGN/MVBs transition likely in a SYP61-dependant manner.

MIN7-GFP pull-downs using the anti-SYP61 antibody (Hachez *et al*., 2014) in stable *Arabidopsis* lines expressing BEN1-GFP (Nomura *et al*., 2011) is the key experiment to carry out to unravel the role of SYP61 in the MIN7-mediated

TGN sorting of FLS2. But in interest of time the pull-downs were not performed because the end of my PhD was close.

While my data provide novel insights into the regulation of FLS2 endocytosis, it also raises several important questions. Nomura and collaborators showed that HopM1 promotes the ubiquitination and destruction of MIN7 via the host proteasome, suggesting that an E3 ligase activity is required in this process (Nomura *et al*., 2006). However, at the time I started investigation on HopM1 it remained unclear whether HopM1: i) exhibits an intrinsic E3 ligase activity; ii) (hijacks and activates a host E3 ligase ubiquitinating MIN7; or iii) HopM1 brings proteins together in a complex to degrade its host targets. To determine the mechanism underlying HopM1-mediated degradation of FLS2 my first hypothesis is that HopM1 is a structural mimic of E3 ligase and thus hijack a host E3 ligase as it has been reported previously for AvrPtoB (Abramovitch *et al*., 2006)). Indeed, the primary HopM1 amino acid sequence showed no similarities to known E3 ligases or any yet known conserved domain using the basic local alignment sequence tool (BLAST) (Figure 5-25).

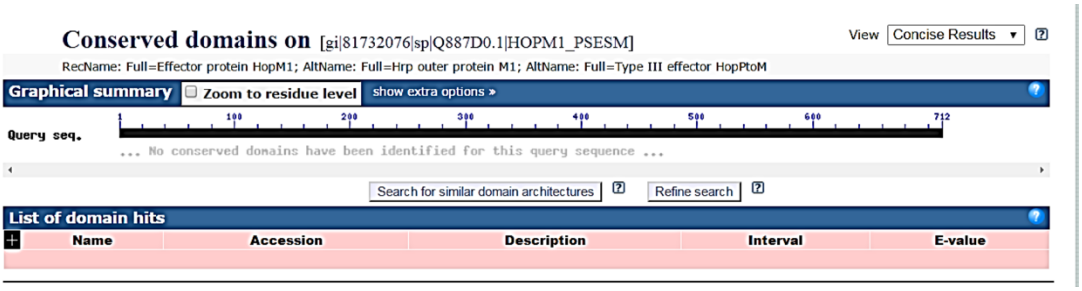

Figure 5-25 HopM1 primary amino acid sequence does not display conserved known domains.

HopM1 primary amino acid sequence in FASTA format was analysed for conserved domains search using BLAST.

This is consistent with the finding that most known bacterial E3 ligases do not share sequence similarities with eukaryotic E3 ligases. By contrast, hijacking of host E3 ligases by bacterial pathogen effectors in animals and plants has been well studied (Hicks and Galán, 2010). For instance, bacterial effectors like AvrPtoB or SapA exhibit no sequence similarities to known E3 ligases but resemble structural mimics of host E3 ligases. Revelation of the biochemical activity can be performed by structure prediction, crystallization and structure determination, and *in vitro* ubiquitination assay as has been done for AvrPtoB (Abramovitch *et al*., 2006) or SapA (Diao *et al*., 2007). Initial structure prediction using Phyre2 (Kelley *et al*., 2015) and IntFold (McGuffin, L *et al*., 2015) revealed no folds that could be strongly linked to its function. Analysis with Phyre2 resulted in 96 residues (13% of HopM1 sequence) that have been modelled with 48.7% confidence by the single highest scoring template. A highly speculative model is shown in Figure 7A. IntFold gives a model quality score of 0.0841 for the predicted structure displayed in Figure 7B, indicating a relatively poor fit. Thus, this approach failed to address my hypothesis. To

perform biochemical assay that will uncover E3 ligase activity of HopM1 I generated *LacI::GST-HopM1-His.* Nevertheless, I did not perform the ubiquitination assay experiment because i) while I generated material data showed HopM1 forms complex with host E3 ligases, thus, it is likely that HopM1 does not display an E3 ligase activity ii) when discuss with competitors working on elucidation of HopM1's activity they were already investigating this mechanism and I agreed not to work on this area. Besides, my PhD project did not aim at unravelling HopM1 activity in the first place.

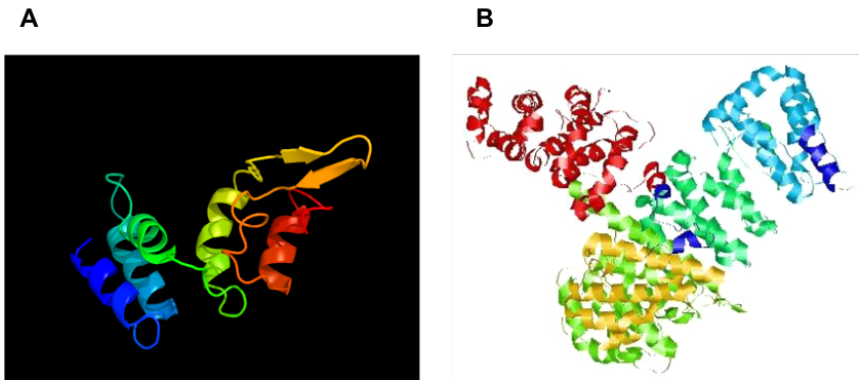

Figure 5-26 Structure prediction of HopM1.

(A) Phyre2 structure prediction on 96 residues (13% of HopM1 sequence). Image coloured by rainbow N → C terminus. Model dimensions (Å):X:39.760 Y:44.464 Z:30.364. (B) InFold structure prediction by RasMol generated image of domain prediction for HopM1. Domains are coloured in accordance with the predicted domain boundaries, using a gradient from blue through green, yellow and orange to red. A change in colour indicates a likely domain boundary. Model quality score poor 0.0841.

Notably, a recent study suggests HopM1 form complex with host E3 ligases in *N. benthamiana* (Üstün *et al.*, 2016). Therefore, I speculated that HopM1 recruits a TGN-localised E3 ligase. To test this possibility, a literature-based

search is currently on going to identify putative TGN-localised E3 ligases showing a role in immunity. An overlap with the TGN-localised SYP61 vesicle proteome will be investigating to found candidates (Drakakaki *et al*., 2012).

5.7 **Effector interference with FLS2 internalisation.**

Effector targeting trafficking components has emerged as a strategy to uncover important pathways. In order to investigate whether effector targeting of trafficking components is a conserved mechanism, I examined effectors interference with flg22-mediated internalisation and degradation of FLS2 via three collaborations with laboratories working on effectors described as inhibitors of MAMP-induced responses. The data I obtained are not displayed in my thesis because of high competition in this area our collaborators whished the data to be kept confidential until they publish the results into a publication.

5.7.1 **Effector secreted by Aphids**

Aphids are parasites insects responsible for disease transmission in plants (Gilbert and Gutierrez, 1973). Aphids feeding delivers effectors that can modulate plant responses to promote infestation (Jaouannet *et al*., 2014). The aphid effector Mp10 is secreted in salivary glands of *M. persicae* and can suppress flg22-induced ROS burst in *N. benthamiana* (Drurey *et al*., 2017). Thus, I tested the effect of Mp10 expression on the late endosomal trafficking in *N. benthamiana* (Saskia Hogenhout, JIC, UK).

5.7.2 **Effector secreted by *Xanthomonas*.**

Xanthomonas campestris pv. vesicatoria effector XopB suppresses flg22-mediated ROS burst and modulates flg22-responses genes in *Arabidopsis* (Priller *et al*., 2016). Our collaborators, Dr Sophia Sonnewald, division of biochemistry, Universitat Erlangen-Nurnberg, Germany wanted to investigate XopB-mediated suppression of PTI in more detail. Hence, upon her request I tested whether XopB interferes with FLS2 internalisation. I observed flg22-induced endocytosis of FLS2-mCherry by confocal microscopy in *N. benthamiana* plants transiently expressing XopB-GFP.

5.7.3 **RIN4**

RESISTANCE TO P. *SYRINGAE PV MACULICOLA* 1 (RPM1) interacting protein 4 (RIN4) is targeted by numerous effectors indicating a central role in immunity or pathogenicity (Mackey *et al*., 2002). RIN4 plays both positive and negative roles in various defence pathways (Van der Hoorn and Kamoun, 2008). Pr Gitta Coaker and postdoctorate researcher Dr Tania Torino- (department of plant pathology at the university of California, Davis) obtained data supporting a link between the RIN4 and traffic regulation. Thus, they established a collaboration with our team to test whether RIN4 protein complex acts as a molecular switch, hence, regulates abundance of PRRs at the PM. I tested flg22-induced degradation of FLS2 in *Arabidopsis* mutant lines linked to RIN4. I observed internalisation of FLS2-GFP in *N. benthamiana* plants transiently expressing different T7-RIN4 phosphodead and phosphomimetic variants.

5.8 General Conclusions

In the present study, together with Dr Martina Beck we demonstrated that in *Arabidopsis* tissues both activated and non-activated FLS2 traffics via the trans-Golgi network/early endosome (Figure 5-1;Figure 5-2). Using live-cell imaging and vesicles trafficking inhibitors we showed that FLS2 traffics to the MVBs/LE via the TGN/EE upon flg22 perception (Figure 5-3). A genetic approach using *min7* mutants and effector interference indicated that post-Golgi trafficking of FLS2 is dependent on the Arf-GEF MIN7. Thus, I demonstrated TGN sorting of FLS2 upon flg22 perception is mediated by MIN7. This is the first time a link between an ArfGEF and PRR trafficking is unravelled. Thus, my PhD work brings new insight into ArfGEF role in trafficking that have broad implication for our understanding of the spatiotemporal control of PRRs during PTI. My study showed MIN7 is a key player in PRRs trafficking upon MAMP perception. Hence, analysing MIN7 interactors can decipher the molecular mechanism involved in TGN maturation into MVBs during MAMP-induced internalisation of PRRs.

Using effector interference on PRRs subcellular trafficking I indirectly showed that FLS2 and EFR follow the same endosomal pathway at the TGN/EE (Figure 5-17;Figure 5-18). I showed the bacterial effector HopM1 blocks PAMP-triggered internalisation of PRRs at the SYP61-labelled TGN domain in a MIN7-dependent manner *in N. benthamiana* (Figure 5-23;Figure 5-24). This consisted in localisation studies of PRRs and different markers along the trafficking pathway together with the effector.

Overall, I demonstrated MIN7 is mediating post-Golgi trafficking of PRRs upon MAMPs perception and is targeted by bacterial effector HopM1 (Figure 5-27). FLS2 subcellular trafficking model is updated and includes a passage through the TGN which was not clear before. This brings novel insight to our understanding of the regulation of FLS2 subcellular trafficking. Besides, pathogen-induced PRRs internalisation follow a conserved pathway (Mbengue *et al*., 2016). It is most likely that the TGN sorting of PRRs is a conserved mechanism between plants species as PRRs and ArfGEFs orthologous are both present in plants genomes. My data extend our understanding on how PRR sorting is mediated upon MAMP perception Overall, my project uncovered a step of the spatio-temporal control of a major immune receptor in plants. This finding is of particular relevance as attempts to unravel PRR subcellular trafficking and its contribution to defence are ongoing.

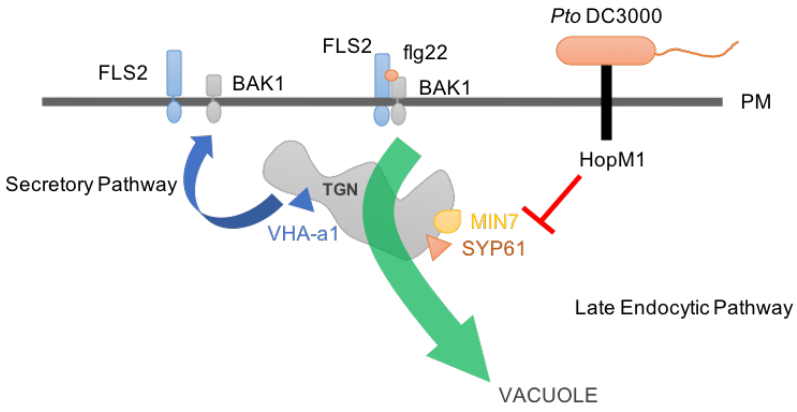

Figure 5-27 MIN7-mediated Post-Golgi trafficking of FLS2 is targeted by HopM1.

Overview of FLS2 subcellular trafficking along the *trans*-Golgi network (TGN). Secretory trafficking of FLS2 to the PM (dark blue arrow), and ligand-induced endocytosis pathways (green arrow) both are mediated by the TGN but likely by different domains. Upon ligand binding FLS2 travels via TGN for vacuolar degradation whereas upon secretion FLS2 traffics via the TGN to the plasma membrane. MIN7 is required for FLS2 internalisation but not for its secretion. The bacterial effector HopM1 targets FLS2 endocytosis in a MIN7-dependent manner likely mediated by SYP61. PM, plasma membrane; TGN, *trans*-Golgi network.

5.9 **Discussion**

While my study provides novel insights into the regulation of FLS2 endocytosis, it also raises several important questions.

1) Is FLS2 internalisation involved in establishment of defence responses?
2) Where does the coupling between receptor internalisation and newly synthetized accumulation occur?
3) How does MIN7 mediate maturation of FLS2 from TGN/EE to MVBs?

FLS2 endocytosis is uncoupled from receptor activation

The subcellular trafficking pathway of PRRs is now well described in plants (Erwig *et al*., 2017; Irani and Russinova, 2009; Mbengue *et al*., 2016; Miya *et al*., 2011; Postma. *et al*., 2016; Richter *et al*., 2007; Russinova *et al*., 2004), but the role of PRR endocytosis in PTI (PRR-triggered immunity) remains poorly understood. Trafficking components are important players during PTI but only indirect evidence exists for the involvement of receptor mediated endocytosis (RME) in establishment of PTI. For instance, genetic mutation in endocytic motif Yxxϕ of the *Le*EIX receptor compromised xylanase-induced HR in tomato (Ron and Avni, 2004). But no localisation studies of mutated *Le*EIX were performed to confirm a direct link between genetic mutation in the motif with *Le*EIX endocytosis. Although impairment in FLS2 trafficking components such as dynamin and ESCRT are associated with reduced resistance to bacterial infection (Mbengue *et al*., 2016; Smith *et al*., 2014a; Spallek *et al*., 2013) this has been found to be due to the broad role of these components in plant processes rather than being FLS2 specific. Indeed, it has

recently been shown that impairment of FLS2 endocytosis at the receptor level is not required for activation of flg22-induced immune response (Ben Khaled *unpublished*). This data shows that FLS2 endocytosis is uncoupled from receptor activation and suggests that FLS2 endocytosis follows its activation. Using a *min7* mutant background my data demonstrated that FLS2 endocytosis is uncoupled with flg22-induced MAPK activation and seedling growth inhibition (SGI) (Figure 5-14). This is supported by the fact that canonical flg22 responses are not affected in *min7* mutant background (Figure 5-14;Figure 5-15) whereas FLS2 endocytosis is strongly reduced (Figure 5-8). Thus, my results agree with previous data and indicate no role for FLS2 endocytosis in establishment of PTI.

Coupling between receptor internalisation and accumulation does not occur at the TGN/EE

Recent data support the notion that PTM of PRRs regulates accumulation of activated receptor at the PM (Ben Khaled *et al.,* unpublished). This model proposes that FLS2 is inactivated by PTM prior to its endocytosis, thus, abolishment of FLS2 endocytosis leads to accumulation of inactive receptors at the PM. Therefore, removal of inactive PRRs from the PM is required to replenish the PM with newly synthesized receptors to maintain sensitivity to bacteria (Ben Khaled *et al.,* unpublished);(Smith *et al*., 2014b). This suggests that there could be a link between internalisation of the inactive receptor pool and secretion of the newly synthesized pool. Nevertheless, how this mechanism is regulated and where the coupling occurs remains unknown.

The TGN/EE is a hub where cargoes from the secretory and endocytic pathways converge (Viotti *et al*., 2010). Using live-cell imaging and vesicle trafficking inhibitors, together with Dr Martina Beck I demonstrated that both early and late endosomal FLS2 pathways are shared by the TGN/EE, thus making the TGN a prime compartment for the coupling to take place. Using a *min7* mutant background I showed that reduction of FLS2 endocytosis and degradation are not coupled with newly synthesized receptors at the TGN/EE. This is supported by the fact that I observed over accumulation of FLS2 protein level previously described to be from *de novo* synthesis (Smith *et al*., 2014b) in Col-0 and *min7* after 120 min flg22 treatment.

Additionally, I demonstrated that this pool of receptors is signalling-competent (is able to recognise flg22 and activates signal responses). I observed a SGI and MAPK activation comparable to Col-0 in plants lacking MIN7 after long-term flg22 perception, even with abolishment of endocytosis (Figure 5-14;Figure 5-15). My observation seems in contradiction with two other studies where blocking FLS2 endocytosis has an effect on newly synthesised receptor and sensitivity to flg22 and bacteria (Smith *et al*., 2014b) (Ben Khaled *et al.*, unpublished). These experiments show that accumulation of FLS2 at the PM reduces sensitivity to flg22 and FLS2 degradation is required to re-sensitise the cell to flg22. An explanation could be that in the *min7* mutant background FLS2 does not accumulate at the PM but at the TGN/EE, thus, allowing replenishment of signalling-competent newly synthesised receptors at the PM. Besides, I observed an over accumulation of FLS2 protein level in *min7* after long term flg22 treatment, but this experiment cannot determine the

localisation of this receptor pool and it is possible this overaccumulation occurs at the TGN/EE. Detailed co-localisation studies with endomembrane markers could shed further light on the localisation of the pool of FLS2 receptor in *min7*. Furthermore, this result indicates that MIN7 does not mediate FLS2 trafficking from the PM to the TGN/EE but from TGN/EE into LE/MVBs. Importantly, this result revealed that MIN7 is required for FLS2 endocytosis at the TGN/EE but not for accumulation of signalling-competent receptor at the PM. Hence, I demonstrated that the coupling between receptor internalisation and newly synthetized accumulation does not occur at the TGN/EE.

Post-Golgi trafficking of FLS2 dependent on MIN7

MIN7 is a member of the BIG subclass in the Arf-GEF family (Sandra *et al*., 2009). This class includes five members, BIG1-4 and BIG5/BEN1/MIN7. Evidence shows that BIG1-4 perform essential functions in the late secretory pathway and post-Golgi trafficking, whereas the role of MIN7 in post-Golgi trafficking remains elusive (Richter *et al*., 2014). However, there is a role in the early endocytic pathway for PIN1 proteins during development in roots (Tanaka *et al*., 2009). I observed that FLS2 localisation at the PM is unaffected in a *min7* mutant background (Figure 5-7), showing secretion of FLS2 at the PM is not dependent on MIN7. By contrast, flg22-induced FLS2 endocytosis and degradation were both strongly reduced (Figure 5-7;Figure 5-8;Figure 5-12). FLS2 degradation in the vacuole is mediated by recognition of ubiquitinated FLS2 by the VACUOLAR PROTEIN SORTING (VPS37) of the ENDOSOMAL SORTING COMPLEX REQUIRED FOR TRANSPORT

(ESCRT-I) machinery (Göhre *et al*., 2008; Lu *et al*., 2011; Spallek *et al*., 2013). This led us to speculate that FLS2 ubiquitination at the PM is unaltered in *min7*, however because ubiquitinated FLS2 cannot mature into LE/MVBs it is consequently not recognized by the VPS37 subunit and therefore unable to undergo degradation. This places MIN7 at the post-Golgi trafficking pathway of FLS2. FLS2 ubiquitination assays and co-localisation with VPS37 in *min7* would be important experiments to investigate this hypothesis.

Flg22-induced FLS2 endocytosis requires a functional ARA7/RAbF2b pathway (Beck *et al*., 2012). I observed that the localisation and endosomal numbers of late endocytosis ARA7/RabF2b was not affected in the *min7* mutant background (Figure 5-11) showing that MIN7 is specifically involved in PRRs post-Golgi trafficking during PAMPs perception but not generally in late endocytosis. Notably, ARA7/Rab F2b mainly labels the LE/MVB endosomal population but also, to a lower extent, the TGN/EE endosomal population (Takashi *et al*., 2004). I cannot rule out the possibility that only one population is affected but it is not observable without co-localisation studies.

Chemical interference

BFA is a non-competitive inhibitor of the Arf-GEF GNOM and has been extensively used with *Arabidopsis* roots (Robinson *et al*., 2008b). Previously, GNOM was described as a TGN-localised Arf-GEF (Geldner *et al*., 2003), thus, BFA was use to observe secretory and recycling pathways (Viotti *et al*., 2010). However, recent data has reassessed GNOM localisation at the GA, and only after long-term BFA treatment is translocated into the TGN/EE

(Naramoto *et al*., 2014), suggesting a role in TGN stability. Consequently, BFA has a broad effect and must be used and interpreted while bearing this in mind. Different vesicle trafficking inhibitors could be used to dissect the identity of the endosomal population observed in *min7/*FLS2-GFP but must be used cautiously due to pleotropic effects on development and trafficking.

Effector interference with PRR trafficking

Consistent with the importance of PRR trafficking during immunity, I observed FLS2 endocytosis is targeted by the bacterial effector HopM1 (Figure 5-17). Using live-cell imaging of endomembrane markers, I demonstrated HopM1 interference with FLS2 endocytosis, which occurs at the TGN (Figure 5-23;Figure 5-24), probably in a MIN7-dependent manner. However, the role of MIN7 in immunity has been attributed to its effect on PR-1 secretion (Gangadharan *et al*., 2013) and on creating an aqueous apoplast (Xin *et al*., 2016), rather than on PRR trafficking. This is also supported by the fact that I observed FLS2 internalisation mediated by MIN7 is not required for sensitivity to flg22 (Figure 5-13;Figure 5-14;Figure 5-15).

Using HopM1 interference with PRR trafficking, I indirectly demonstrated that FLS2 and EFR both traffic via the TGN/EE after ligand perception, in a MIN7-dependent manner, confirming EFR and FLS2 share a common endosomal pathway (Mbengue *et al*., 2016). I observed ligand-induced internalisation of both FLS2 and EFR were strongly reduced in the presence of HopM1 showing that it is a suitable model to study PRR trafficking (Figure 5-17;Figure 5-18). I also demonstrated that constitutive BRI1 internalisation is not altered while co-

expressed with HopM1, indirectly showing MIN7 is not involved in recycling but specifically in the late endosomal pathway in *N. benthamiana* (Figure 5-19).

Interestingly, MG132 a proteasome inhibitor, blocks both FLS2 endocytosis and HopM1-mediated degradation of MIN7. I speculate the ubiquitination status of MIN7 is important for FLS2 sorting at the TGN, thus, for the virulence effect of HopM1 in *Arabidopsis*. Identifying the lysine(s) that can be ubiquitinated by HopM1 may unravel the mechanism by which HopM1 mediates MIN7 degradation. This could also resolve why HopM1 specifically targets MIN7 but no other members of the BIG family. Indeed, it is possible that the other BIG members cannot be ubiquitinated.

In *N. benthamiana* SYP61 and ARA7/Rab F2b only co-localise to compartments carrying endocytosed FLS2 (Choi *et al*., 2013). I speculate that MIN7 forms a complex with SYP61 to mediate FLS2 maturation from TGN/EE into LE/MVBs in *N. benthamiana*. This is supported by the observation that similarly to MIN7 (Nomura *et al*., 2006) accumulation of SYP61 is strongly reduced in the presence of HopM1 (Figure 5-23;Figure 5-24). Due to the fact that HopM1 has several targets in *Arabidopsis*, I cannot exclude that the effect observed on endomembrane markers is solely due to HopM1-mediated degradation of MIN7. Detailed co-localisation studies of FLS2-GFP with SYP61 and ARA7/Rab F2b in stable *Arabidopsis* lines expressing HopM1 under an inducible promotor, would dissect the pathway to validate this hypothesis. Nevertheless, such material is difficult to generate due to the effect

of HopM1 on the TGN/EE. Indeed, the TGN is a central organelle playing role in secretion necessary for seedling growth and development at early stages. To test whether MIN7 mediates FLS2 maturation into LE/MVBs in a SYP61-dependent manner FLS2 localisation and accumulation in *osm1* mutant background can be tested (Zhu *et al*., 2002). SYP61 is involved in embryogenesis, as a consequence *syp61* knock-out mutation is lethal (Sanderfoot *et al*., 2001b). To overcome this, transgenic *osm1* line which exhibits abnormal SYP61 transcripts, but no growth phenotype is a suitable option (Hachez *et al*., 2014). Nonetheless, where the coupling between receptor endocytosis and secretion occurs and whether MIN7 associates with SYP61 to mediate FLS2 maturation into LE/MBVs, remain to be addressed. Besides, proteomic analysis of SYP61 pull-downs are available and MIN7 was not found in SYP61 complexes (Drakakaki *et al*., 2012). MIN7 is present in low amount in *Arabidopsis* but increased after flg22 treatment (Gangadharan *et al*., 2013), thus, this could explain why MIN7 is not find in SYP61 pull-downs. To consolidate my data showing MIN7 is required for TGN/EE trafficking of activated FLS2 in a SYP61-dependant manner, SYP61 pull-downs upon flg22 perception followed by MS analysis need to be performed. Nevertheless, an endogenous MIN7 accumulation and detection need to be tested prior to such experiment.

To summarise, my work presented in this thesis aimed to better understand the spatio-temporal control of PRRs during PTI. I have successfully demonstrated: both non-activated and activated FLS2 traffic via the TGN; how is this mediated by the Arf-GEF MIN7 during flg22-induced internalisation; and

this pathway is targeted by the bacterial effector HopM1. I have studied the subcellular trafficking of FLS2 during PTI and its interference with effectors, and this will provide valuable insight for other MAMPs/PRRs systems. More details on why MIN7 among the other members of the Arf-GEF family is a key player in PRRs trafficking during PTI will require refined techniques. To understand why activated FLS2 travels via the TGN in a MIN7-dependent manner but not non-activated FLS2, looking at flg22-induced PTM of FLS2 and recognition by MIN7 complex can be useful. Ultimately, my work confirms the TGN is a key organelle where FLS2 is sorted, understanding the mechanistic underlying PRRs internalisation at the TGN would provide valuable knowledge on why PRRs are internalised after bacterial attack?

6 References

Abramovitch, R.B., Janjusevic, R., Stebbins, C.E., and Martin, G.B. (2006). Type III effector AvrPtoB requires intrinsic E3 ubiquitin ligase activity to suppress plant cell death and immunity. Proc. Natl. Acad. Sci. U. S. A. *103*, 2851–2856.

Aducci, P., Camoni, L., Marra, M., and Visconti, S. (2002). From Cytosol to Organelles: 14-3-3 Proteins as Multifunctional Regulators of Plant Cell. IUBMB Life *53*, 49–55.

Aitken, A. (2006). 14-3-3 proteins: A historic overview. Semin. Cancer Biol. *16*, 162–172.

Albert, I., Böhm, H., Albert, M., Feiler, C.E., Imkampe, J., Wallmeroth, N., Brancato, C., Raaymakers, T.M., Oome, S., Zhang, H., *et al*. (2015). An RLP23–SOBIR1–BAK1 complex mediates NLP-triggered immunity. *1*, 15140.

Albrecht, C., Russinova, E., Kemmerling, B., Kwaaitaal, M., and De Vries, S.C. (2008). *Arabidopsis* SOMATIC EMBRYOGENESIS RECEPTOR KINASE Proteins Serve Brassinosteroid-Dependent and -Independent Signaling Pathways. Plant Physiol. *148*, 611–619.

Alfano, J.R., and Collmer, A. (2004). TYPE III SECRETION SYSTEM EFFECTOR PROTEINS: Double Agents in Bacterial Disease and Plant Defense. Annu. Rev. Phytopathol. *42*, 385–414.

Ali, G.S., and Reddy, A.S.N. (2008). PAMP-triggered immunity: Early events in the activation of FLAGELLIN SENSITIVE2. Plant Signal. Behav. *3*, 423–426.

Anders, N., and Jürgens, G. (2008). Large ARF guanine nucleotide exchange factors in membrane trafficking. Cell. Mol. Life Sci. *65*, 3433–3445.

Anelli, T., and Sitia, R. (2008). Protein quality control in the early secretory pathway. EMBO J. *27*, 315–327.

Asano, T., Miwa, A., Maeda, K., Kimura, M., and Nishiuchi, T. (2013). The Secreted Antifungal Protein Thionin 2.4 in *Arabidopsis thaliana* Suppresses the Toxicity of a Fungal Fruit Body Lectin from *Fusarium graminearum*. PLoS Pathog. *9*, e1003581.

Assaad, F.F., Qiu, J.-L., Youngs, H., Ehrhardt, D., Zimmerli, L., Kalde, M., Wanner, G., Peck, S.C., Edwards, H., Ramonell, K., *et al*. (2004). The PEN1 Syntaxin Defines a Novel Cellular Compartment upon Fungal Attack and Is Required for the Timely Assembly of Papillae. Mol. Biol. Cell *15*, 5118–5129.

Badel, J.L., Shimizu, R., Oh, H.-S., and Collmer, A. (2006). A Pseudomonas syringae pv. tomato avrE1/hopM1 Mutant Is Severely Reduced in Growth and Lesion Formation in Tomato. Mol. Plant-Microbe Interact. *19*, 99–111.

Barth, M., and Holstein, S.E.H. (2004). Identification and functional characterization of Arabidopsis AP180, a binding partner of plant αC-adaptin. J. Cell Sci. *117*, 2051 LP-2062.

Bauer, Z., Gómez-Gómez, L., Boller, T., and Felix, G. (2001). Sensitivity of Different Ecotypes and Mutants ofArabidopsis thaliana toward the Bacterial Elicitor Flagellin Correlates with the Presence of Receptor-binding Sites. J. Biol. Chem. *276*, 45669–45676.

Beck, M., Zhou, J., Faulkner, C., MacLean, D., and Robatzek, S. (2012). Spatio-Temporal Cellular Dynamics of the *Arabidopsis* Flagellin Receptor Reveal Activation Status-Dependent Endosomal Sorting. Plant Cell *24*, 4205–4219.

Bednarek, P., Kwon, C., and Schulze-Lefert, P. (2010). Not a peripheral issue: secretion in plant–microbe interactions. Curr. Opin. Plant Biol. *13*, 378–387.

Bell, J.K., Mullen, G.E.D., Leifer, C.A., Mazzoni, A., Davies, D.R., and Segal, D.M. (2017). Leucine-rich repeats and pathogen recognition in Toll-like receptors. Trends Immunol. *24*, 528–533.

De Boer, A.H., Van Kleeff, P.J.M., and Gao, J. (2013). Plant 14-3-3 proteins as spiders in a web of phosphorylation. Protoplasma *250*, 425–440.

Bottanelli, F., Foresti, O., Hanton, S., and Denecke, J. (2011). Vacuolar Transport in Tobacco Leaf Epidermis Cells Involves a Single Route for Soluble Cargo and Multiple Routes for Membrane Cargo. Plant Cell *23*, 3007 LP-3025.

Bozkurt, T.O., Schornack, S., Win, J., Shindo, T., Ilyas, M., Oliva, R., Cano, L.M., Jones, A.M.E., Huitema, E., Van der Hoorn, R.A.L., *et al*. (2011). Phytophthora infestans effector AVRblb2 prevents secretion of a plant immune protease at the haustorial interface. Proc. Natl. Acad. Sci. *108*, 20832–20837.

Bozkurt, T.O., Belhaj, K., Dagdas, Y.F., Chaparro-Garcia, A., Wu, C.-H., Cano, L.M., and Kamoun, S. (2015). Rerouting of Plant Late Endocytic Trafficking Toward a Pathogen Interface. Traffic *16*, 204–226.

Brutus, A., Sicilia, F., Macone, A., Cervone, F., and De Lorenzo, G. (2010). A domain swap approach reveals a role of the plant wall-associated kinase 1 (WAK1) as a receptor of oligogalacturonides. Proc. Natl. Acad. Sci. *107*, 9452–9457.

Bücherl, C.A., Van Esse, G.W., Kruis, A., Luchtenberg, J., Westphal, A.H., Aker, J., van Hoek, A., Albrecht, C., Borst, J.W., and De Vries, S.C. (2013). Visualization of BRI1 and BAK1(SERK3) Membrane Receptor Heterooligomers during Brassinosteroid Signaling. Plant Physiol. *162*, 1911 LP-1925.

Bücherl, C.A., Bader, A., Westphal, A.H., Laptenok, S.P., and Borst, J.W. (2014). FRET-FLIM applications in plant systems. Protoplasma *251*, 383–394.

Bücherl, C.A., Jarsch, I.K., Schudoma, C., Segonzac, C., Mbengue, M., Robatzek, S., MacLean, D., Ott, T., and Zipfel, C. (2017). Plant immune and growth receptors share common signalling components but localise to distinct plasma membrane nanodomains. Elife *6*, e25114.

Cai, R., Lewis, J., Yan, S., Liu, H., Clarke, C.R., Campanile, F., Almeida, N.F., Studholme, D.J., Lindeberg, M., Schneider, D., *et al*. (2011). The Plant Pathogen Pseudomonas syringae pv. tomato Is Genetically Monomorphic and under Strong Selection to Evade Tomato Immunity. PLOS Pathog. *7*, e1002130.

Cao, Y., Liang, Y., Tanaka, K., Nguyen, C.T., Jedrzejczak, R.P., Joachimiak, A., and Stacey, G. (2014). The kinase LYK5 is a major chitin receptor in Arabidopsis and forms a chitin-induced complex with related kinase CERK1. Elife *3*, e03766.

Carrasco, J.L., Castelló, M.J., Naumann, K., Lassowskat, I., Navarrete-Gómez, M., Scheel, D., and Vera, P. (2014). *Arabidopsis* Protein Phosphatase DBP1 Nucleates a Protein Network with a Role in Regulating Plant Defense. PLoS One *9*, e90734.

Cesari, S., Bernoux, M., Moncuquet, P., Kroj, T., and Dodds, P. (2014). A novel conserved mechanism for plant NLR protein pairs: the 'integrated decoy' hypothesis. Front. Plant Sci. *5*, 606.

Chang, Y.-F., Curran, A., Woolsey, R., Quilici, D., Cushman, J, C., Mittler, R., Harmon, A., and Harper, J, F. (2009). Proteomic profiling of tandem affinity purified 14-3-3 protein complexes in *Arabidopsis thaliana*. Proteomics *9*, 2967–2985.

Chaparro-Garcia, A., Schwizer, S., Sklenar, J., Yoshida, K., Petre, B., Bos, J.I.B., Schornack, S., Jones, A.M.E., Bozkurt, T.O., and Kamoun, S. (2015). Phytophthora infestans RXLR-WY Effector AVR3a Associates with Dynamin-Related Protein 2 Required for Endocytosis of the Plant Pattern Recognition Receptor FLS2. PLoS One *10*, e0137071.

Chinchilla, D., Zipfel, C., Robatzek, S., Kemmerling, B., Nurnberger, T., Jones, J.D.G., Felix, G., and Boller, T. (2007). A flagellin-induced complex of the receptor FLS2 and BAK1 initiates plant defence. Nature *448*, 497–500.

Chinchilla, D., Shan, L., He, P., De Vries, S., and Kemmerling, B. (2009). One for all: the receptor-associated kinase BAK1. Trends Plant Sci. *14*, 535–541.

Chisholm, S.T., Coaker, G., Day, B., and Staskawicz, B.J. (2017). Host-Microbe Interactions: Shaping the Evolution of the Plant Immune Response. Cell *124*, 803–814.

Choi, S., Tamaki, T., Ebine, K., Uemura, T., Ueda, T., and Nakano, A. (2013). RABA Members Act in Distinct Steps of Subcellular Trafficking of the FLAGELLIN SENSING2 Receptor. Plant Cell *25*, 1174 LP-1187.

Clark, S.E., Williams, R.W., and Meyerowitz, E.M. (1997). The CLAVATA1 Gene Encodes a Putative Receptor Kinase That Controls Shoot and Floral Meristem Size in *Arabidopsis*. Cell *89*, 575–585.

Clarke, C.R., Chinchilla, D., Hind, S.R., Taguchi, F., Miki, R., Ichinose, Y., Martin, G.B., Leman, S., Felix, G., and Vinatzer, B.A. (2013). Allelic variation in two distinct Pseudomonas syringae flagellin epitopes modulates the strength of plant immune responses but not bacterial motility. New Phytol. *200*, 847–860.

Clouse, S.D., Langford, M., and McMorris, T.C. (1996). A Brassinosteroid-Insensitive Mutant in *Arabidopsis thaliana* Exhibits Multiple Defects in Growth and Development. Plant Physiol. *111*, 671 LP-678.

Collmer, A. (1998). Determinants of pathogenicity and avirulence in plant pathogenic bacteria. Curr. Opin. Plant Biol. *1*, 329–335.

Conner, S.D., and Schmid, S.L. (2003). Regulated portals of entry into the cell. Nature *422*, 37.

Cook, D.E., Mesarich, C.H., and Thomma, B.P.H.J. (2015). Understanding Plant Immunity as a Surveillance System to Detect Invasion. Annu. Rev. Phytopathol. *53*, 541–563.

Couto, D., and Zipfel, C. (2016). Regulation of pattern recognition receptor

signalling in plants. Nat. Rev. Immunol. *16*, 537.

Cram, W.J. (1980). Pinocytosis in Plants. New Phytol. *84*, 1–17.

Da Cunha, L., McFall, A.J., and Mackey, D. (2006). Innate immunity in plants: a continuum of layered defenses. Microbes Infect. *8*, 1372–1381.

Cunnac, S., Lindeberg, M., and Collmer, A. (2009). Pseudomonas syringae type III secretion system effectors: repertoires in search of functions. Curr. Opin. Microbiol. *12*, 53–60.

Cutler, S.R., Ehrhardt, D.W., Griffitts, J.S., and Somerville, C.R. (2000). Random GFP::cDNA fusions enable visualization of subcellular structures in cells of *Arabidopsis* at a high frequency. Proc. Natl. Acad. Sci. U. S. A. *97*, 3718–3723.

Dagdas, Y.F., Belhaj, K., Maqbool, A., Chaparro-Garcia, A., Pandey, P., Petre, B., Tabassum, N., Cruz-Mireles, N., Hughes, R.K., Sklenar, J., *et al*. (2016). An effector of the Irish potato famine pathogen antagonizes a host autophagy cargo receptor. Elife *5*, e10856.

Dangl, J.L., Horvath, D.M., and Staskawicz, B.J. (2013). Pivoting the Plant Immune System from Dissection to Deployment. Science *341*, 10.1126/science.1236011.

DebRoy, S., Thilmony, R., Kwack, Y.-B., Nomura, K., and He, S.Y. (2004). A family of conserved bacterial effectors inhibits salicylic acid-mediated basal immunity and promotes disease necrosis in plants. Proc. Natl. Acad. Sci. U. S. A. *101*, 9927 LP-9932.

Denison, F.C., Paul, A.-L., Zupanska, A.K., and Ferl, R.J. (2011). 14-3-3 proteins in plant physiology. Semin. Cell Dev. Biol. *22*, 720–727.

Dettmer, J., Hong-Hermesdorf, A., Stierhof, Y.-D., and Schumacher, K. (2006). Vacuolar H(+)-ATPase Activity Is Required for Endocytic and Secretory Trafficking in *Arabidopsis*. Plant Cell *18*, 715–730.

Diao, J., Zhang, Y., Huibregtse, J.M., Zhou, D., and Chen, J. (2007). Crystal structure of SopA, a Salmonella effector protein mimicking a eukaryotic ubiquitin ligase. Nat. Struct. &Amp;amp; Mol. Biol. *15*, 65.

Dikran, T., S., A.G., and C., H.S. (1998). Site-specific regulatory interaction between spinach leaf sucrose-phosphate synthase and 14-3-3 proteins. FEBS Lett. *435*, 110–114.

Dodds, P.N., and Rathjen, J.P. (2010). Plant immunity: towards an integrated view of plant–pathogen interactions. Nat. Rev. Genet. *11*, 539.

Donaldson, J.G., and Jackson, C.L. (2000). Regulators and effectors of the ARF GTPases. Curr. Opin. Cell Biol. *12*, 475–482.

Drakakaki, G., and Dandekar, A. (2013). Protein secretion: How many secretory routes does a plant cell have? Plant Sci. *203–204*, 74–78.

Drakakaki, G., van de Ven, W., Pan, S., Miao, Y., Wang, J., Keinath, N.F., Weatherly, B., Jiang, L., Schumacher, K., Hicks, G., *et al*. (2012). Isolation and proteomic analysis of the SYP61 compartment reveal its role in exocytic trafficking in *Arabidopsis*. Cell Res. *22*, 413–424.

Drurey, C., Mathers, T.C., Prince, D.C., Wilson, C., Caceres-Moreno, C., Mugford, S.T., and Hogenhout, S.A. (2017). Chemosensory proteins in the CSP4 clade evolved as plant immunity suppressors before two suborders of plant-feeding hemipteran insects diverged. BioRxiv.

Elena, O.-Z., Esther, S.-O., Jesús, M.M., Dolores, O.-M., and Fernando, A. (2006). Trafficking of the human transferrin receptor in plant cells: effects of tyrphostin A23 and brefeldin A. Plant J. *48*, 757–770.

Erwig, J., Ghareeb, H., Kopischke, M., Hacke, R., Matei, A., Petutschnig, E., and Lipka, V. (2017). Chitin-induced and CHITIN ELICITOR RECEPTOR KINASE1 (CERK1) phosphorylation-dependent endocytosis of *Arabidopsis thaliana* LYSIN MOTIF-CONTAINING RECEPTOR-LIKE KINASE5 (LYK5).

New Phytol. *215*, 382–396.

Faulkner, C., Petutschnig, E., Benitez-Alfonso, Y., Beck, M., Robatzek, S., Lipka, V., and Maule, A.J. (2013). LYM2-dependent chitin perception limits molecular flux via plasmodesmata. Proc. Natl. Acad. Sci. U. S. A. *110*, 9166–9170.

Felix, G., Duran, J.D., Volko, S., and Boller, T. (1999). Plants have a sensitive perception system for the most conserved domain of bacterial flagellin. Plant J. *18*, 265–276.

Frescatada-Rosa, M., Robatzek, S., and Kuhn, H. (2015). Should I stay or should I go? Traffic control for plant pattern recognition receptors. Curr. Opin. Plant Biol. *28*, 23–29.

Gampala, S.S., Kim, T.-W., He, J.-X., Tang, W., Deng, Z., Bai, M., Guan, S., Lalonde, S., Sun, Y., Gendron, J.M., *et al*. (2007). An Essential Role for 14-3-3 Proteins in Brassinosteroid Signal Transduction in *Arabidopsis*. Dev. Cell *13*, 177–189.

Gangadharan, A., Sreerekha, M.-V., Whitehill, J., Ham, J.H., and Mackey, D. (2013). The Pseudomonas syringae pv. tomato Type III Effector HopM1 Suppresses *Arabidopsis* Defenses Independent of Suppressing Salicylic Acid Signaling and of Targeting AtMIN7. PLoS One *8*, e82032.

Ganz, T. (2003). Defensins: antimicrobial peptides of innate immunity. Nat. Rev. Immunol. *3*, 710.

Gao, M., Wang, X., Wang, D., Xu, F., Ding, X., Zhang, Z., Bi, D., Cheng, Y.T., Chen, S., Li, X., *et al*. (2009). Regulation of Cell Death and Innate Immunity by Two Receptor-like Kinases in *Arabidopsis*. Cell Host Microbe *6*, 34–44.

Gardino, A.K., Smerdon, S.J., and Yaffe, M.B. (2006). Structural determinants of 14-3-3 binding specificities and regulation of subcellular localization of 14-3-3-ligand complexes: A comparison of the X-ray crystal structures of all

human 14-3-3 isoforms. Semin. Cancer Biol. *16*, 173–182.

Geldner, N., and Jürgens, G. (2006). Endocytosis in signalling and development. Curr. Opin. Plant Biol. *9*, 589–594.

Geldner, N., Friml, J., Stierhof, Y.-D., Jürgens, G., and Palme, K. (2001). Auxin transport inhibitors block PIN1 cycling and vesicle trafficking. Nature *413*, 425.

Geldner, N., Anders, N., Wolters, H., Keicher, J., Kornberger, W., Muller, P., Delbarre, A., Ueda, T., Nakano, A., and Jürgens, G. (2003). The *Arabidopsis* GNOM ARF-GEF Mediates Endosomal Recycling, Auxin Transport, and Auxin-Dependent Plant Growth. Cell *112*, 219–230.

Geldner, N., Hyman, D.L., Wang, X., Schumacher, K., and Chory, J. (2007). Endosomal signaling of plant steroid receptor kinase BRI1. Genes Dev. *21*, 1598–1602.

Geldner, N., Dénervaud-Tendon, V., Hyman, D.L., Mayer, U., Stierhof, Y.-D., and Chory, J. (2009). Rapid, combinatorial analysis of membrane compartments in intact plants with a multicolor marker set. Plant J. *59*, 169–178.

Gerd, J., and Niko, G. (2002). Protein Secretion in Plants: from the trans-Golgi Network to the Outer Space. Traffic *3*, 605–613.

Ghosh, P. (2004). Process of protein transport by the type III secretion system. Microbiol. Mol. Biol. Rev. *68*, 771–795.

Gilbert, N., and Gutierrez, A.P. (1973). A Plant-Aphid-Parasite Relationship. J. Anim. Ecol. *42*, 323–340.

Göhre, V., Spallek, T., Häweker, H., Mersmann, S., Mentzel, T., Boller, T., de Torres, M., Mansfield, J.W., and Robatzek, S. (2008). Plant Pattern-Recognition Receptor FLS2 Is Directed for Degradation by the Bacterial Ubiquitin Ligase AvrPtoB. Curr. Biol. *18*, 1824–1832.

Gómez-Gómez, L., and Boller, T. (2000). FLS2 An LRR Receptor–like Kinase Involved in the Perception of the Bacterial Elicitor Flagellin in <i>Arabidopsis</i<. Mol. Cell *5*, 1003–1011.

Gómez-Gómez, L., and Boller, T. (2018). FLS2: An LRR Receptor–like Kinase Involved in the Perception of the Bacterial Elicitor Flagellin in *Arabidopsis*. Mol. Cell *5*, 1003–1011.

Gómez-Gómez, L., Felix, G., and Boller, T. (1999). A single locus determines sensitivity to bacterial flagellin in *Arabidopsis thaliana*. Plant J. *18*, 277–284.

Grant, S.R., Fisher, E.J., Chang, J.H., Mole, B.M., and Dangl, J.L. (2006). Subterfuge and Manipulation: Type III Effector Proteins of Phytopathogenic Bacteria. Annu. Rev. Microbiol. *60*, 425–449.

Gust, A.A., and Felix, G. (2014). Receptor like proteins associate with SOBIR1-type of adaptors to form bimolecular receptor kinases. Curr. Opin. Plant Biol. *21*, 104–111.

Hachez, C., Laloux, T., Reinhardt, H., Cavez, D., Degand, H., Grefen, C., De Rycke, R., Inzé, D., Blatt, M.R., Russinova, E., *et al*. (2014). *Arabidopsis* SNAREs SYP61 and SYP121 Coordinate the Trafficking of Plasma Membrane Aquaporin PIP2;7 to Modulate the Cell Membrane Water Permeability. Plant Cell *26*, 3132 LP-3147.

Häweker, H., Rips, S., Koiwa, H., Salomon, S., Saijo, Y., Chinchilla, D., Robatzek, S., and von Schaewen, A. (2010). Pattern Recognition Receptors Require N-Glycosylation to Mediate Plant Immunity. J. Biol. Chem. *285*, 4629–4636.

He, Z., Wang, Z.-Y., Li, J., Zhu, Q., Lamb, C., Ronald, P., and Chory, J. (2000). Perception of Brassinosteroids by the Extracellular Domain of the Receptor Kinase BRI1. Science (80-.). *288*, 2360 LP-2363.

Heard, W., Sklenář, J., Tomé, D.F.A., Robatzek, S., and Jones, A.M.E. (2015).

Identification of Regulatory and Cargo Proteins of Endosomal and Secretory Pathways in *Arabidopsis thaliana* by Proteomic Dissection. Mol. Cell. Proteomics *14*, 1796–1813.

Heath, M.C. (2000). Nonhost resistance and nonspecific plant defenses. Curr. Opin. Plant Biol. *3*, 315–319.

Heese, A., Hann, D.R., Gimenez-Ibanez, S., Jones, A.M.E., He, K., Li, J., Schroeder, J.I., Peck, S.C., and Rathjen, J.P. (2007). The receptor-like kinase SERK3/BAK1 is a central regulator of innate immunity in plants. Proc. Natl. Acad. Sci. U. S. A. *104*, 12217–12222.

Helft, L., Thompson, M., and Bent, A.F. (2016). Directed Evolution of FLS2 towards Novel Flagellin Peptide Recognition. PLoS One *11*, e0157155.

van Heusden, G, P., van der Zanden, A, L., Ferl, R.J., and de Steensma, H, Y. (1996). Four Arabidopsis thaliana 14-3-3 protein isoforms can complement the lethal yeast bmh1 bmh2 double disruption. FEBS Lett. *391*, 252–256.

Hicks, S.W., and Galán, J.E. (2010). Hijacking the Host Ubiquitin Pathway: Structural Strategies of Bacterial E3 Ubiquitin Ligases. Curr. Opin. Microbiol. *13*, 41.

Hind, S.R., Strickler, S.R., Boyle, P.C., Dunham, D.M., Bao, Z., O'Doherty, I.M., Baccile, J.A., Hoki, J.S., Viox, E.G., Clarke, C.R., *et al*. (2016). Tomato receptor FLAGELLIN-SENSING 3 binds flgII-28 and activates the plant immune system. Nat. Plants *2*, 16128.

Holstein, S.E.H. (2002). Clathrin and Plant Endocytosis. Traffic *3*, 614–620.

Holstein, S.E.H., and Oliviusson, P. (2005). Sequence analysis of *Arabidopsis thaliana* E/ANTH-domain-containing proteins: membrane tethers of the clathrin-dependent vesicle budding machinery. Protoplasma *226*, 13–21.

Van der Hoorn, R.A.L., and Kamoun, S. (2008). From Guard to Decoy: A New Model for Perception of Plant Pathogen Effectors. Plant Cell *20*, 2009–2017.

Howe, C.L., Valletta, J.S., Rusnak, A.S., and Mobley, W.C. (2001). NGF Signaling from Clathrin-Coated Vesicles. Neuron *32*, 801–814.

Hsu, V.W., and Prekeris, R. (2010). Transport at the Recycling Endosome. Curr. Opin. Cell Biol. *22*, 528–534.

Hu, C.-D., Grinberg, A. V, and Kerppola, T.K. (2001). Visualization of Protein Interactions in Living Cells Using Bimolecular Fluorescence Complementation (BiFC) Analysis. In Current Protocols in Protein Science, (John Wiley & Sons, Inc.), p.

Irani, N.G., and Russinova, E. (2009). Receptor endocytosis and signaling in plants. Curr. Opin. Plant Biol. *12*, 653–659.

Jaouannet, M., Rodriguez, P.A., Thorpe, P., Lenoir, C.J.G., MacLeod, R., Escudero-Martinez, C., and Bos, J.I.B. (2014). Plant immunity in plant–aphid interactions. Front. Plant Sci. *5*, 663.

Jaspert, N., Throm, C., and Oecking, C. (2011). *Arabidopsis* 14-3-3 Proteins: Fascinating and Less Fascinating Aspects. Front. Plant Sci. *2*, 96.

Jones, J.D.G., and Dangl, J.L. (2006). The plant immune system. Nature *444*, 323–329.

Kadota, Y., Sklenar, J., Derbyshire, P., Stransfeld, L., Asai, S., Ntoukakis, V., Jones, J.D., Shirasu, K., Menke, F., Jones, A., *et al*. (2014). Direct Regulation of the NADPH Oxidase RBOHD by the PRR-Associated Kinase BIK1 during Plant Immunity. Mol. Cell *54*, 43–55.

Kaku, H., Nishizawa, Y., Ishii-Minami, N., Akimoto-Tomiyama, C., Dohmae, N., Takio, K., Minami, E., and Shibuya, N. (2006). Plant cells recognize chitin fragments for defense signaling through a plasma membrane receptor. Proc. Natl. Acad. Sci. U. S. A. *103*, 11086–11091.

Kang, Y., Jelenska, J., Cecchini, N.M., Li, Y., Lee, M.W., Kovar, D.R., and Greenberg, J.T. (2014). HopW1 from *Pseudomonas syringae* Disrupts the

Actin Cytoskeleton to Promote Virulence in Arabidopsis. PLOS Pathog. *10*, e1004232.

Keinath, N.F., Kierszniowska, S., Lorek, J., Bourdais, G., Kessler, S.A., Shimosato-Asano, H., Grossniklaus, U., Schulze, W.X., Robatzek, S., and Panstruga, R. (2010). PAMP (Pathogen-associated Molecular Pattern)-induced Changes in Plasma Membrane Compartmentalization Reveal Novel Components of Plant Immunity. J. Biol. Chem. *285*, 39140–39149.

Kelley, L.A., Mezulis, S., Yates, C.M., Wass, M.N., and Sternberg, M.J.E. (2015). The Phyre2 web portal for protein modeling, prediction and analysis. Nat. Protoc. *10*, 845.

Ben Khaled, S., Postma, J., and Robatzek, S. (2015). A Moving View: Subcellular Trafficking Processes in Pattern Recognition Receptor–Triggered Plant Immunity. Annu. Rev. Phytopathol. *53*, 379–402.

Kim, S.-J., and Federica, B. (2014). The Plant Secretory Pathway: An Essential Factory for Building the Plant Cell Wall. Plant Cell Physiol. *55*, 687–693.

Kim, T.-W., and Wang, Z.-Y. (2010). Brassinosteroid Signal Transduction from Receptor Kinases to Transcription Factors. Annu. Rev. Plant Biol. *61*, 681–704.

Lacombe, S., Rougon-Cardoso, A., Sherwood, E., Peeters, N., Dahlbeck, D., van Esse, H.P., Smoker, M., Rallapalli, G., Thomma, B.P.H.J., Staskawicz, B., *et al*. (2010). Interfamily transfer of a plant pattern-recognition receptor confers broad-spectrum bacterial resistance. Nat Biotech *28*, 365–369.

Lamaze, C. & Schmid, S.L. Recruitment of epidermal growth factor receptors into coated pits requires their activated tyrosine kinase. J. Cell Biol. *129*, 47–54.

Langhans, M., Förster, S., Helmchen, G., and D.G., R. (2011). Differential

effects of the brefeldin A analogue (6R)-hydroxy-BFA in tobacco and *Arabidopsis*. J. Exp. Bot. *62*, 2949–2957.

Le Roux, C., Huet, G., Jauneau, A., Camborde, L., Trémousaygue, D., Kraut, A., Zhou, B., Levaillant, M., Adachi, H., Yoshioka, H., *et al*. (2015). A Receptor Pair with an Integrated Decoy Converts Pathogen Disabling of Transcription Factors to Immunity. Cell *161*, 1074–1088.

Lee, H.Y., Bowen, C.H., Popescu, G.V., Kang, H.-G., Kato, N., Ma, S., Dinesh-Kumar, S., Snyder, M., and Popescu, S.C. (2011). *Arabidopsis* RTNLB1 and RTNLB2 Reticulon-Like Proteins Regulate Intracellular Trafficking and Activity of the FLS2 Immune Receptor. Plant Cell *23*, 3374 LP-3391.

Lehti-Shiu, M.D., Zou, C., Hanada, K., and Shiu, S.-H. (2009). Evolutionary History and Stress Regulation of Plant Receptor-Like Kinase/Pelle Genes. Plant Physiol. *150*, 12–26.

Li, J., Zhao-Hui, C., Batoux, M., Nekrasov, V., Roux, M., Chinchilla, D., Zipfel, C., and Jones, J.D.G. (2009). Specific ER quality control components required for biogenesis of the plant innate immune receptor EFR. Proc. Natl. Acad. Sci. U. S. A. *106*, 15973–15978.

Liebrand, T.W.H., Van Den Berg, G.C.M., Zhang, Z., Smit, P., Cordewener, J.H.G., America, A.H.P., Sklenar, J., Jones, A.M.E., Tameling, W.I.L., Robatzek, S., *et al*. (2013). Receptor-like kinase SOBIR1/EVR interacts with receptor-like proteins in plant immunity against fungal infection. Proc. Natl. Acad. Sci. *110*, 10010 LP-10015.

Liebrand, T.W.H., Van den Burg, H.A., and Joosten, M.H.A.J. (2014). Two for all: receptor-associated kinases SOBIR1 and BAK1. Trends Plant Sci. *19*, 123–132.

Lipka, V., Dittgen, J., Bednarek, P., Bhat, R., Wiermer, M., Stein, M., Landtag, J., Brandt, W., Rosahl, S., Scheel, D., *et al*. (2005). Pre- and Postinvasion Defenses Both Contribute to Nonhost Resistance in *Arabidopsis*. Science (80-

.). *310*, 1180 LP-1183.

Liu, B., Li, J.-F., Ao, Y., Qu, J., Li, Z., Su, J., Zhang, Y., Liu, J., Feng, D., Qi, K., *et al*. (2012). Lysin Motif–Containing Proteins LYP4 and LYP6 Play Dual Roles in Peptidoglycan and Chitin Perception in Rice Innate Immunity. Plant Cell *24*, 3406–3419.

Loiseau, J., and Robatzek, S. (2017). Detection and Analyses of Endocytosis of Plant Receptor Kinases BT - Plant Receptor Kinases: Methods and Protocols. In Plant Receptor Kinases, R.B. Aalen, ed. (New York, NY: Springer New York), pp. 177–189.

Lozano-Durán, R., and Robatzek, S. (2015). 14-3-3 Proteins in Plant-Pathogen Interactions. Mol. Plant-Microbe Interact. *28*, 511–518.

Lozano-Durán, R., Bourdais, G., He, S.Y., and Robatzek, S. (2013). The bacterial effector HopM1 suppresses PAMP-triggered oxidative burst and stomatal immunity. New Phytol. *202*, 259–269.

Lu, Y, J., Schornack, S., Spallek, T., Geldner, N., Chory, J., Schellmann, S., Schumacher, K., Kamoun, S., and Robatzek, S. (2012). Patterns of plant subcellular responses to successful oomycete infections reveal differences in host cell reprogramming and endocytic trafficking. Cell. Microbiol. *14*, 682–697.

Lu, D., Wu, S., Gao, X., Zhang, Y., Shan, L., and He, P. (2010). A receptor-like cytoplasmic kinase, BIK1, associates with a flagellin receptor complex to initiate plant innate immunity. Proc. Natl. Acad. Sci. U. S. A. *107*, 496–501.

Lu, D., Lin, W., Gao, X., Wu, S., Cheng, C., Avila, J., Heese, A., Devarenne, T.P., He, P., and Shan, L. (2011). Direct ubiquitination of pattern recognition receptor FLS2 attenuates plant innate immunity. Science *332*, 1439–1442.

Lu, F., Wang, H., Wang, S., Jiang, W., Shan, C., Liu, B., Yang, J., Zhang, S., and Sun, W. (2015). Enhancement of innate immune system in monocot rice

by transferring the dicotyledonous elongation factor Tu receptor EFR. J. Integr. Plant Biol. *57*, 641–652.

Lucie, T., Olivier, F., Freddy, B., Marie-Claire, H., Jani, K., Xavier, D., Marielle, A., Christophe, C., Cyril, Z., Stéphan, D., *et al*. (2013). The grapevine flagellin receptor VvFLS2 differentially recognizes flagellin-derived epitopes from the endophytic growth-promoting bacterium Burkholderia phytofirmans and plant pathogenic bacteria. New Phytol. *201*, 1371–1384.

Luna, E., Pastor, V., Robert, J., Flors, V., Mauch-Mani, B., and Ton, J. (2010). Callose Deposition: A Multifaceted Plant Defense Response. Mol. Plant-Microbe Interact. *24*, 183–193.

M., M.P., Myron, B., and E., L.J. (2011). Rice 14-3-3 protein (GF14e) negatively affects cell death and disease resistance. Plant J. *68*, 777–787.

Macho, A.P., and Zipfel, C. (2014). Plant PRRs and the Activation of Innate Immune Signaling. Mol. Cell *54*, 263–272.

Mackey, D., Holt III, B.F., Wiig, A., and Dangl, J.L. (2002). RIN4 Interacts with *Pseudomonas syringae* Type III Effector Molecules and Is Required for RPM1-Mediated Resistance in *Arabidopsis*. Cell *108*, 743–754.

De Marchis, F., Bellucci, M., and Pompa, A. (2013). Unconventional pathways of secretory plant proteins from the endoplasmic reticulum to the vacuole bypassing the Golgi complex. Plant Signal. Behav. *8*, e25129.

Mbengue, M., Bourdais, G., Gervasi, F., Beck, M., Zhou, J., Spallek, T., Bartels, S., Boller, T., Ueda, T., Kuhn, H., *et al*. (2016). Clathrin-dependent endocytosis is required for immunity mediated by pattern recognition receptor kinases. Proc. Natl. Acad. Sci. U. S. A. *113*, 11034–11039.

McGuffin, L, G., Atkins, J, D., Salehe, B, R., Shuid, A, N., and Roche, D, B. (2015). IntFOLD: an integrated server for modelling protein structures and functions from amino acid sequences. Nucleic Acids Res. *43*, W169–W173.

Medzhitov, R. (2001). Toll-like receptors and innate immunity. Nat. Rev. Immunol. *1*, 135.

Medzhitov, R., and Janeway Jr., C.A. (1997). Innate Immunity: The Virtues of a Nonclonal System of Recognition. Cell *91*, 295–298.

Meindl, T., Boller, T., and Felix, G. (2000). The Bacterial Elicitor Flagellin Activates Its Receptor in Tomato Cells According to the Address–Message Concept. Plant Cell *12*, 1783–1794.

Melotto, M., Underwood, W., and He, S.Y. (2008). Role of Stomata in Plant Innate Immunity and Foliar Bacterial Diseases. Annu. Rev. Phytopathol. *46*, 101–122.

Miya, A., Albert, P., Shinya, T., Desaki, Y., Ichimura, K., Shirasu, K., Narusaka, Y., Kawakami, N., Kaku, H., and Shibuya, N. (2007). CERK1, a LysM receptor kinase, is essential for chitin elicitor signaling in *Arabidopsis*. Proc. Natl. Acad. Sci. U. S. A. *104*, 19613–19618.

Miya, S., Maya, B., Marcelo, E., Silvia, S., Shiri, M.-B., Ran, E., Guido, S., and Adi, A. (2011). Endosomal signaling of the tomato leucine-rich repeat receptor-like protein LeEix2. Plant J. *68*, 413–423.

Mogensen, T.H. (2009). Pathogen Recognition and Inflammatory Signaling in Innate Immune Defenses. Clin. Microbiol. Rev. *22*, 240–273.

Monaghan, J., and Zipfel, C. (2012). Plant pattern recognition receptor complexes at the plasma membrane. Curr. Opin. Plant Biol. *15*, 349–357.

Monaghan, J., Matschi, S., Shorinola, O., Rovenich, H., Matei, A., Segonzac, C., Malinovsky, F.G., Rathjen, J.P., MacLean, D., Romeis, T., *et al*. (2014). The Calcium-Dependent Protein Kinase CPK28 Buffers Plant Immunity and Regulates BIK1 Turnover. Cell Host Microbe *16*, 605–615.

Mouratou, B., Biou, V., Joubert, A., Cohen, J., Shields, D.J., Geldner, N., Jürgens, G., Melançon, P., and Cherfils, J. (2005). The domain architecture of

large guanine nucleotide exchange factors for the small GTP-binding protein Arf. BMC Genomics *6*, 20.

Mukhtar, M.S., Carvunis, A.-R., Dreze, M., Epple, P., Steinbrenner, J., Moore, J., Tasan, M., Galli, M., Hao, T., Nishimura, M.T., *et al*. (2011). Independently Evolved Virulence Effectors Converge onto Hubs in a Plant Immune System Network. Science (80-.). *333*, 596 LP-601.

Muslin, A.J., Tanner, J.W., Allen, P.M., and Shaw, A.S. (1996). Interaction of 14-3-3 with Signaling Proteins Is Mediated by the Recognition of Phosphoserine. Cell *84*, 889–897.

NAKAGAWA, T., SUZUKI, T., MURATA, S., NAKAMURA, S., HINO, T., MAEO, K., TABATA, R., KAWAI, T., TANAKA, K., NIWA, Y., *et al*. (2007). Improved Gateway Binary Vectors: High-Performance Vectors for Creation of Fusion Constructs in Transgenic Analysis of Plants. Biosci. Biotechnol. Biochem. *71*, 2095–2100.

Naramoto, S., Otegui, M.S., Kutsuna, N., de Rycke, R., Dainobu, T., Karampelias, M., Fujimoto, M., Feraru, E., Miki, D., Fukuda, H., *et al*. (2014). Insights into the Localization and Function of the Membrane Trafficking Regulator GNOM ARF-GEF at the Golgi Apparatus in *Arabidopsis*. Plant Cell *26*, 3062–3076.

Nekrasov, V., Li, J., Batoux, M., Roux, M., Chu, Z.-H., Lacombe, S., Rougon, A., Bittel, P., Kiss-Papp, M., Chinchilla, D., *et al*. (2009). Control of the pattern-recognition receptor EFR by an ER protein complex in plant immunity. EMBO J. *28*, 3428–3438.

Newton, A.C., Fitt, B.D.L., Atkins, S.D., Walters, D.R., and Daniell, T.J. (2010). Pathogenesis, parasitism and mutualism in the trophic space of microbe–plant interactions. Trends Microbiol. *18*, 365–373.

Nicaise, V., Roux, M., and Zipfel, C. (2009). Recent Advances in PAMP-Triggered Immunity against Bacteria: Pattern Recognition Receptors Watch

over and Raise the Alarm. Plant Physiol. *150*, 1638 LP-1647.

Nimchuk, Z.L., Tarr, P.T., Ohno, C., Qu, X., and Meyerowitz, E.M. (2011). Plant Stem Cell Signaling Involves Ligand-Dependent Trafficking of the CLAVATA1 Receptor Kinase. Curr. Biol. *21*, 345–352.

Nomura, K., DebRoy, S., Lee, Y.H., Pumplin, N., Jones, J., and He, S.Y. (2006). A Bacterial Virulence Protein Suppresses Host Innate Immunity to Cause Plant Disease. Science (80-.). *313*, 220 LP-223.

Nomura, K., Mecey, C., Lee, Y.-N., Imboden, L.A., Chang, J.H., and He, S.Y. (2011). Effector-triggered immunity blocks pathogen degradation of an immunity-associated vesicle traffic regulator in *Arabidopsis*. Proc. Natl. Acad. Sci. *108*, 10774 LP-10779.

Ntoukakis, V., Schwessinger, B., Segonzac, C., and Zipfel, C. (2011). Cautionary Notes on the Use of C-Terminal BAK1 Fusion Proteins for Functional Studies. Plant Cell *23*, 3871 LP-3878.

Nühse, T.S., Stensballe, A., Jensen, O.N., and Peck, S.C. (2003). Large-scale Analysis of in Vivo Phosphorylated Membrane Proteins by Immobilized Metal Ion Affinity Chromatography and Mass Spectrometry. Mol. Cell. Proteomics *2*, 1234–1243.

Nürnberger, T., Brunner, F., Kemmerling, B., and Piater, L. (2004). Innate immunity in plants and animals: striking similarities and obvious differences. Immunol. Rev. *198*, 249–266.

O'Neill, L.A.J., and Bowie, A.G. (2007). The family of five: TIR-domain-containing adaptors in Toll-like receptor signalling. Nat. Rev. Immunol. *7*, 353.

Oh, C.-S., and Martin, G.B. (2011). Tomato 14-3-3 Protein TFT7 Interacts with a MAP Kinase Kinase to Regulate Immunity-associated Programmed Cell Death Mediated by Diverse Disease Resistance Proteins. J. Biol. Chem. *286*, 14129–14136.

Paul, A.-L., Sehnke, P.C., and Ferl, R.J. (2005). Isoform-specific Subcellular Localization among 14-3-3 Proteins in *Arabidopsis* Seems to be Driven by Client Interactions. Mol. Biol. Cell *16*, 1735–1743.

Paul, A.-L., Liu, L., McClung, S., Laughner, B., Chen, S., and Ferl, R.J. (2009). Comparative Interactomics: Analysis of *Arabidopsis* 14-3-3 Complexes Reveals Highly Conserved 14-3-3 Interactions between Humans and Plants. J. Proteome Res. *8*, 1913–1924.

Paul, A.-L., Denison, F.C., Schultz, E.R., Zupanska, A.K., and Ferl, R.J. (2012). 14-3-3 phosphoprotein interaction networks – does isoform diversity present functional interaction specification? Front. Plant Sci. *3*, 190.

Peng, K.-C., Wang, C.-W., Wu, C.-H., Huang, C.-T., and Liou, R.-F. (2015). Tomato SOBIR1/EVR Homologs Are Involved in Elicitin Perception and Plant Defense Against the Oomycete Pathogen Phytophthora parasitica. Mol. Plant-Microbe Interact. *28*, 913–926.

Pérez-Gómez, J., and Moore, I. (2007). Plant Endocytosis: It Is Clathrin after All. Curr. Biol. *17*, R217–R219.

Perraki, A., DeFalco, T.A., Derbyshire, P., Avila, J., Séré, D., Sklenar, J., Qi, X., Stransfeld, L., Schwessinger, B., Kadota, Y., *et al*. (2018). Phosphocode-dependent functional dichotomy of a common co-receptor in plant signalling. Nature *561*, 248–252.

Petosa, C., Masters, S.C., Bankston, L.A., Pohl, J., Wang, B., Fu, H., and Liddington, R.C. (1998). 14-3-3ζ Binds a Phosphorylated Raf Peptide and an Unphosphorylated Peptide via Its Conserved Amphipathic Groove. J. Biol. Chem. *273*, 16305–16310.

Piccinini, A.M., and Midwood, K.S. (2010). DAMPening Inflammation by Modulating TLR Signalling. Mediators Inflamm. *2010*, 672395.

Postma., J., Liebrand, T.W.H., Bi, G., Evrard, A., Ruby, R.B., Mbengue, M.,

Kuhn, H., Joosten, M.H.A., and Robatzek, S. (2016). Avr4 promotes Cf-4 receptor-like protein association with the BAK1/SERK3 receptor-like kinase to initiate receptor endocytosis and plant immunity. New Phytol. *210*, 627–642.

Priller, J.P.R., Reid, S., Konein, P., Dietrich, P., and Sonnewald, S. (2016). The *Xanthomonas campestris pv. vesicatoria* Type-3 Effector XopB Inhibits Plant Defence Responses by Interfering with ROS Production. PLoS One *11*, e0159107.

Ranf, S., Gisch, N., Schäffer, M., Illig, T., Westphal, L., Knirel, Y.A., Sánchez-Carballo, P.M., Zähringer, U., Hückelhoven, R., Lee, J., *et al*. (2015). A lectin S-domain receptor kinase mediates lipopolysaccharide sensing in *Arabidopsis thaliana*. Nat. Immunol. *16*, 426.

Richter, S., Geldner, N., Schrader, J., Wolters, H., Stierhof, Y.-D., Rios, G., Koncz, C., Robinson, D.G., and Jürgens, G. (2007). Functional diversification of closely related ARF-GEFs in protein secretion and recycling. Nature *448*, 488.

Richter, S., Müller, L.M., Stierhof, Y.-D., Mayer, U., Takada, N., Kost, B., Vieten, A., Geldner, N., Koncz, C., and Jürgens, G. (2011). Polarized cell growth in *Arabidopsis* requires endosomal recycling mediated by GBF1-related ARF exchange factors. Nat. Cell Biol. *14*, 80.

Richter, S., Kientz, M., Brumm, S., Nielsen, M.E., Park, M., Gavidia, R., Krause, C., Voss, U., Beckmann, H., Mayer, U., *et al*. (2014). Delivery of endocytosed proteins to the cell–division plane requires change of pathway from recycling to secretion. Elife *3*, e02131.

Rivas, S., and Thomas, C.M. (2005). Molecular Interactions Between Tomato and the Leaf Mold Pathogen Cladosporium fulvum. Annu. Rev. Phytopathol. *43*, 395–436.

Robatzek, S., Chinchilla, D., and Boller, T. (2006). Ligand-induced endocytosis of the pattern recognition receptor FLS2 in *Arabidopsis*. Genes

Dev. *20*, 537–542.

Robatzek, S., Bittel, P., Chinchilla, D., Köchner, P., Felix, G., Shiu, S.-H., and Boller, T. (2007). Molecular identification and characterization of the tomato flagellin receptor LeFLS2, an orthologue of *Arabidopsis* FLS2 exhibiting characteristically different perception specificities. Plant Mol. Biol. *64*, 539–547.

Robert, S., Chary, S.N., Drakakaki, G., Li, S., Yang, Z., Raikhel, N. V, and Hicks, G.R. (2008). Endosidin1 defines a compartment involved in endocytosis of the brassinosteroid receptor BRI1 and the auxin transporters PIN2 and AUX1. Proc. Natl. Acad. Sci. *105*, 8464 LP-8469.

Robinson, D.G., Langhans, M., Saint-Jore-Dupas, C., and Hawes, C. (2008a). BFA effects are tissue and not just plant specific. Trends Plant Sci. *13*, 405–408.

Robinson, D.G., Jiang, L., and Schumacher, K. (2008b). The Endosomal System of Plants: Charting New and Familiar Territories. Plant Physiol. *147*, 1482–1492.

Robinson, J.S., Albert, A.C., and Morris, D.A. (1999). Differential Effects of Brefeldin A and Cycloheximide on the Activity of Auxin Efflux Carriers in Cucurbita pepo L. J. Plant Physiol. *155*, 678–684.

Ron, M., and Avni, A. (2004). The Receptor for the Fungal Elicitor Ethylene-Inducing Xylanase Is a Member of a Resistance-Like Gene Family in Tomato. Plant Cell *16*, 1604 LP-1615.

Russinova, E., Borst, J.-W., Kwaaitaal, M., Caño-Delgado, A., Yin, Y., Chory, J., and De Vries, S.C. (2004). Heterodimerization and Endocytosis of *Arabidopsis* Brassinosteroid Receptors BRI1 and AtSERK3 (BAK1). Plant Cell *16*, 3216 LP-3229.

Saijo, Y., Tintor, N., Lu, X., Rauf, P., Pajerowska-Mukhtar, K., Häweker, H.,

Dong, X., Robatzek, S., and Schulze-Lefert, P. (2009). Receptor quality control in the endoplasmic reticulum for plant innate immunity. EMBO J. *28*, 3439 LP-3449.

Sanderfoot, A.A., Kovaleva, V., Bassham, D.C., and Raikhel, N. V (2001a). Interactions between Syntaxins Identify at Least Five SNARE Complexes within the Golgi/Prevacuolar System of the *Arabidopsis* Cell. Mol. Biol. Cell *12*, 3733–3743.

Sanderfoot, A.A., Pilgrim, M., Adam, L., and Raikhel, N. V (2001b). Disruption of Individual Members of *Arabidopsis* Syntaxin Gene Families Indicates Each Has Essential Functions. Plant Cell *13*, 659 LP-666.

Sandor, R., Der, C., Grosjean, K., Anca, I., Noirot, E., Leborgne-Castel, N., Lochman, J., Simon-Plas, F., and Gerbeau-Pissot, P. (2016). Plasma membrane order and fluidity are diversely triggered by elicitors of plant defence. J. Exp. Bot. *67*, 5173–5185.

Sandra, R., Ute, V., and Gerd, J. (2009). Post-Golgi Traffic in Plants. Traffic *10*, 819–828.

Sarris, P.F., Duxbury, Z., Huh, S.U., Ma, Y., Segonzac, C., Sklenar, J., Derbyshire, P., Cevik, V., Rallapalli, G., Saucet, S.B., *et al*. (2015). A Plant Immune Receptor Detects Pathogen Effectors that Target WRKY Transcription Factors. Cell *161*, 1089–1100.

Scheuring, D., Viotti, C., Krüger, F., Künzl, F., Sturm, S., Bubeck, J., Hillmer, S., Frigerio, L., Robinson, D.G., Pimpl, P., *et al*. (2011). Multivesicular Bodies Mature from the Trans-Golgi Network/Early Endosome in *Arabidopsis*. Plant Cell *23*, 3463–3481.

Schoonbeek, H.-J., Wang, H.-H., Stefanato, F.L., Craze, M., Bowden, S., Wallington, E., Zipfel, C., and Ridout, C.J. (2015). Arabidopsis EF-Tu receptor enhances bacterial disease resistance in transgenic wheat. New Phytol. *206*, 606–613.

Schwessinger, B., Roux, M., Kadota, Y., Ntoukakis, V., Sklenar, J., Jones, A., and Zipfel, C. (2011). Phosphorylation-Dependent Differential Regulation of Plant Growth, Cell Death, and Innate Immunity by the Regulatory Receptor-Like Kinase BAK1. PLoS Genet. *7*, e1002046.

Serrano, M., Coluccia, F., Torres, M., L'Haridon, F., and Métraux, J.-P. (2014). The cuticle and plant defense to pathogens. Front. Plant Sci. *5*, 274.

Shan, L., He, P., Li, J., Heese, A., Peck, S.C., Nürnberger, T., Martin, G.B., and Sheen, J. (2008). Bacterial Effectors Target the Common Signaling Partner BAK1 to Disrupt Multiple MAMP Receptor-Signaling Complexes and Impede Plant Immunity. Cell Host Microbe *4*, 17–27.

Shiu, S.-H., and Bleecker, A.B. (2001). Receptor-like kinases from *Arabidopsis* form a monophyletic gene family related to animal receptor kinases. Proc. Natl. Acad. Sci. U. S. A. *98*, 10763–10768.

Shpak, E.D., McAbee, J.M., Pillitteri, L.J., and Torii, K.U. (2005). Stomatal Patterning and Differentiation by Synergistic Interactions of Receptor Kinases. Science (80-.). *309*, 290 LP-293.

Shuang, H., Pin-Fang, L., Dominic, F., E., P.J., M., T.J., and Subhas, C. (1991). Growth modulation by epidermal growth factor (EGF) in human colonic carcinoma cells: Constitutive expression of the human EGF gene. J. Cell. Physiol. *148*, 220–227.

Sigismund, S., Argenzio, E., Tosoni, D., Cavallaro, E., Polo, S., and Di Fiore, P.P. (2008). Clathrin-Mediated Internalization Is Essential for Sustained EGFR Signaling but Dispensable for Degradation. Dev. Cell *15*, 209–219.

Smith, J.M., Mitchell, A., Li, G., Ding, S., Fitzmaurice, A.M., Ryan, K., Crowe, S., and Goldberg, J.B. (2003). Toll-like Receptor (TLR) 2 and TLR5, but Not TLR4, Are Required for Helicobacter pylori-induced NF-κB Activation and Chemokine Expression by Epithelial Cells. J. Biol. Chem. *278*, 32552–32560.

Smith, J.M., Leslie, M.E., Robinson, S.J., Korasick, D.A., Zhang, T., Backues, S.K., Cornish, P. V, Koo, A.J., Bednarek, S.Y., and Heese, A. (2014a). Loss of Arabidopsis thaliana Dynamin-Related Protein 2B Reveals Separation of Innate Immune Signaling Pathways. PLOS Pathog. *10*, e1004578.

Smith, J.M., Salamango, D.J., Leslie, M.E., Collins, C.A., and Heese, A. (2014b). Sensitivity to Flg22 Is Modulated by Ligand-Induced Degradation and de Novo Synthesis of the Endogenous Flagellin-Receptor FLAGELLIN-SENSING2. Plant Physiol. *164*, 440–454.

Spallek, T., Beck, M., Ben Khaled, S., Salomon, S., Bourdais, G., Schellmann, S., and Robatzek, S. (2013). ESCRT-I Mediates FLS2 Endosomal Sorting and Plant Immunity. PLoS Genet. *9*, e1004035.

Speth, E.B., Imboden, L., Hauck, P., and He, S.Y. (2009). Subcellular Localization and Functional Analysis of the *Arabidopsis* GTPase RabE. Plant Physiol. *149*, 1824–1837.

Stanislas, T., Bouyssie, D., Rossignol, M., Vesa, S., Fromentin, J., Morel, J., Pichereaux, C., Monsarrat, B., and Simon-Plas, F. (2009). Quantitative Proteomics Reveals a Dynamic Association of Proteins to Detergent-resistant Membranes upon Elicitor Signaling in Tobacco. Mol. Cell. Proteomics *8*, 2186–2198.

Stein, M., Dittgen, J., Sánchez-Rodríguez, C., Hou, B.-H., Molina, A., Schulze-Lefert, P., Lipka, V., and Somerville, S. (2006). *Arabidopsis* PEN3/PDR8, an ATP Binding Cassette Transporter, Contributes to Nonhost Resistance to Inappropriate Pathogens That Enter by Direct Penetration. Plant Cell *18*, 731–746.

Su, W., Liu, Y., Xia, Y., Hong, Z., and Li, J. (2011). Conserved endoplasmic reticulum-associated degradation system to eliminate mutated receptor-like kinases in *Arabidopsis*. Proc. Natl. Acad. Sci. U. S. A. *108*, 870–875.

Sun, W., Dunning, F.M., Pfund, C., Weingarten, R., and Bent, A.F. (2006).

Within-Species Flagellin Polymorphism in Xanthomonas campestris pv campestris and Its Impact on Elicitation of Arabidopsis FLAGELLIN SENSING2–Dependent Defenses. Plant Cell *18*, 764 LP-779.

Sun, Y., Li, L., Macho, A.P., Han, Z., Hu, Z., Zipfel, C., Zhou, J.-M., and Chai, J. (2013). Structural Basis for flg22-Induced Activation of the *Arabidopsis* FLS2-BAK1 Immune Complex. Science (80-.). *342*, 624 LP-628.

Takashi, U., Tomohiro, U., H., S.M., and Akihiko, N. (2004). Functional differentiation of endosomes in *Arabidopsis* cells. Plant J. *40*, 783–789.

Takeo, K., and Ito, T. (2017). Subcellular localization of VIP1 is regulated by phosphorylation and 14-3-3 proteins. FEBS Lett. *591*, 1972–1981.

Tanaka, H., Kitakura, S., De Rycke, R., De Groodt, R., and Friml, J. (2009). Fluorescence Imaging-Based Screen Identifies ARF GEF Component of Early Endosomal Trafficking. Curr. Biol. *19*, 391–397.

Tanji, T., and Ip, Y.T. (2005). Regulators of the Toll and Imd pathways in the *Drosophila* innate immune response. Trends Immunol. *26*, 193–198.

Tao, Y., Xie, Z., Chen, W., Glazebrook, J., Chang, H.-S., Han, B., Zhu, T., Zou, G., and Katagiri, F. (2003). Quantitative Nature of *Arabidopsis* Responses during Compatible and Incompatible Interactions with the Bacterial Pathogen Pseudomonas syringae. Plant Cell *15*, 317–330.

Thomma, B.P.H.J., Nürnberger, T., and Joosten, M.H.A.J. (2011). Of PAMPs and Effectors: The Blurred PTI-ETI Dichotomy. Plant Cell *23*, 4 LP-15.

Tintor, N., and Saijo, Y. (2014). ER-mediated control for abundance, quality, and signaling of transmembrane immune receptors in plants. Front. Plant Sci. *5*, 65.

Ton, J., and Mauch-Mani, B. (2004). β-amino-butyric acid-induced resistance against necrotrophic pathogens is based on ABA-dependent priming for callose. Plant J. *38*, 119–130.

Tsuda, K., and Katagiri, F. (2010). Comparing signaling mechanisms engaged in pattern-triggered and effector-triggered immunity. Curr. Opin. Plant Biol. *13*, 459–465.

Ueda,Takashi, Yamaguchi, M., Uchimiya, H., and Nakano, A. (2001). Ara6, a plant-unique novel type Rab GTPase, functions in the endocytic pathway of Arabidopsis thaliana. EMBO J. *20*, 4730–4741.

Underwood, W., and Somerville, S.C. (2013). Perception of conserved pathogen elicitors at the plasma membrane leads to relocalization of the *Arabidopsis* PEN3 transporter. Proc. Natl. Acad. Sci. U. S. A. *110*, 12492–12497.

Üstün, S., Sheikh, A., Gimenez-Ibanez, S., Jones, A., Ntoukakis, V., and Börnke, F. (2016). The Proteasome Acts as a Hub for Plant Immunity and Is Targeted by Pseudomonas Type III Effectors. Plant Physiol. *172*, 1941–1958.

Vetter, M.M., Kronholm, I., He, F., Häweker, H., Reymond, M., Bergelson, J., and Robatzek, S. (2012). Flagellin perception varies quantitatively in *Arabidopsis thaliana* and its relatives. Mol. Biol. Evol. *26*, 1655–1667.

Viotti, C., Bubeck, J., Stierhof, Y.-D., Krebs, M., Langhans, M., Van den Berg, W., Van Dongen, W., Richter, S., Geldner, N., Takano, J., *et al*. (2010). Endocytic and Secretory Traffic in *Arabidopsis* Merge in the Trans-Golgi Network/Early Endosome, an Independent and Highly Dynamic Organelle. Plant Cell *22*, 1344–1357.

Vorwerk, S., Somerville, S., and Somerville, C. (2004). The role of plant cell wall polysaccharide composition in disease resistance. Trends Plant Sci. *9*, 203–209.

De Vries, S.C. (2007). 14-3-3 Proteins in Plant Brassinosteroid Signaling. Dev. Cell *13*, 162–164.

Wang, B., Yang, H., Liu, Y.-C., Jelinek, T., Zhang, L., Ruoslahti, E., and Fu,

H. (1999). Isolation of High-Affinity Peptide Antagonists of 14-3-3 Proteins by Phage Display. Biochemistry *38*, 12499–12504.

Wang, D., Weaver, N.D., Kesarwani, M., and Dong, X. (2005). Induction of Protein Secretory Pathway Is Required for Systemic Acquired Resistance. Science (80-.). *308*, 1036 LP-1040.

Wang, G., Roux, B., Feng, F., Guy, E., Li, L., Li, N., Zhang, X., Lautier, M., Jardinaud, M.-F., Chabannes, M., *et al*. (2015a). The Decoy Substrate of a Pathogen Effector and a Pseudokinase Specify Pathogen-Induced Modified-Self Recognition and Immunity in Plants. Cell Host Microbe *18*, 285–295.

Wang, L., Albert, M., Einig, E., Fürst, U., Krust, D., and Felix, G. (2016). The pattern-recognition receptor CORE of Solanaceae detects bacterial cold-shock protein. Nat. Plants *2*, 16185.

Wang, S., Sun, Z., Wang, H., Liu, L., Lu, F., Yang, J., Zhang, M., Zhang, S., Guo, Z., Bent, A.F., *et al*. (2015b). Rice OsFLS2-Mediated Perception of Bacterial Flagellins Is Evaded by *Xanthomonas oryzae pvs. oryzae* and *oryzicola*. Mol. Plant *8*, 1024–1037.

Wang, X., Kota, U., He, K., Blackburn, K., Li, J., Goshe, M.B., Huber, S.C., and Clouse, S.D. (2017). Sequential Transphosphorylation of the BRI1/BAK1 Receptor Kinase Complex Impacts Early Events in Brassinosteroid Signaling. Dev. Cell *15*, 220–235.

Williamson, B. (1998). Plant Pathology, Fourth Edition. By G. N. Agrios. London: Academic Press (1997), pp. 635, hardback US$59.95. ISBN 0-12-044564-6. Exp. Agric. *34*, 125–130.

Willmann, R., Lajunen, H.M., Erbs, G., Newman, M.-A., Kolb, D., Tsuda, K., Katagiri, F., Fliegmann, J., Bono, J.-J., Cullimore, J. V, *et al*. (2011). *Arabidopsis* lysin-motif proteins LYM1 LYM3 CERK1 mediate bacterial peptidoglycan sensing and immunity to bacterial infection. Proc. Natl. Acad. Sci. U. S. A. *108*, 19824–19829.

Xiang, T., Zong, N., Zou, Y., Wu, Y., Zhang, J., Xing, W., Li, Y., Tang, X., Zhu, L., Chai, J., *et al*. (2008). *Pseudomonas syringae* Effector AvrPto Blocks Innate Immunity by Targeting Receptor Kinases. Curr. Biol. *18*, 74–80.

Xin, X.-F., Nomura, K., Aung, K., Velásquez, A.C., Yao, J., Boutrot, F., Chang, J.H., Zipfel, C., and He, S.Y. (2016). Bacteria establish an aqueous living space in plants crucial for virulence. Nature *539*, 524–529.

Yaffe, M.B., Rittinger, K., Volinia, S., Caron, P.R., Aitken, A., Leffers, H., Gamblin, S.J., Smerdon, S.J., and Cantley, L.C. (2017). The Structural Basis for 14-3-3:Phosphopeptide Binding Specificity. Cell *91*, 961–971.

Yamaguchi, Y., Pearce, G., and Ryan, C.A. (2006). The cell surface leucine-rich repeat receptor for AtPep1, an endogenous peptide elicitor in *Arabidopsis*, is functional in transgenic tobacco cells. Proc. Natl. Acad. Sci. U. S. A. *103*, 10104–10109.

Yamaguchi, Y., Huffaker, A., Bryan, A.C., Tax, F.E., and Ryan, C.A. (2010). PEPR2 Is a Second Receptor for the Pep1 and Pep2 Peptides and Contributes to Defense Responses in *Arabidopsis*. Plant Cell *22*, 508–522.

von Zastrow, M., and Sorkin, A. (2007). Signaling on the endocytic pathway. Curr. Opin. Cell Biol. *19*, 436–445.

Zhang, J., Shao, F., Li, Y., Cui, H., Chen, L., Li, H., Zou, Y., Long, C., Lan, L., Chai, J., *et al*. (2007). A *Pseudomonas syringae* Effector Inactivates MAPKs to Suppress PAMP-Induced Immunity in Plants. Cell Host Microbe *1*, 175–185.

Zhang, J., Li, W., Xiang, T., Liu, Z., Laluk, K., Ding, X., Zou, Y., Gao, M., Zhang, X., Chen, S., *et al*. (2017). Receptor-like Cytoplasmic Kinases Integrate Signaling from Multiple Plant Immune Receptors and Are Targeted by a *Pseudomonas syringae* Effector. Cell Host Microbe *7*, 290–301.

Zhang, X., Zhao, H., Gao, S., Wang, W.-C., Katiyar-Agarwal, S., Huang, H.-D., Raikhel, N., and Jin, H. (2011). *Arabidopsis* Argonaute 2 regulates innate

immunity via miRNA393*-mediated silencing of a Golgi-localized SNARE gene MEMB12. Mol. Cell *42*, 356–366.

Zhou, J.-M., and Chai, J. (2008). Plant pathogenic bacterial type III effectors subdue host responses. Curr. Opin. Microbiol. *11*, 179–185.

Zhu, J., Gong, Z., Zhang, C., Song, C.-P., Damsz, B., Inan, G., Koiwa, H., Zhu, J.-K., Hasegawa, P.M., and Bressan, R.A. (2002). OSM1/SYP61: A Syntaxin Protein in *Arabidopsis* Controls Abscisic Acid–Mediated and Non-Abscisic Acid–Mediated Responses to Abiotic Stress. Plant Cell *14*, 3009 LP-3028.

Zipfel, C., and Robatzek, S. (2010). Pathogen-Associated Molecular Pattern-Triggered Immunity: Veni, Vidi…? Plant Physiol. *154*, 551 LP-554.

Zipfel, C., Robatzek, S., Navarro, L., Oakeley, E.J., Jones, J.D.G., Felix, G., and Boller, T. (2004). Bacterial disease resistance in *Arabidopsis* through flagellin perception. Nature *428*, 764–767.

Zipfel, C., Kunze, G., Chinchilla, D., Caniard, A., Jones, J.D.G., Boller, T., and Felix, G. (2006). Perception of the Bacterial PAMP EF-Tu by the Receptor EFR Restricts Agrobacterium-Mediated Transformation. Cell *125*, 749–760.